Final Report

FDOT Contract No.: BDV31-977-13
UF Contract No.: 113099

Embedded Data Collector (EDC) Phase II Load and Resistance Factor Design (LRFD)

Principal Investigators: Michael C. McVay
Scott J. Wasman

Department of Civil and Coastal Engineering
Engineering School of Sustainable Infrastructure and Environment
University of Florida
P.O. Box 116580
Gainesville, Florida 32611-6580

Developed for the

Rodrigo Herrera, P.E., Project Manager
Juan Castellanos, P.E., Co-Project Manager

September 2015

DISCLAIMER

The opinions, findings, and conclusions expressed in this publication are those of the authors and not necessarily those of the Florida Department of Transportation or the U.S. Department of Transportation.

Prepared in cooperation with the State of Florida Department of Transportation and the U.S. Department of Transportation.

SI (MODERN METRIC) CONVERSION FACTORS (from FHWA)

APPROXIMATE CONVERSIONS TO SI UNITS

SYMBOL	WHEN YOU KNOW	MULTIPLY BY	TO FIND	SYMBOL
LENGTH				
in	inches	25.4	millimeters	mm
ft	feet	0.305	meters	m
yd	yards	0.914	meters	m
mi	miles	1.61	kilometers	km

SYMBOL	WHEN YOU KNOW	MULTIPLY BY	TO FIND	SYMBOL
AREA				
in^2	square inches	645.2	square millimeters	mm^2
ft^2	square feet	0.093	square meters	m^2
yd^2	square yard	0.836	square meters	m^2
ac	acres	0.405	hectares	ha
mi^2	square miles	2.59	square kilometers	km^2

SYMBOL	WHEN YOU KNOW	MULTIPLY BY	TO FIND	SYMBOL
VOLUME				
fl oz	fluid ounces	29.57	milliliters	mL
gal	gallons	3.785	liters	L
ft^3	cubic feet	0.028	cubic meters	m^3
yd^3	cubic yards	0.765	cubic meters	m^3
NOTE: volumes greater than 1000 L shall be shown in m^3				

SYMBOL	WHEN YOU KNOW	MULTIPLY BY	TO FIND	SYMBOL
MASS				
oz	ounces	28.35	grams	g
lb	pounds	0.454	kilograms	kg
T	short tons (2000 lb)	0.907	megagrams (or "metric ton")	Mg (or "t")

SYMBOL	WHEN YOU KNOW	MULTIPLY BY	TO FIND	SYMBOL
TEMPERATURE (exact degrees)				
°F	Fahrenheit	5 (F-32)/9 or (F-32)/1.8	Celsius	°C

SYMBOL	WHEN YOU KNOW	MULTIPLY BY	TO FIND	SYMBOL
ILLUMINATION				
fc	foot-candles	10.76	lux	lx
fl	foot-Lamberts	3.426	candela/m^2	cd/m^2

SYMBOL	WHEN YOU KNOW	MULTIPLY BY	TO FIND	SYMBOL
FORCE and PRESSURE or STRESS				
Lbf*	poundforce	4.45	newtons	N
kip	kip force	1000	pounds	lbf
lbf/in^2	poundforce per square inch	6.89	kilopascals	kPa

APPROXIMATE CONVERSIONS TO SI UNITS

SYMBOL	WHEN YOU KNOW	MULTIPLY BY	TO FIND	SYMBOL
LENGTH				
mm	millimeters	0.039	inches	in
m	meters	3.28	feet	ft
m	meters	1.09	yards	yd
km	kilometers	0.621	miles	mi

SYMBOL	WHEN YOU KNOW	MULTIPLY BY	TO FIND	SYMBOL
AREA				
mm^2	square millimeters	0.0016	square inches	in^2
m^2	square meters	10.764	square feet	ft^2
m^2	square meters	1.195	square yards	yd^2
ha	hectares	2.47	acres	ac
km^2	square kilometers	0.386	square miles	mi^2

SYMBOL	WHEN YOU KNOW	MULTIPLY BY	TO FIND	SYMBOL
VOLUME				
mL	milliliters	0.034	fluid ounces	fl oz
L	liters	0.264	gallons	gal
m^3	cubic meters	35.314	cubic feet	ft^3
m^3	cubic meters	1.307	cubic yards	yd^3

SYMBOL	WHEN YOU KNOW	MULTIPLY BY	TO FIND	SYMBOL
MASS				
g	grams	0.035	ounces	oz
kg	kilograms	2.202	pounds	lb
Mg (or "t")	megagrams (or "metric ton")	1.103	short tons (2000 lb)	T

SYMBOL	WHEN YOU KNOW	MULTIPLY BY	TO FIND	SYMBOL
TEMPERATURE (exact degrees)				
°C	Celsius	1.8C+32	Fahrenheit	°F

SYMBOL	WHEN YOU KNOW	MULTIPLY BY	TO FIND	SYMBOL
ILLUMINATION				
lx	lux	0.0929	foot-candles	fc
cd/m^2	candela/m^2	0.2919	foot-Lamberts	fl

SYMBOL	WHEN YOU KNOW	MULTIPLY BY	TO FIND	SYMBOL
FORCE and PRESSURE or STRESS				
N	newtons	0.225	poundforce	lbf
kPa	kilopascals	0.145	poundforce per square inch	lbf/in^2

*SI is the symbol for International System of Units. Appropriate rounding should be made to comply with Section 4 of ASTM E380.
(Revised March 2003)

TECHNICAL REPORT DOCUMENTATION PAGE

1. Report No.	2. Government Accession No.	3. Recipient's Catalog No.
4. Title and Subtitle Embedded Data Collector (EDC) Phase II Load and Resistance Factor Design (LRFD)		5. Report Date September 2015 6. Performing Organization Code
7. Author(s) Michael C. McVay and Scott J. Wasman		8. Performing Organization Report No.
9. Performing Organization Name and Address University of Florida – Dept. of Civil and Coastal Engineering Engineering School of Sustainable Infrastructure and Environment 365 Weil Hall – P.O. Box 116580 Gainesville, FL 32611-6580		10. Work Unit No. (TRAIS) 11. Contract or Grant No. BDV31-977-13
12. Sponsoring Agency Name and Address Florida Department of Transportation 605 Suwannee Street, MS 30 Tallahassee, FL 32399		13. Type of Report and Period Covered Final Report 1/1/14 – 9/30/15 14. Sponsoring Agency Code
15. Supplementary Notes		

16. Abstract

A total of 16 static load test results was collected in Florida and Louisiana. New static load tests on five test piles in Florida (four of which were voided) were monitored with Embedded Data Collector (EDC) instrumentation and contributed to the total of 16. For the voided test piles, EDC instrumentation was placed in the piles at different locations relative to the void to compare the estimated resistances. In the four test piles, the measured top compressive stresses measured in the solid section of the pile were typically about 25% smaller than the measured values in the voided section of the pile. However, when the top stresses were adjusted by area (i.e., divide by 645 in^2 / 900 in^2 = 0.72), then the stresses were very comparable. Two methods were used to estimate the pile capacities: The UF method and the Tran et al. methods. The UF method (employed in SmartPile Review) uses the Case capacity equation with variable case damping, J_c, to assess total capacity and the Unloading Point Method for tip resistance, (i.e., skin friction = total – tip resistance). The Tran et al. method computes side friction using a segmental approach and tip resistance using conservation of force and energy. The Tran et al. method for side friction showed a smaller difference (6%) in predicted capacities between top solid and voided gauge sets than the UF method (23%) using the Case Equation for the four voided test piles.

Load and Resistance Factor Design (LRFD) resistance factors (Φ) for piles with EDC were calculated for a reliability, β, of 2.33 using the First Order Second Moment (FOSM) method and the First Order Reliability Method (FORM). For the UF method, a total of 42 pairs (measured vs. predicted; bias, λ = 0.998, standard deviation, σ = 0.212, and CV = 0.212) were analyzed for the cases of EDC in both the solid and voided sections (four new test piles supported in present project)). The Φ_{FORM} = 0.75 and Φ_{FOSM} = 0.64. A smaller data set of 34 pairs (measured vs. predicted; bias, λ = 0.918, standard deviation, σ = 0.172, and CV = 0.188) were analyzed for the cases of EDC only in the solid sections. The Φ_{FORM} = 0.73 and Φ_{FOSM} = 0.62. For the Tran et al. method, a total of 39 pairs (measured vs. predicted; bias, λ = 0.991, standard deviation, σ = 0.169, and CV = 0.17) were analyzed for the cases of EDC in both the solid and voided sections. The Φ_{FORM} = 0.81 and Φ_{FOSM} = 0.68. A smaller data set of 33 pairs (measured vs. predicted; bias, λ = 0.979, standard deviation, σ = 0.182, and CV = 0.186) were analyzed for the cases of EDC only in the solid sections. The Φ_{FORM} = 0.78 and Φ_{FOSM} = 0.66. For the Fixed J_c method, Φ_{FORM} and Φ_{FOSM} were calculated for limited data sets (solid/voided and only solid sections). The listed resistance factors should be used with caution due to the limited data set and the conditions they were obtained (e.g., limited soil types tested, time between BOR and static load test, lack of fully instrumented tests piles).

17. Key Words	18. Distribution Statement
Deep Foundations, LRFD Resistance Factor, Embedded Data Collectors (EDC), Prestressed Concrete Piles, Skin, Tip, and Total Resistance and Case Studies	No restrictions.

19. Security Classif. (of this report)	20. Security Classif. (of this page)	21. No. of Pages	22. Price
Unclassified	Unclassified	139	

Form DOT F 1700.7 (8-72) Reproduction of completed page authorized

ACKNOWLEDGMENTS

The researchers would like to thank the Florida Department of Transportation (FDOT) for the financial support to carry out this research, as well as the input of the FDOT central office's geotechnical engineers in the collection of site data. They would also like to thank the Louisiana Department of Transportation (LaDOT) for providing data on four piles.

EXECUTIVE SUMMARY

The focus of this research was the evaluation of the Load and Resistance Factor Design (LRFD) resistance factors (Φ) for available predictive pile capacity methods that use Embedded Data Collectors (EDC). Data from 16 piles (12 in Florida and four in Louisiana) with four piles (US-331 Choctawhatchee Bay) employing gauge sets in both the solid and void top sections of the piles. A maximum of 42 side, tip, and total resistances were predicted for the piles. The Florida Department of Transportation (FDOT) project BDK75-977-24 collected data for 12 of the piles, and this project collected data on four US-331 Choctawhatchee Bay piles, as well as skin and tip resistance on two Bayou Lacassine piles.

For the study, Davisson Capacity was used to assess the total nominal measured resistance. Similarly, at Davisson Capacity and movement, the measured nominal side and base resistances were obtained and compared (bias - measured/predicted) with predicted response. In the case of static load tests which did not reach Davisson Capacity, the side, tip, and total resistances at peak measured static load and displacement were compared (i.e., bias, CV, etc.).

For the assessment of LRFD Φ values, the First Order Reliability Method (FORM), as developed by Hasofer and Lind (1974) and described in detail in Paikowsky et al. (2004) and Styler (2005), was employed. The FORM was used by Paikowsky et al. (2004) in the NCHRP 507 project to develop Φ values for Pile Driving Analyzer/Case Pile Wave Analysis Program (PDA/CAPWAP) determined resistance, and which were later adopted by the American Association of State Highway and Transportation Officials (AASHTO). Resistance factors using the First Order Second Moment (FOSM) method are also included for comparison.

In the case of where the SmartPile Review software (UF Method) was used, which employs the Case capacity equation with variable case damping, J_c, (i.e., calculated for every

hammer blow), to assess total capacity and Unloading Point Method (Middendorp et al., 1992) for tip resistance, (skin friction = total - tip resistance), a total of 42 pairs (measured vs. predicted; bias, $\lambda = 0.998$, standard deviation, $\sigma = 0.212$, and CV = 0.212) were analyzed. The data set included solid and voided piles with EDC gauges at the top and tip of the piles, and around the void for 4 piles. The computed LRFD Φ, for a reliability, β, of 2.33, are Φ_{FORM} = 0.75 and Φ_{FOSM} = 0.64 for the UF method.

For newer methods (Tran et al., 2012A and 2012B), which compute side friction using a segmental approach and tip resistance using conservation of force and energy, a total of 39 pairs (measured vs. predicted; bias, λ =0.991 , standard deviation, $\sigma = 0.169$, and CV = 0.17) were analyzed for solid and voided sections. The computed LRFD Φ, for a reliability, β, of 2.33, are Φ_{FORM} = 0.81 and Φ_{FOSM} = 0.68 for the Tran et al. method.

For the Fixed J_c method, which estimates the nominal (total) resistance a total of 15 pairs (measured vs. predicted; bias, $\lambda = 1.05$, standard deviation, $\sigma = 0.235$, and CV = 0.224) were analyzed for solid and voided sections. The computed LRFD Φ, for a reliability, β, of 2.33, are Φ_{FORM} = 0.76 and Φ_{FOSM} = 0.66.

The differences in EDC gauge location in the test piles (at the top and tip of a pile or around the void) was investigated for four voided piles by comparing capacity estimates from the UF method and the Tran et al. method. The Tran et al. method for skin friction, which employs a segmental approach to the pile, exhibited smaller difference (6%) in predicted capacities between top solid and voided gauge sets than the UF method (23%) using the Case capacity equation. Finally, the measured top compressive stresses measured in the solid section of the pile were typically about 25% smaller than the measured values in the voided section of

the pile. However, when the top stresses were adjusted by area (i.e., divide by 645 in^2 / 900 in^2 = 0.72), then the stresses were very comparable.

Current FDOT design standard index number 20602 specifies that the EDC instrumentation be embedded at 2D (D = pile diameter) from the top of the pile and 3 feet from the tip of the pile. Considering this specification on the use of EDC in concrete piles driven in Florida, smaller data sets that exclude the skin, tip, and total resistance predictions based on the EDC in the voided section of the test piles (four test piles from the US-331 Choctawhatchee Bay) were considered. For the UF method (measured vs. predicted; bias, $\lambda = 0.918$, standard deviation, $\sigma = 0.172$, and CV = 0.188) the computed LRFD Φ, for a reliability, β, of 2.33, are $\Phi_{FORM} = 0.73$ and $\Phi_{FOSM} = 0.62$. For the Tran et al. method (measured vs. predicted; bias, $\lambda = 0.979$, standard deviation, $\sigma = 0.182$, and CV = 0.186) the computed LRFD Φ, for a reliability, β, of 2.33, are $\Phi_{FORM} = 0.78$ and $\Phi_{FOSM} = 0.66$. For the Fixed J_c method (measured vs. predicted; bias, $\lambda = 1.01$, standard deviation, $\sigma = 0.256$, and CV = 0.253) the computed LRFD Φ, for a reliability, β, of 2.33, are $\Phi_{FORM} = 0.69$ and $\Phi_{FOSM} = 0.60$.

TABLE OF CONTENTS

LIST OF TABLES

LIST OF FIGURES

CHAPTER 1
INTRODUCTION

1.1 Background

Monitoring the installation of driven pile foundations is critical for assessing capacities, stresses, and final pile lengths for Florida Department of Transportation (FDOT) bridge structures. Dynamic load testing of driven test piles (ASTM Specifications D4945-12) is currently the preferred approach used by industry on the grounds that it is a cost effective and a reliable method for assessing total capacity. Until 2008, the primary method used was the Pile Driving Analyzer/Case Pile Wave Analysis Program (PDA/CAPWAP), which involved external gauges attached to the top of the pile, from which stresses and capacity vs. depth were computed/displayed using Case capacity equation with J_c assessed from the CAPWAP analysis.

With the development of the Embedded Data Collector (EDC) system, strain and accelerometer gauges were cast-in the top and bottom of the pile, from which stresses at top and bottom of pile, the total pile capacity and end bearing were displayed for every blow of the hammer. In addition, since the instrumentation was cast-in the piles at the casting yard, there was no need to climb the driving leads to attach gauges, speeding up the driving process.

In an effort to evaluate the effectiveness of the EDC system, the FDOT engaged in an evaluation program (Phase I) of comparison with dynamic load testing methods and wave matching software (i.e., CAPWAP), which is used by industry. Phase I yielded promising results, prompting the FDOT central office's geotechnical team to pursue the implementation of EDC as well as evaluation of its reliability by comparing the recorded results with static load tests, i.e., Phase II. To adopt the EDC technology as an alternative to current pile driving monitoring practice, the FDOT requires Load and Resistance Factor Design (LRFD) resistance factors (Φ) for the technology, which should be established from a sufficiently large database of

instrumented static load test results. This final effort is the continuation of phase II, to collect sufficient data for LRFD Φ assessment of methods in existing software (e.g., SmartPile Review) as well as newer methods (Tran et. al, 2012A and 2012B) which can be used with EDC measurements. Since the EDC allows independent assessment of tip, skin, and total, all three will be evaluated. Note, independent assessment of LRFD Φ for skin (e.g., uplift piles) and tip is of interest, and could be useful in cases where superposition of skin and tip from different blows (e.g., End Of Initial Drive (EOID) and Beginning Of Re-strike (BOR), NCHRP 418) are applicable.

1.2 Objective and Supporting Tasks

The primary objectives of this project is the continuation of phase II activities:

- Collect dynamic and static load test results from planned load test program at Choctawhatchee Bay project in District 3;
- Evaluate stresses and capacities with EDC instruments located in both the solid and voided sections of the piles;
- Analyze all the data collected to date and develop resistance factors (side, tip and total) for piles with EDC using the following resistance estimate approaches:
    - UF Method (SmartPile Review)
    - UF Method on test piles and Fixed Method on production piles
    - Recently developed methods (Tran et al, 2012A and 2012B) for independent assessment of side and tip resistance.

For EDC technology, LRFD resistance factors must be determined for FDOT practice. The assessment requires high quality static pile load tests obtained from either top down compression testing, or bottom-up Osterberg Testing for the various soil/rock conditions

throughout the state. Since the technology is capable of separating skin from tip resistance, the resistance factor may be determined from independent measurements (e.g., total, tip or skin in the case of pullout tests) if sufficient data is collected.

The outcomes of this continuation of the EDC Phase II research are 1) evaluation of EDC estimates of static resistance (i.e., total, skin friction and tip resistance) when compared to static load tests; 2) development of LRFD resistance factors for EDC pile monitoring (i.e., skin friction, tip resistance, etc.). The work was accomplished through the following tasks.

1.2.1 Task 1 – Dynamic Monitoring of Test Piles at Choctawhatchee Bay

Completion of Task 1 required coordination of activities with the District 3 project administrator and hiring a consultant (Applied Foundation Testing Inc. [AFT], Jacksonville, FL) to monitor the initial drives and set checks of the five piles with EDC. AFT was also hired to read the EDC gauges on each of the test piles during static load test. The researchers collected the raw data (e.g., BDF files, Excel files, etc.) as well as AFT's prediction (using SmartPile Review) of tip, skin and total capacity of each test at EOID and BOR. The BDF files were sent to Dr. Khiem Tran (Clarkson University) to make predictions of pile resistances (skin, tip and total) using the Tran et al. methods.

The strain and acceleration data collected using the EDC gauges (strain gauge and accelerometer), located in the solid and voided sections of the pile, were used to compare stresses (e.g., compression, tension) in the pile, and capacity estimates.

1.2.2 Task 2 – Static Load Tests and Analysis of Test Piles at Choctawhatchee Bay

The objective of Task 2 was to perform over the shoulder monitoring of the first static load tests and analyze the data. Skanska performed static load tests on each of the five test piles. The top of each test pile was cut-off prior to the static load test, which made the EDC gauges inaccessible because the wires were cut. Accessing the wires by chipping away the pile's

concrete from the cut wires was discussed by the FDOT project manager, UF researchers, and AFT (consultant). A decision was made not to access the wires and that the EDC gauges could not be read during the static load test. As a result, the measured skin friction and tip resistance could not be obtained for comparison to the predicted skin friction and tip resistance (UF and Tran et al.). The only data collected from the load test was the load and vertical displacement at the top of the pile (assessment of total pile capacity). The measured Davisson capacities were plotted against the load displacement for each test pile and provided to the UF researchers. The measured total resistance were compared to the Fixed J_c, UF, and Tran et al. predictions based on the EDC gauges monitored during driving.

1.2.3 Task 3 – Calibration of LRFD Resistance Factors for Fixed J_c, UF, and Tran et al. Methods

All the static load test results were collected for the calibration of the LRFD resistance factors for total, side and tip resistance for the Fixed J_c, UF, and Tran et al. method. As part of FDOT project BDK75-977-24, static load test data from 6 sites, 12 piles (17 independent values: tip and total) were been collected with EDC results. With the addition of the data from the new five test piles at US-331 Choctawhatchee Bay (only four were usable) and two piles at Bayou Lacassine, 12 independent measures (total, and tip) were collected for a minimum total of 29 values. With this larger data set, LRFD resistance factors were assessed for the Fixed J_c, UF, and Tran et al. methods.

1.2.4 Task 4 – Final Report and Recommendations

The final task involves reporting the on the analysis of the method bias and the subsequent calculated LRFD resistance factors using the FOSM method and the FORM. In the bias analysis, both the mean bias (measured/predicted resistance) and coefficient of variation, CV, of bias were obtained. For the study, Davisson Capacity was used to assess the total nominal

measured resistance. Similarly, at Davisson Capacity and movement, the measured nominal side and base resistance was obtained and compared (bias - measured/predicted) with predicted response. In the case of static load tests which did not reach Davisson Capacity, the side, tip and total resistance at peak measured static load and displacements was compared (i.e., bias, CV, etc).

Also, since EDC pile instrumentation included strain and acceleration data, both in the solid and voided section of the piles, comparison of stresses (e.g., compression, tension) and capacities was performed based on both cross-sections.

CHAPTER 2
EDC MONITORED PILES AT US-331 CHOCTAWHATCHEE BAY

2.1 Introduction

Task 1 was to coordinate with the district's project administrator and hire a consultant to install the EDCs (Embedded Data Collector), monitor the initial drive and perform set checks (restrikes) using EDC for 5 test piles at US-331 over Choctawhatchee Bay in Walton County, FL. The raw data, in the form of BDF and excel files, was collected from the consultant in addition to their SmartPile Review predictions of tip, skin and total capacity for each test pile. The BDF format files were needed for the Task 2 for predicting skin and tip capacity using recently developed methods by Tran et al. (2012A and 2012B). The Task 2 predictions of pile capacity will be based on End of Initial Drive (EOID) and Beginning of restrike (BOR). Also note, the previously reported measured and predicted (FDOT BDK75-977-24) will be used in the LRFD Φ assessment, Task 3.

2.2 Collection of Raw Test Data

A new bridge on US-331 over Choctawhatchee Bay (currently under construction) was identified as a site to install EDC in five test piles. The test piles were 30-inch square prestressed concrete and 160 feet in length. Four of the piles had a 134 feet long, 18-inch diameter void that started 15 feet from the top of the pile (Figure 2.1). The other test pile was a solid prestressed concrete pile.

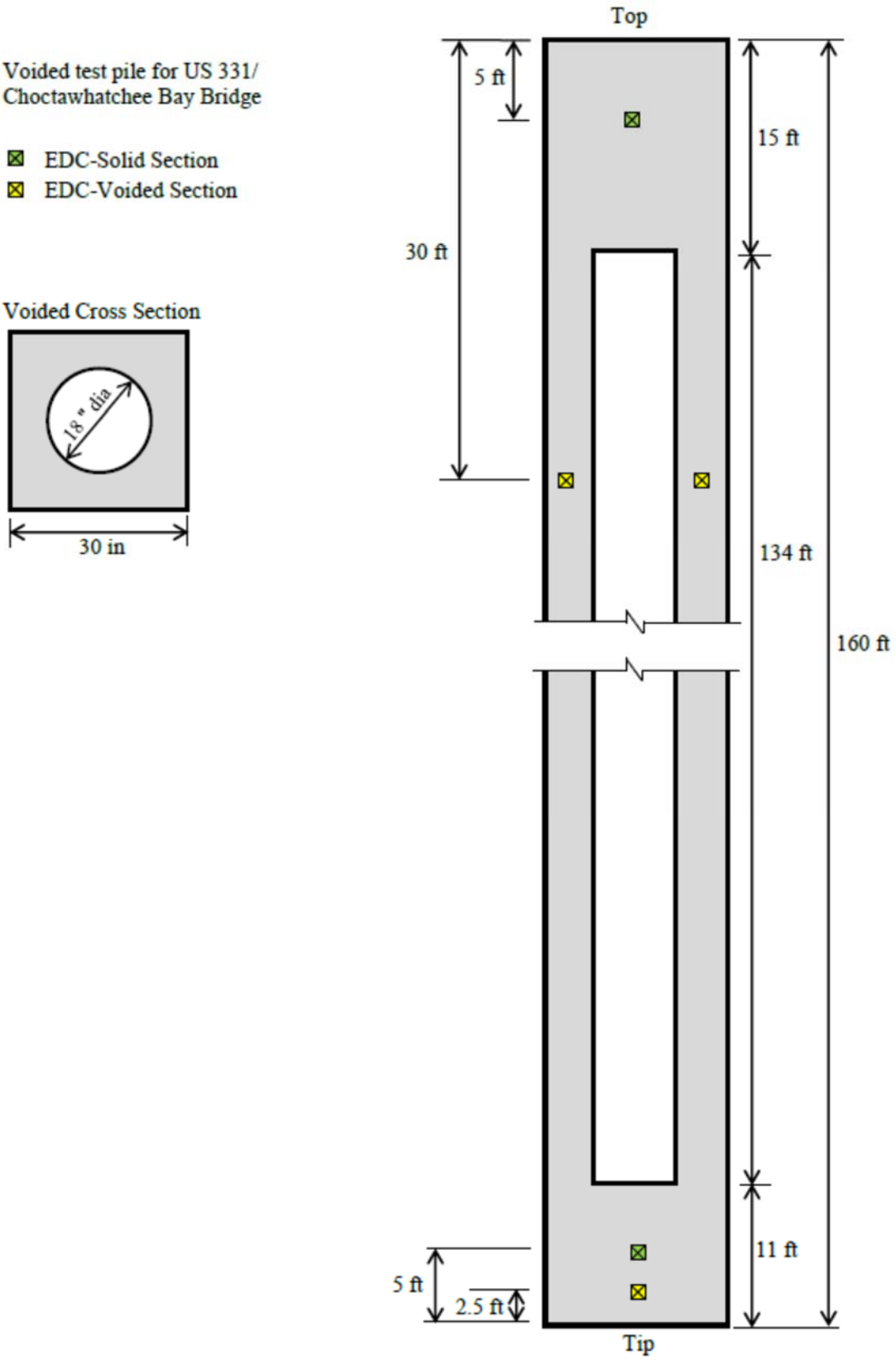

Figure 2.1 Voided 30-inch-Square Prestressed Concrete Test Pile

Applied Foundation Testing (AFT) out of Green Cove Springs, Florida was hired as the subcontractor on the project. In January 2014, their engineers traveled to the casting yard in Mississippi and placed the EDCs on the 5 test piles. At that time, the initial readings, prior to casting, and post casting, the gauges were recorded to assess their functionality. All EDCs were found to be working correctly. Following casting, the test piles were delivered via barge to the project site in south central Walton County, Florida. The EDC measurements of the 5 test piles are discussed next.

2.2.1 Pier 13

The test pile at pier 13 was a solid pile and its initial drive was on 2/24/14, followed by restrikes on 2/27/14, and a static load test on 4/6/14. The pile was driven with an ICE I-100 hammer to a tip elevation of -125 feet, then was cut-off in order to fit equipment for the static load test. As a result, the wire leads to the EDC were also cut-off, making them inaccessible to read during the static load test. Furthermore, SKANSKA (driving contractor) had to drive the pile an additional 8.8 feet deeper to the proposed cut-off elevation of +3.2 feet after the static load test. The EDCs were placed, on center, 5 feet from the top of the pile and 2.5 feet from the tip.

Figure 2.2 are the estimates of total capacity versus pile tip elevation using the Fixed Jc method and the UF method (dynamic Jc method). For the Fixed Jc method, AFT set Jc to be 0.5 (engineer operator experience – personal communication). The total capacity exceeded 600 kip at the final tip elevation (-125 feet).

Figure 2.3 shows the blow count record and Figure 2.4 shows the top and tip preload delta (change in pile pre-load stress) and measured Pile Integrity (MPI) versus pile tip elevation. A change of 50 microstrain ($\mu\varepsilon$) in pre-load stress for 10 consecutive blows indicates that the

tensile stresses or compressive stresses during driving have led to pile damage (loss of pile integrity). The MPI reported in the output of SmartPile Review is the change in the pile impedance output. Generally, if the pre-load stress is reduced by 50 percent then pile damage occurs (SmartPile, 2013). From the MPI presented in Figure 2.5, the pre-stress analysis, test pile at Pier 13, Figure 2.4 indicates the pile integrity was not compromised during installation.

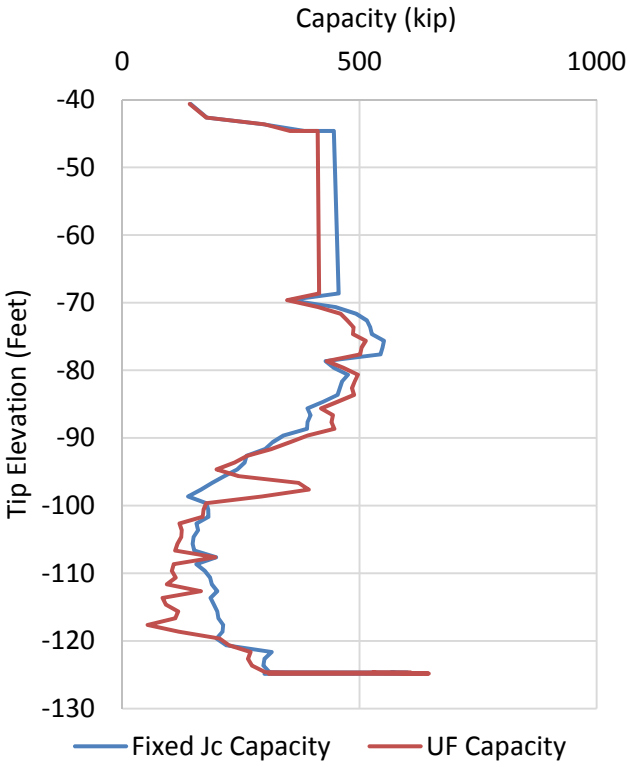

Figure 2.2 Total Capacity Versus Tip Elevation for Test Pile at Pier 13

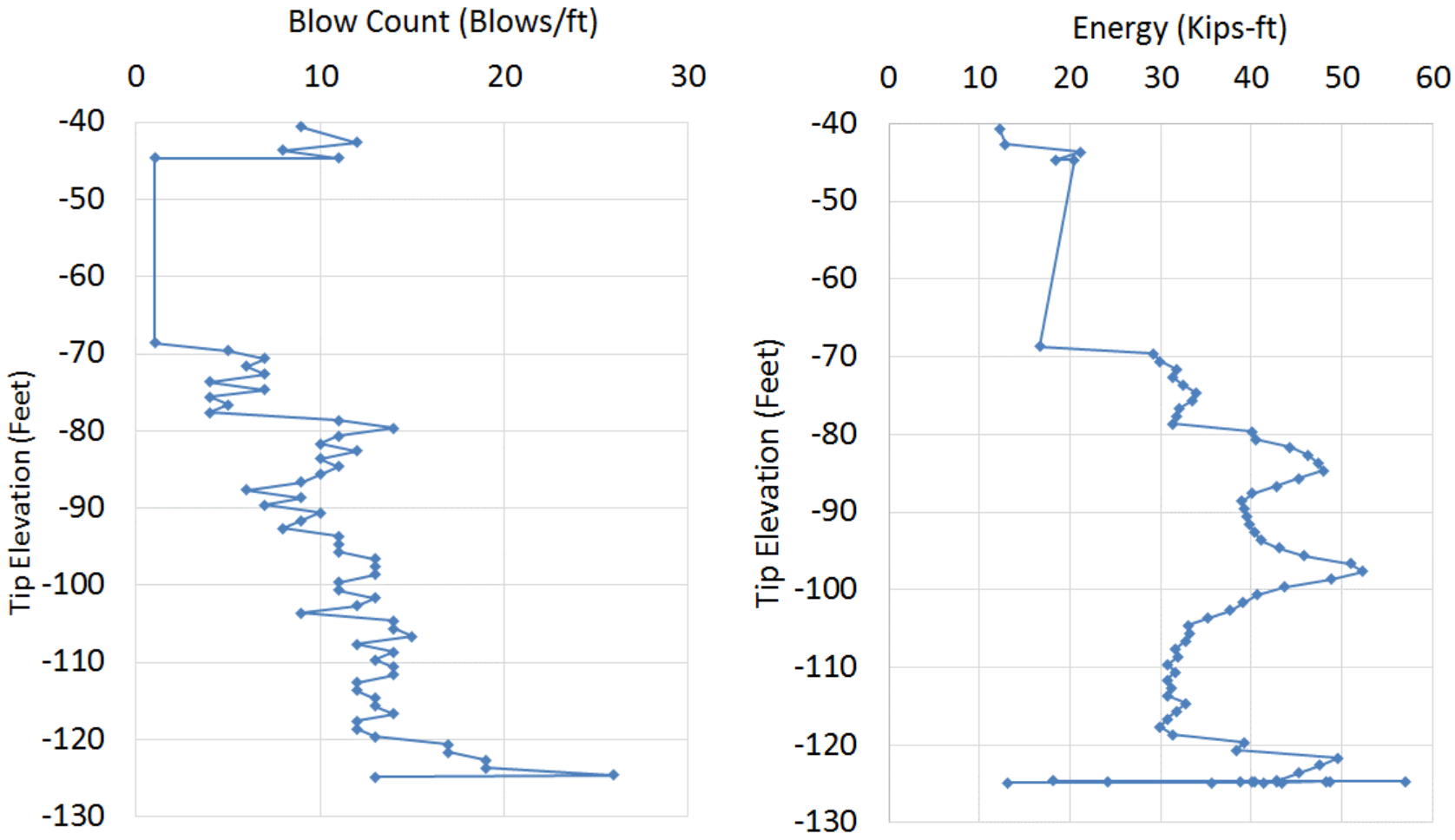

Figure 2.3 Record of Blow Counts and Energy During Driving of Test Pile at Pier 13

MPI	Pile Impedance based damage analysis	Pre-stress based damage analysis
100 %	No issues detected	No Issues detected
99 – 80 %	Minor signal issues detected possibly indicating slight pile damage	No Issues detected
79 – 60 %	More significant issues detected indicating possible pile damage	No Issues detected
59 -51 %	Major issues detected indicating likely pile damage; seek qualified professional assessment	No Issues detected
50 %	No issues detected	Issues detected indicating likely pile damage; seek qualified professional assessment
49-30 %	Minor signal issues detected possibly indicating slight pile damage	Issues detected indicating likely pile damage; seek qualified professional assessment
29 – 10 %	More significant issues detected indicating possible pile damage	Issues detected indicating likely pile damage; seek qualified professional assessment
9 – 0 %	Major issues detected indicating likely pile damage; seek qualified professional assessment	Issues detected indicating likely pile damage; seek qualified professional assessment

Figure 2.4 MPI Interpretation Guidelines (SmartPile, 2013)

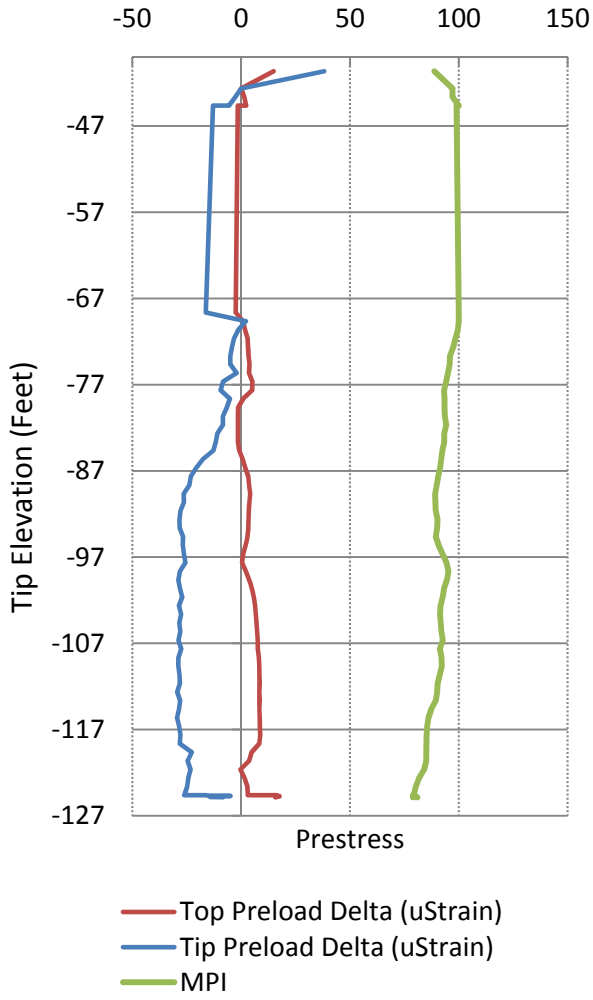

Figure 2.5 Top and Tip Preload Delta and MPI for Test Pile at Pier 13

2.2.2 Pier 25

The test pile at pier 25 was a voided pile with sets of EDC placed at the top of the pile in the solid section, on either side of the void and two sets at the tip of the pile at 5 feet and 2.5 feet from the tip (Figure 2.1). The pile was initially driven on 3/12/14 and restrikes were performed on 3/20/14 and 3/24/14; however, AFT was not notified prior to the restrike on 3/24/14, so data was not collected. The pile was then driven an additional 10 feet on 3/26/14 to a tip elevation of -125 feet, followed by a restrike on 4/1/14, and a static load test on 4/22/14. All phases of

installation were done with an ICE I-100 hammer. Table 3.4 summarizes the nominal resistance estimates using dynamic methods and static load test (SLT) results.

Figure 2.6 are the estimates of total capacity versus pile tip elevation using the Fixed Jc method and the UF method (dynamic Jc method). For the Fixed Jc method, AFT set Jc to be 0.5. The total capacity exceeds 600 kip at the final tip elevation (-125 feet).

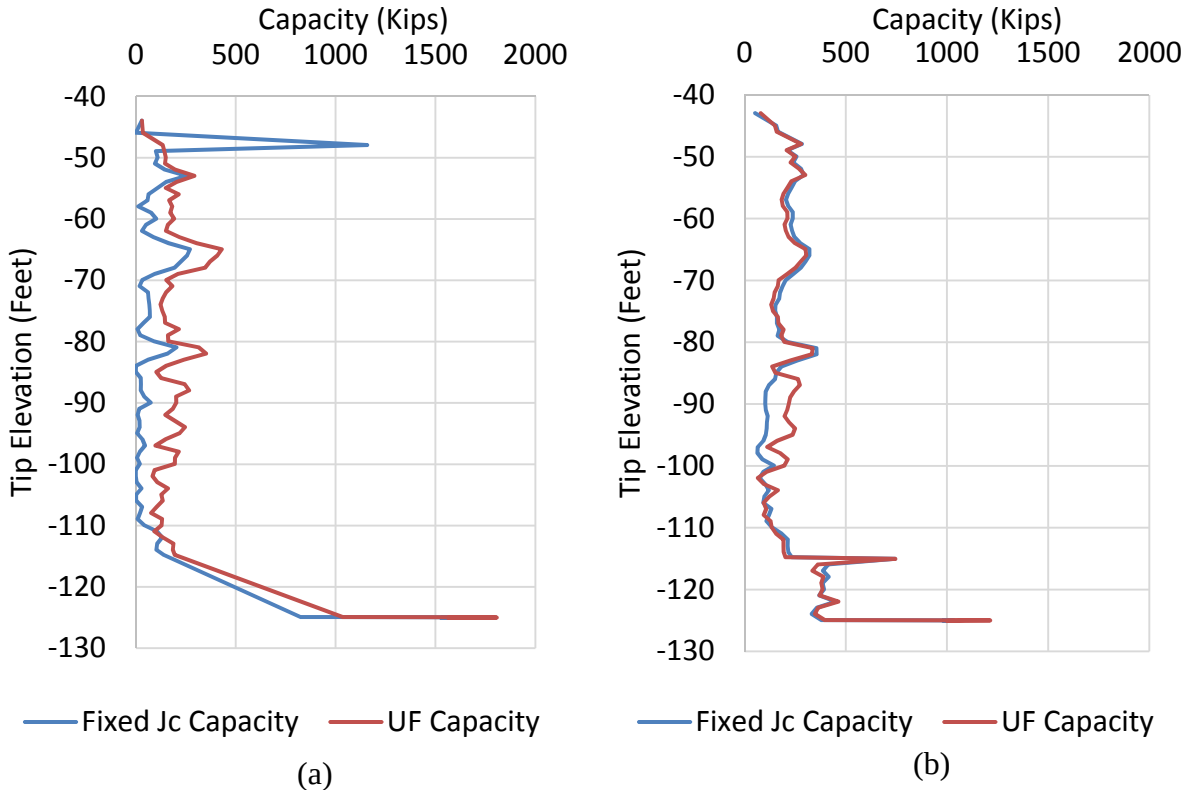

Figure 2.6 Total Capacity Versus Tip Elevation for Test Pile at Pier 25: (a) Solid Section EDC; (b) Voided Section EDC

Figure 2.7 shows the blow count record and Figure 2.8 shows the top and tip preload delta (change in pile pre-load stress) and MPI versus pile tip elevation. The use of EDC in the solid section and the voided section of the pile provide MPI at three locations (Figure 2.1). Figures 2.8 (a) and (b) show that the change in pre-load stress does not exceed 50 με and the MPI does not indicate a pile integrity issue.

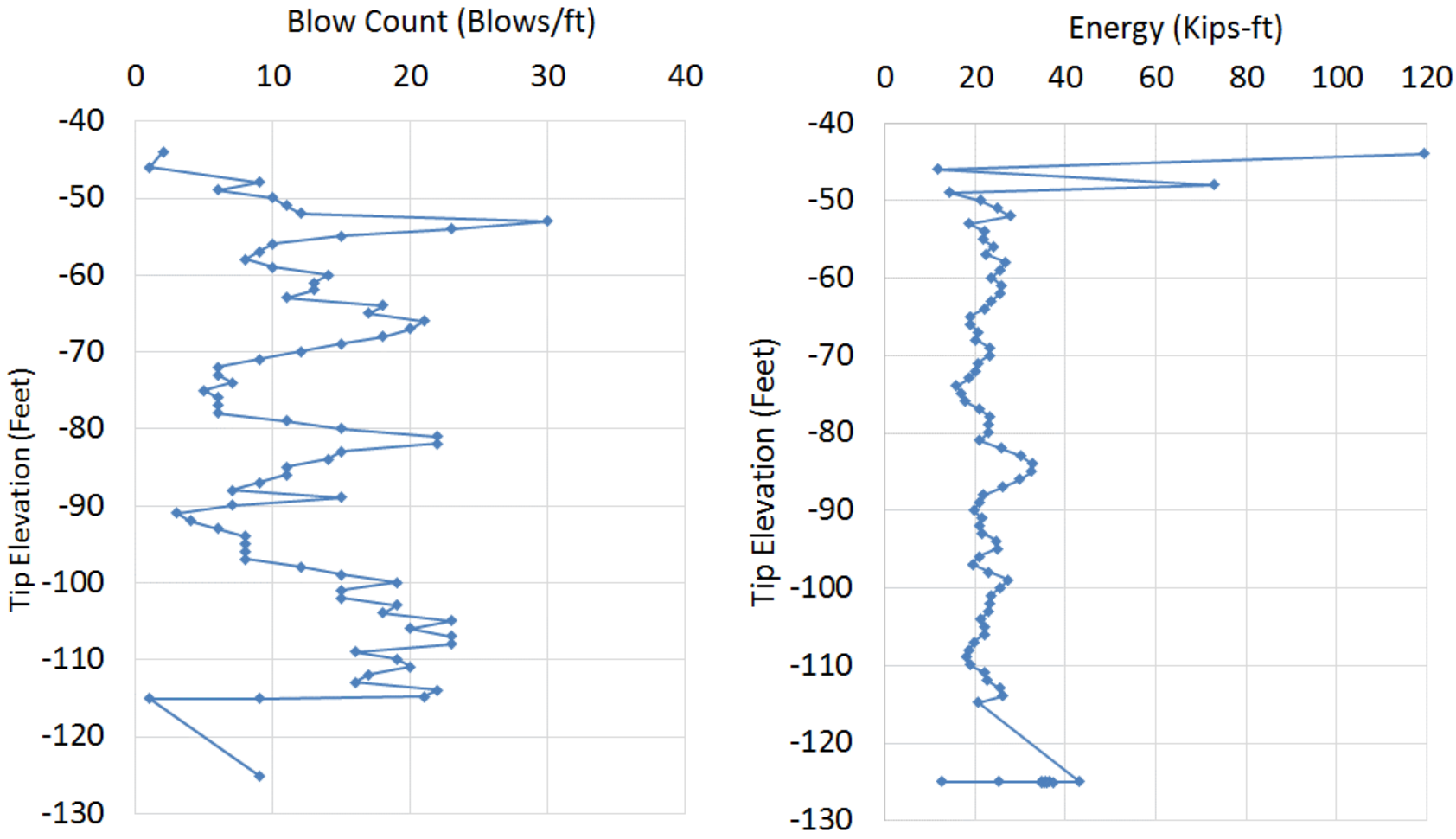

Figure 2.7 Record of Blow Counts and Energy During Driving of Test Pile at Pier 25

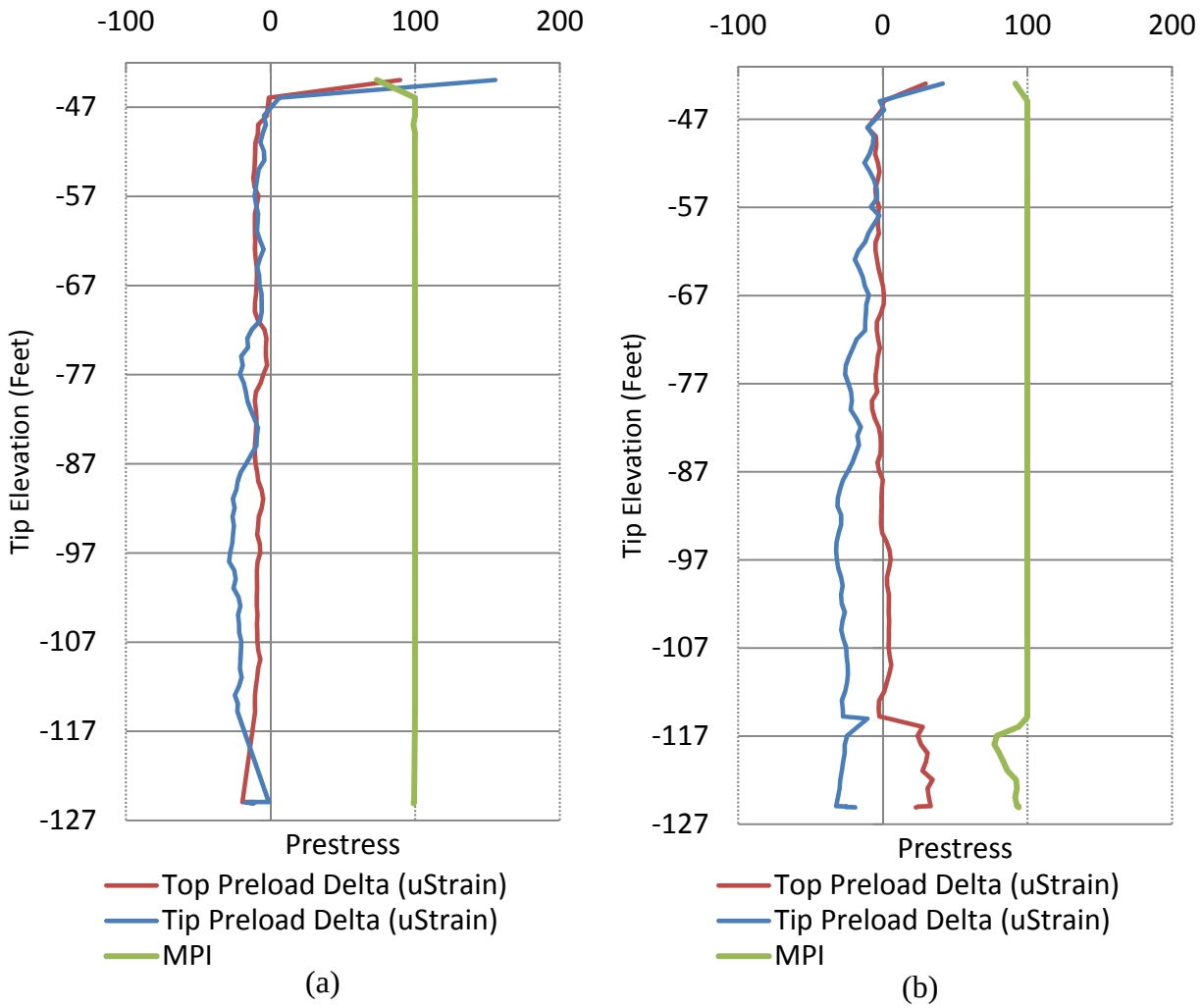

Figure 2.8 Top and Tip Preload Delta and MPI for Test Pile at Pier 25: (a) Solid Section EDC; (b) Voided Section EDC

2.2.3 Pier 33

The test pile at pier 33 was a voided pile with sets of EDC placed at the top of the pile in the solid section, on either side of the void and two sets at the tip of the pile at 5 feet and 2.5 feet from the tip (Figure 2.1). The pile was initially driven to a final tip elevation of -129.8 feet on 3/26/14, followed by a restrike on 4/1/14, and a static load test on 5/3/14. All phases of installation were done with an ICE I-100 hammer.

Figure 2.9 are the estimates of total capacity versus pile tip elevation using the Fixed Jc method and the UF method (dynamic Jc method). For the Fixed Jc method, AFT set Jc to be 0.5. The total capacity exceeds 2,000 kip at the final tip elevation (-129.8 feet).

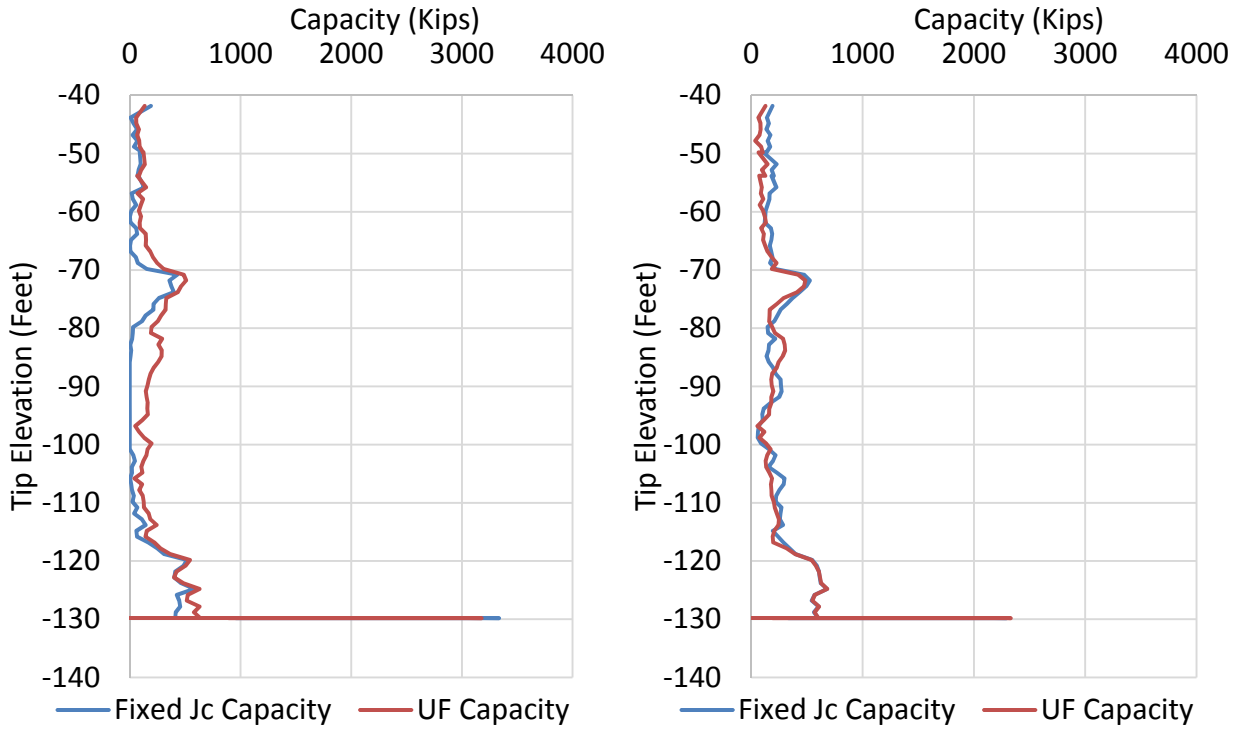

Figure 2.9 Total Capacity Versus Tip Elevation for Test Pile at Pier 33: (a) Solid Section EDC; (b) Voided Section EDC

Figure 2.10 shows the blow count record and Figure 2.11 shows the top and tip preload delta (change in pile pre-load stress) and MPI versus pile tip elevation. The use of EDC in the solid section and the voided section of the pile provide MPI at three locations (Figure 2.1). Figures 2.11 (a) and (b) show that the change in pre-load stress does not exceed 50 με and the MPI does not indicate a pile integrity issue.

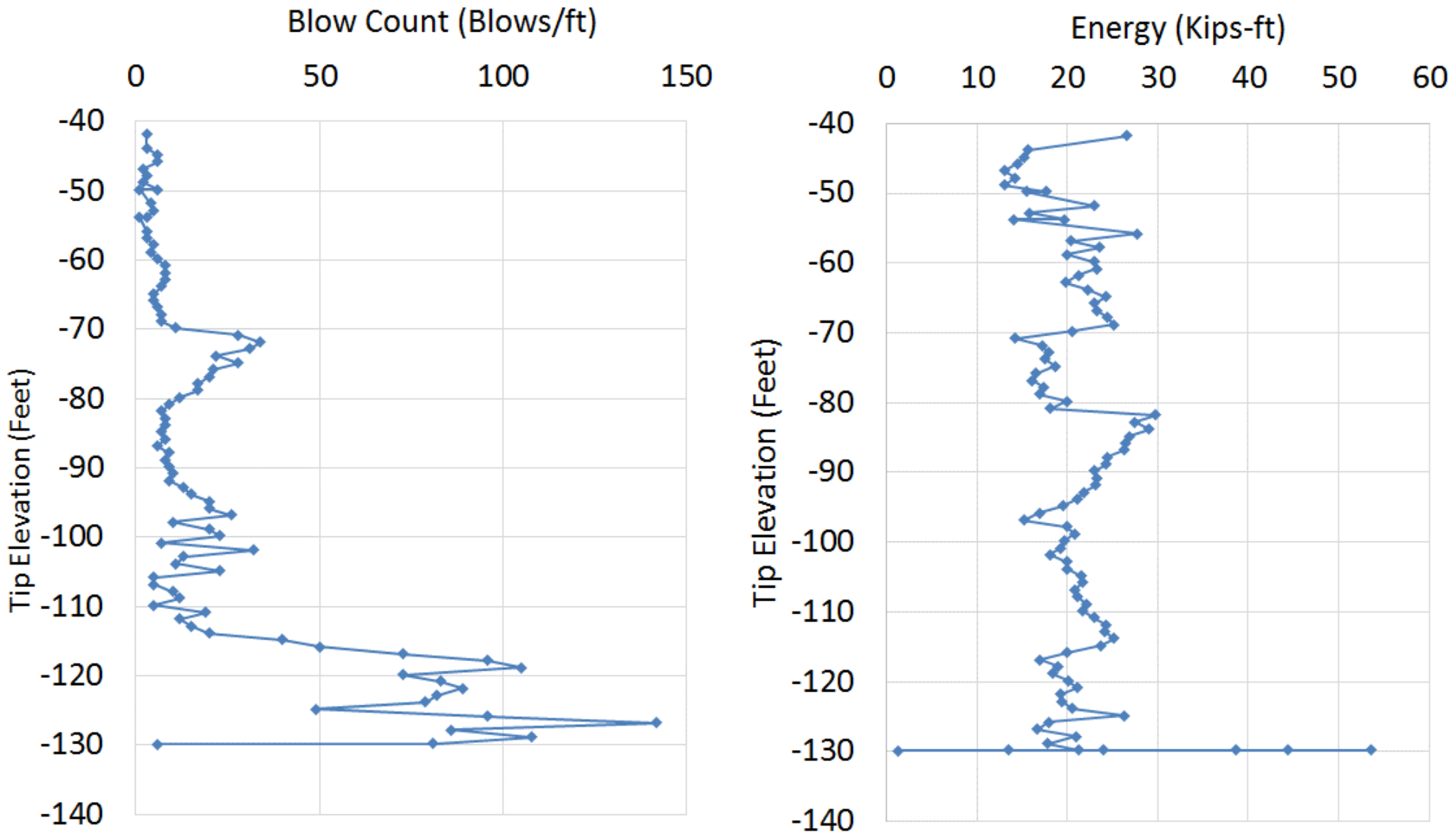

Figure 2.10 Record of Blow Counts and Energy During Driving of Test Pile at Pier 33

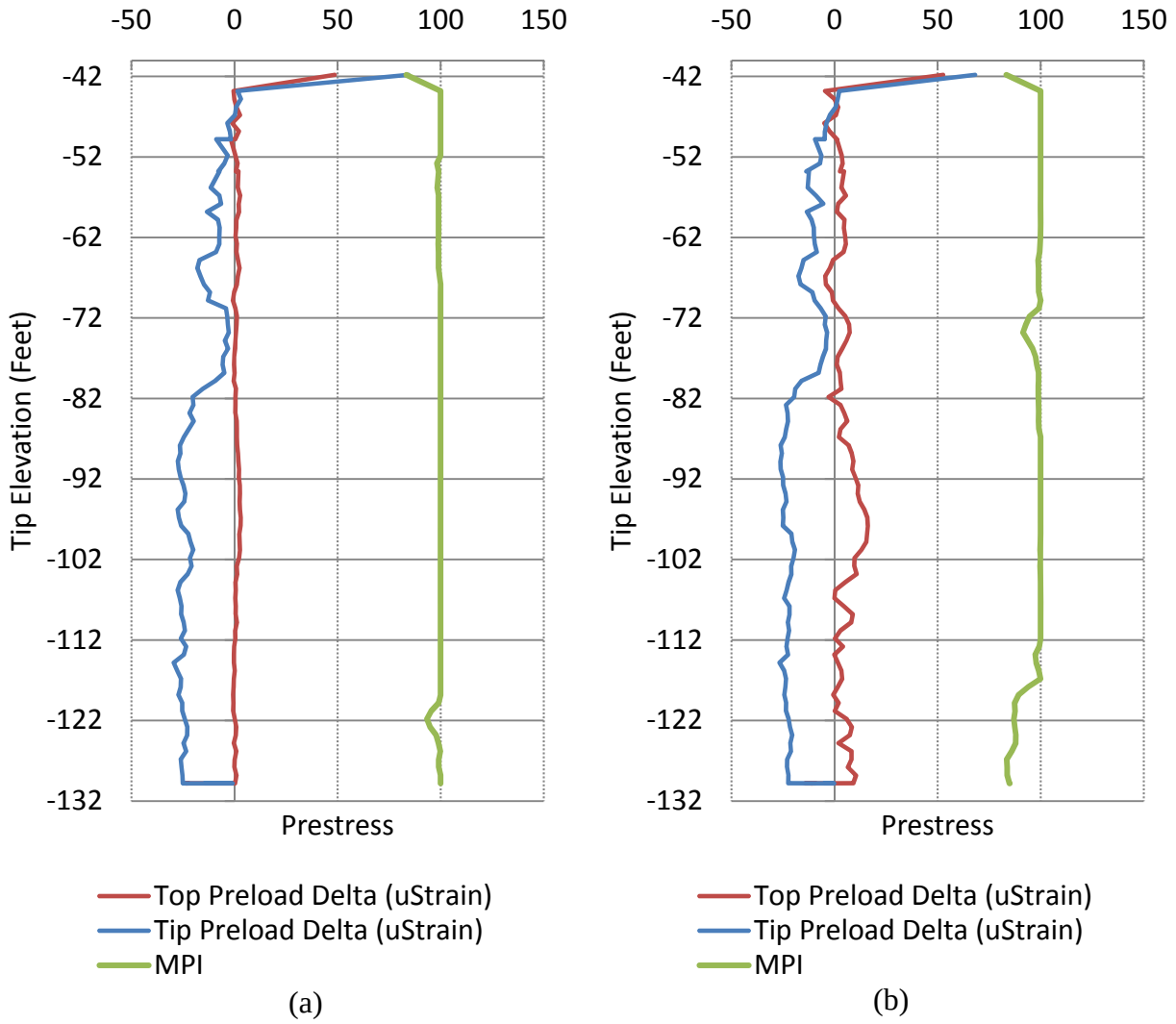

Figure 2.11 Top and Tip Preload Delta and MPI for Test Pile at Pier 33: (a) Solid Section EDC; (b) Voided Section EDC

2.2.4 Pier 59

The test pile at pier 59 was a voided pile with sets of EDC placed at the top of the pile in the solid section, on either side of the void and two sets at the tip of the pile at 5 feet and 2.5 feet from the tip (Figure 2.1). The pile was driven on 4/22/14 to a final tip elevation of -106.1 feet, followed by restrikes 1.5 hours after end of drive, and a static load test on 5/9/14. All phases of installation were done with an ICE I-100 hammer.

Figure 2.12 are the estimates of total capacity versus pile tip elevation using the Fixed Jc method and the UF method (dynamic Jc method). For the Fixed Jc method, AFT set Jc to be 0.5. The total capacity exceeds 1,500 kip at the final tip elevation (-106.1 feet).

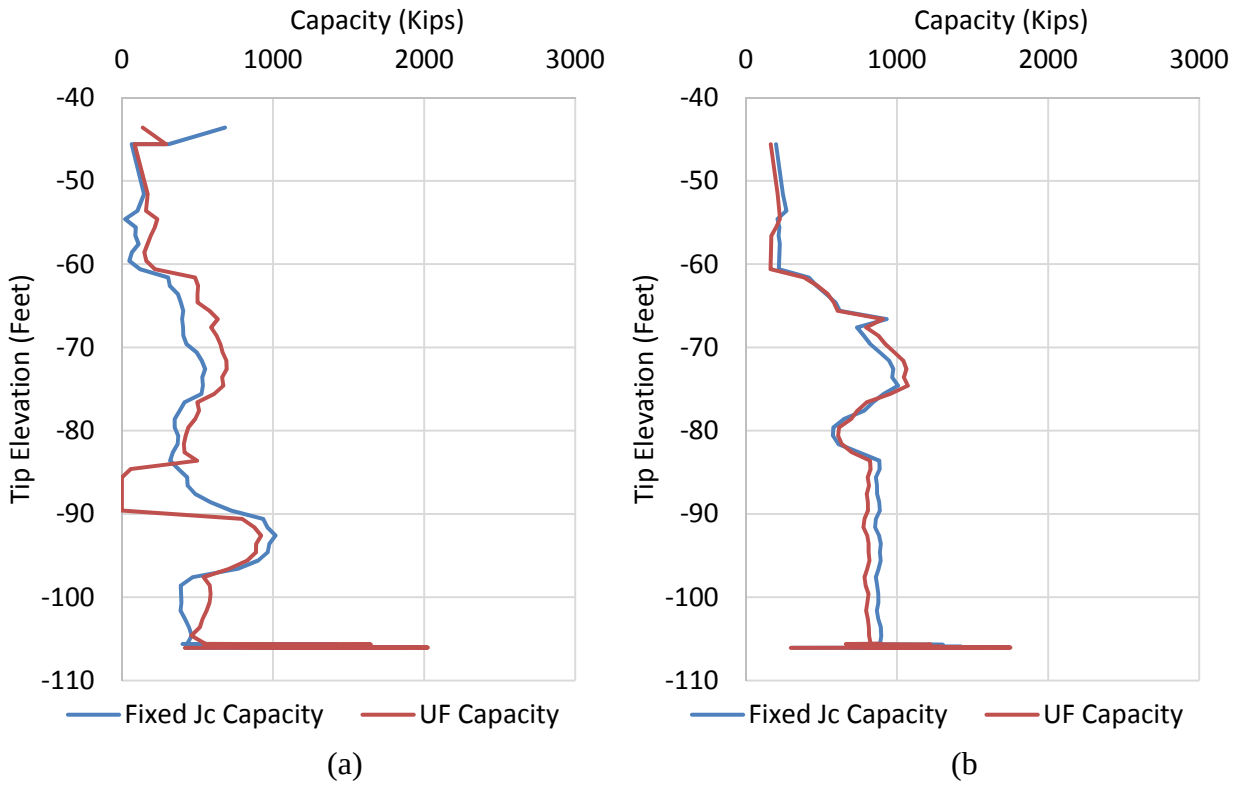

Figure 2.12 Total Capacity Versus Tip Elevation for Test Pile at Pier 59: (a) Solid Section EDC; (b) Voided Section EDC

Figure 2.13 shows the blow count record and Figure 2.14 shows the top and tip preload delta (change in pile pre-load stress) and MPI versus pile tip elevation. The use of EDC in the solid section and the voided section of the pile provide MPI at three locations (Figure 2.1). Figures 2.14 (a) and (b) show that the change in pre-load stress does not exceed 50 με and the MPI does not indicate a pile integrity issue.

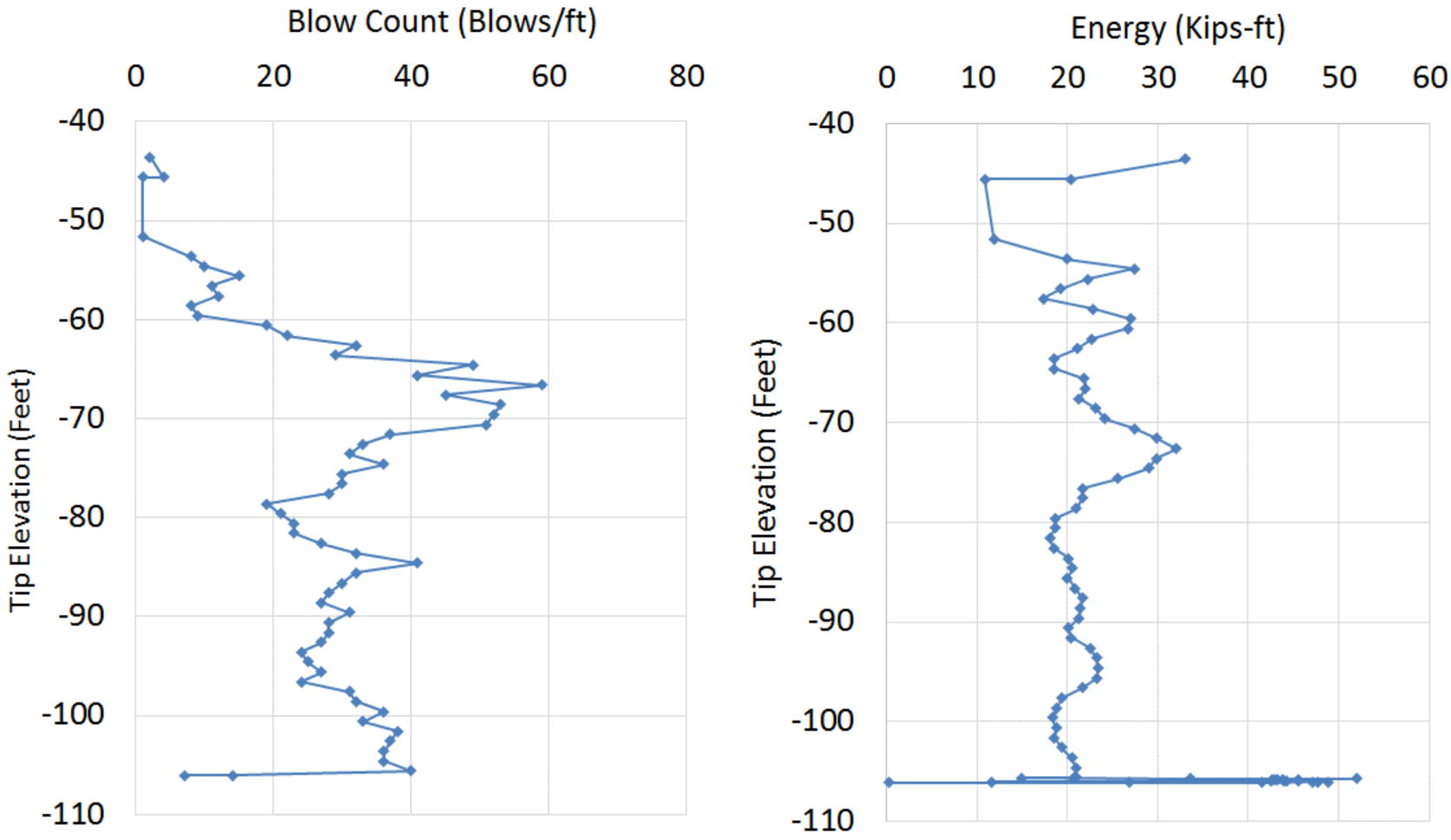

Figure 2.13 Record of Blow Counts and Energy During Driving of Test Pile at Pier 59

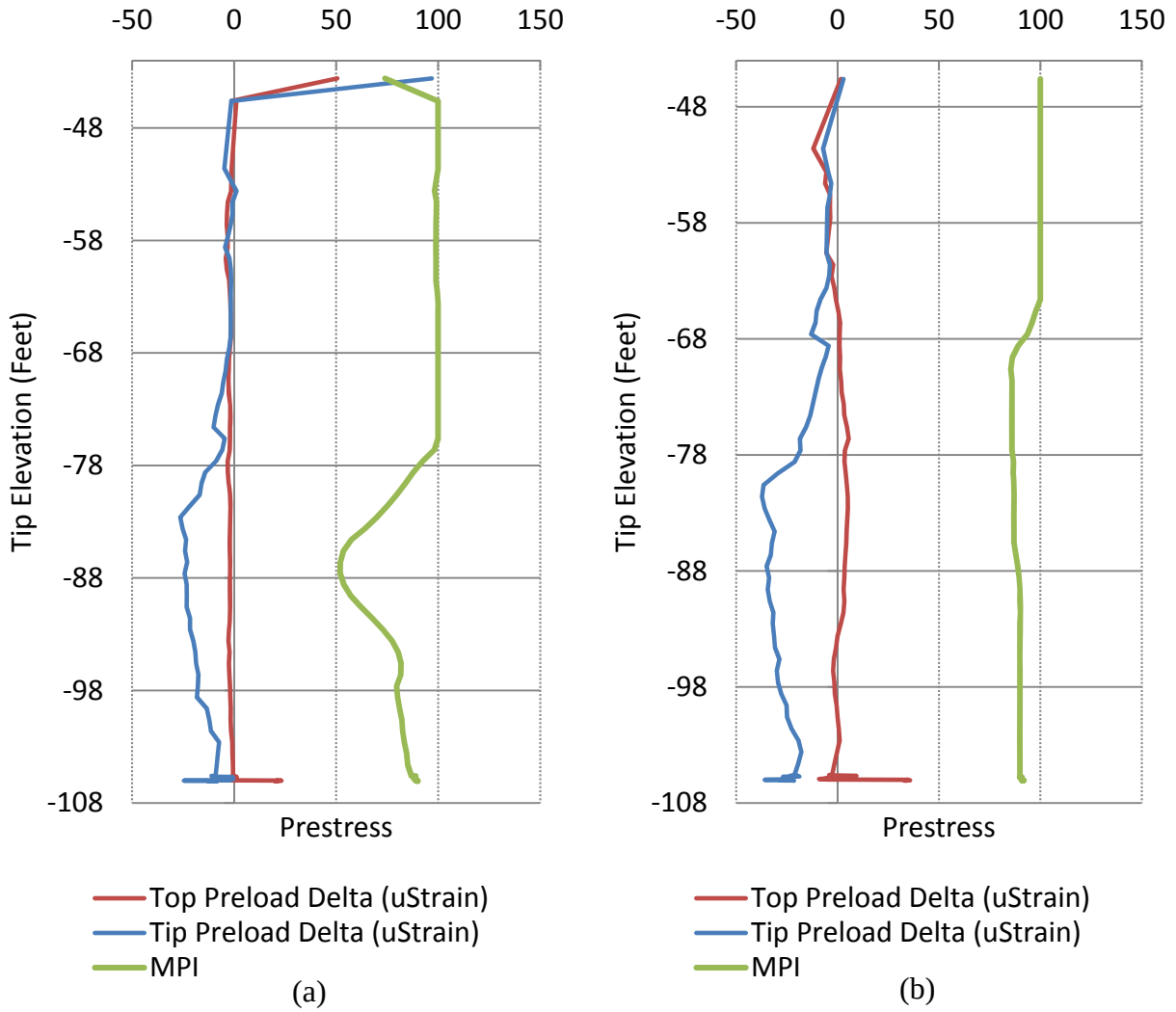

Figure 2.14 Top and Tip Preload Delta and MPI for Test Pile at Pier 59: (a) Solid Section EDC; (b) Voided Section EDC

2.2.5 Pier 84

The test pile at pier 84 was a voided pile with sets of EDC placed at the top of the pile in the solid section, on either side of the void and two sets at the tip of the pile at 5 feet and 2.5 feet from the tip (Figure 2.1). The pile was driven on 4 different days (5/7/14, 5/9/14, 5/13/14 and 5/15/14). The pile was initially driven to a tip elevation of -85.5 feet on 5/7/14, then driven to a tip elevation of -95.75 feet on 5/9/14, then driven to a tip elevation of -104.7 feet on 5/13/14 and finally driven to a tip elevation of -115.2 feet on 5/15/14. Restrikes were performed at the

beginning of each drive phase and 32 minutes after the final driving on 5/15/14. The static load test was performed on 5/19/14. All phases of installation were done with an ICE I-100 hammer.

Figure 2.15 are the estimates of total capacity versus pile tip elevation using the Fixed Jc method and the UF method (dynamic Jc method). For the Fixed Jc method, AFT set Jc to be 0.5. The total capacity exceeds 1,200 kip at the final tip elevation (-106.1 feet).

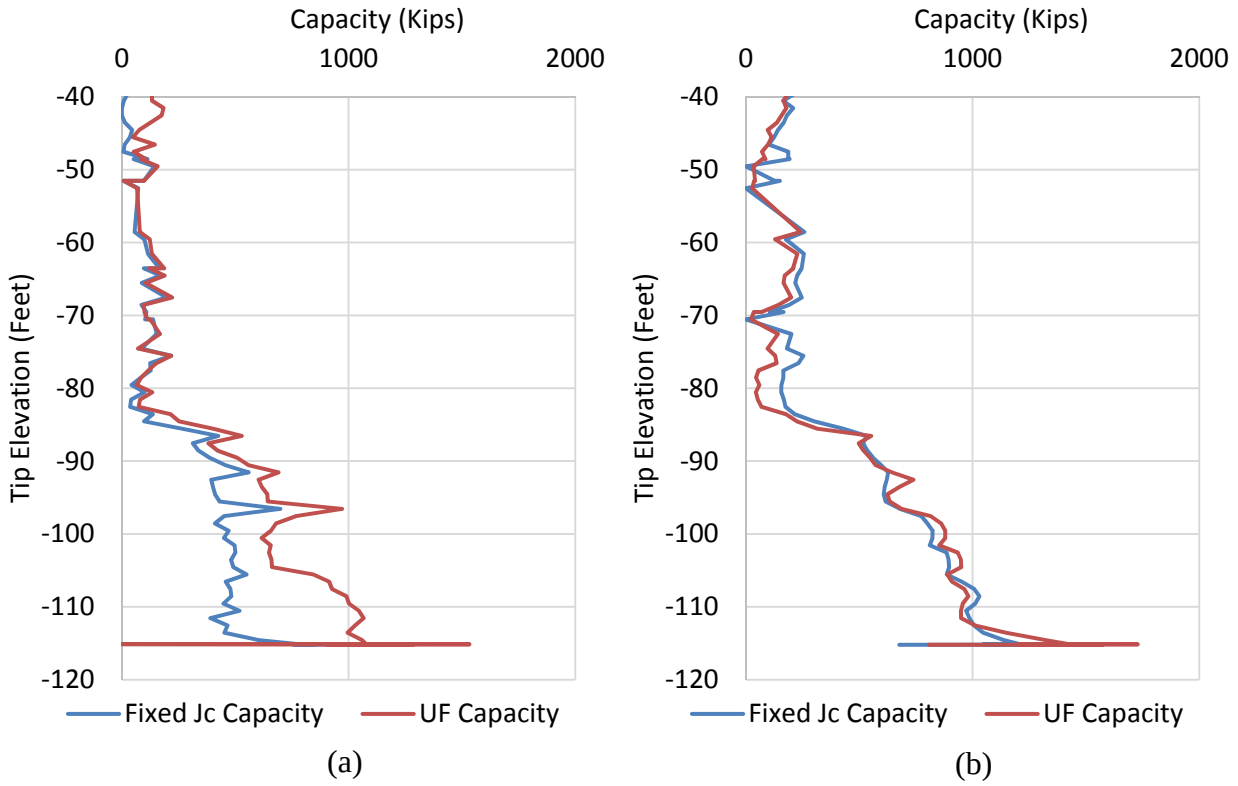

Figure 2.15 Total Capacity Versus Tip Elevation for Test Pile at Pier 84: (a) Solid Section EDC; (b) Voided Section EDC

Figure 2.16 shows the blow count record and Figure 2.17 shows the top and tip preload delta (change in pile pre-load stress) and MPI versus pile tip elevation. The use of EDC in the solid section and the voided section of the pile provide MPI at three locations (Figure 2.1). Figures 2.17 (a) and (b) show that the change in pre-load stress does not exceed 50 με and the MPI does not indicate a pile integrity issue.

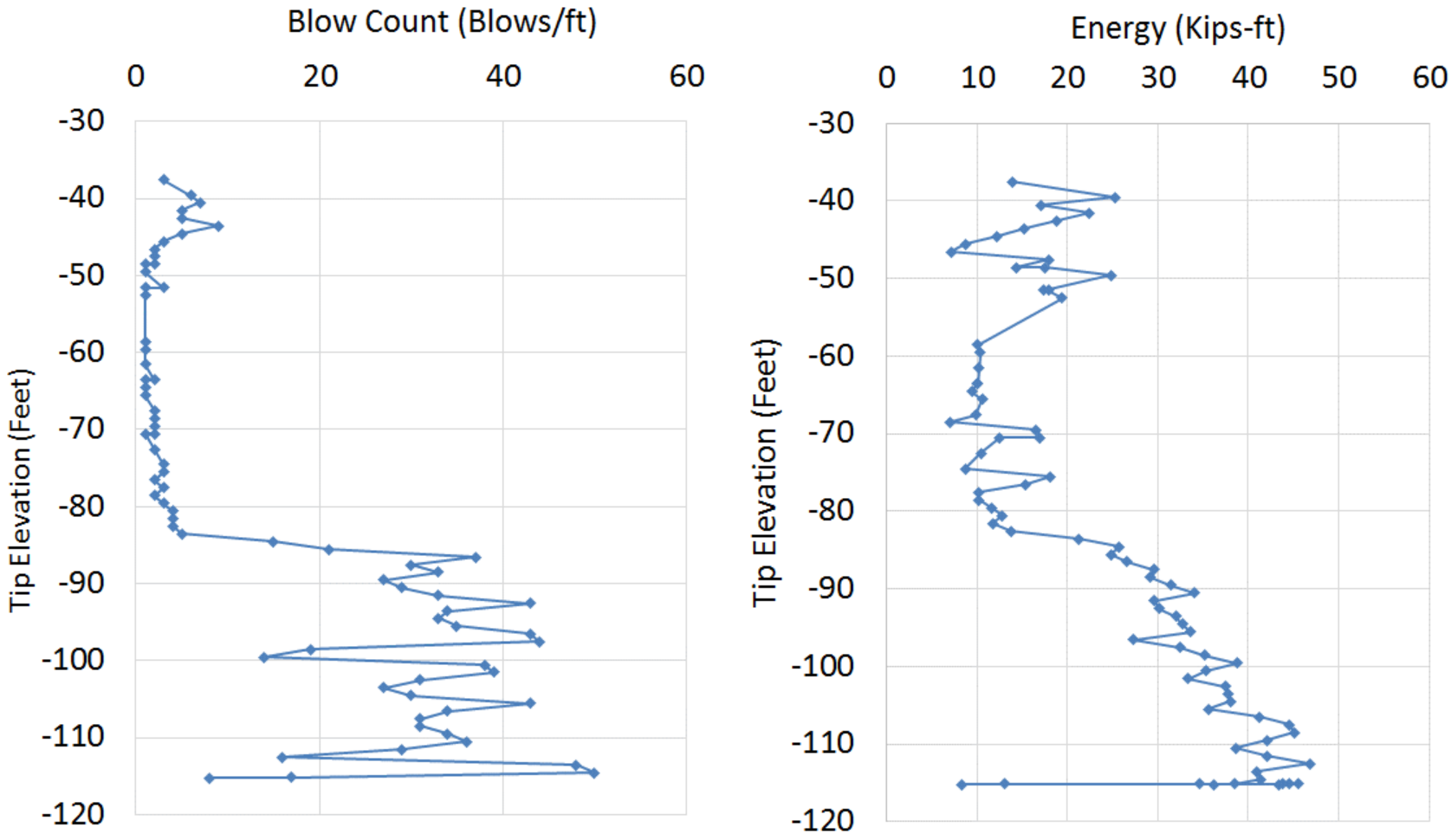

Figure 2.16 Record of Blow Counts and Energy During Driving of Test Pile at Pier 84

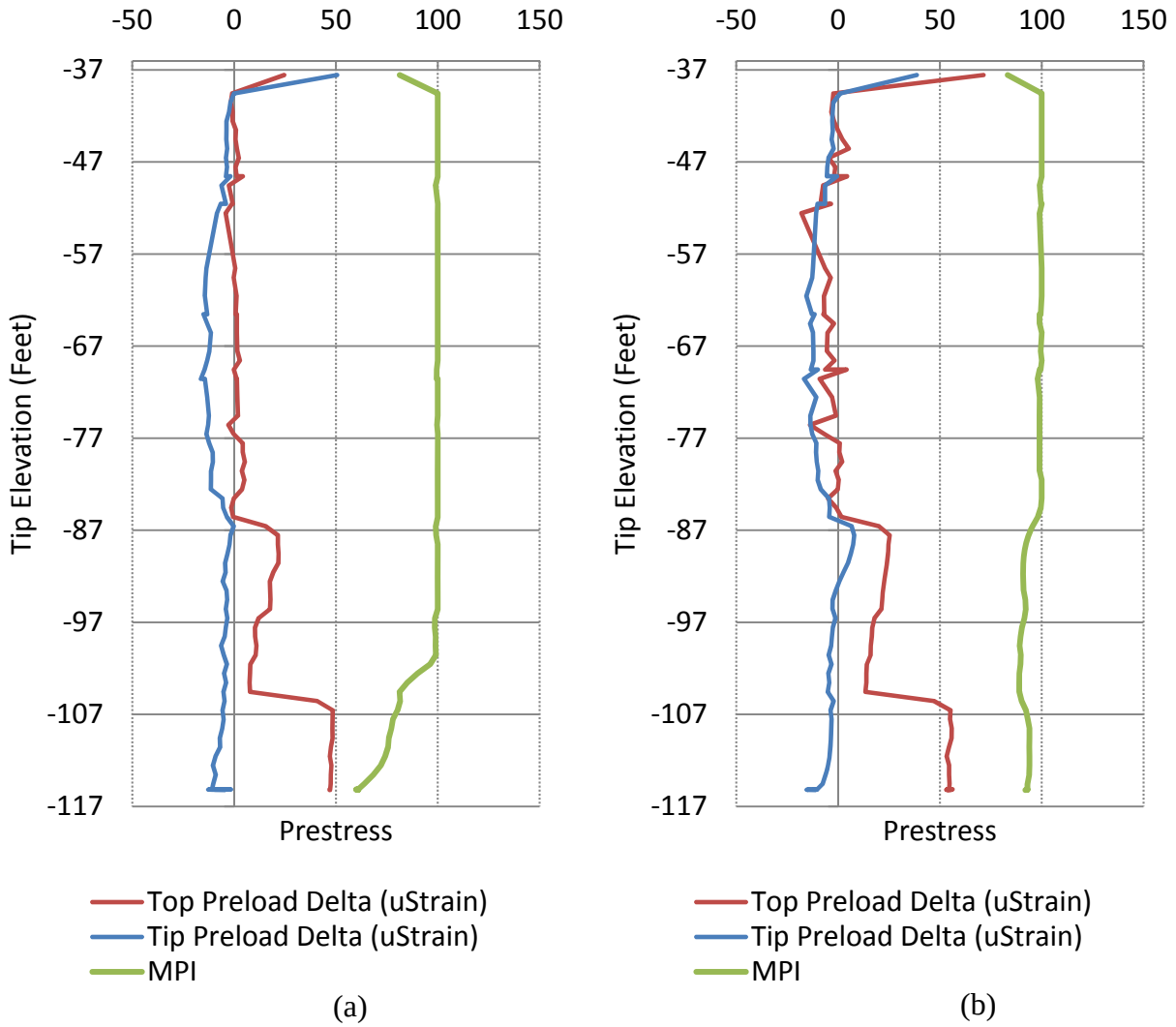

Figure 2.17 Top and Tip Preload Delta and MPI for Test Pile at Pier 84 (a) Solid Section EDC (b) Voided Section EDC

CHAPTER 3
PREDICTIONS OF EDC-MONITORED PILES AND STATIC LOAD TESTS

3.1 Introduction

As part of this research project, the static load tests of the five test piles were monitored by the consultant (AFT). AFT provided to the researchers both Fixed Jc, as well as UF Method predictions for total, tip, and side resistances for each pile based on their analysis using SmartPile Review. The project's geotechnical consultant (Florida Geotechnical Engineering Inc, [FGE], Tampa, FL) also monitored the tests piles with PDA and provided to the contractor CAPWAP results.

Dr. Khiem Tran (Clarkson University) analyzed the SmartPile Review data (strain and velocity) for all five test piles at End of Drive (EOD) as well as the final set of Restrike blows (BOR) prior to load testing to estimate independent skin and tip resistance as well as total (skin + tip) using the Tran et al. methods. His results were received by the researchers prior to the static load results.

Unfortunately, each of the test piles was cut-off by the contractor, with no provision made to splice the wiring. Only, the load versus displacement at the top of each pile was monitored by the project's geotechnical consultant (FGE), in order to assess nominal resistance. The nominal resistance was assessed from Davisson capacity from the load deformation response of the tested piles. For piles which did not reach failure, resistance at similar displacements was compared. To estimate measured skin and tip resistance of the piles which reached failure, DeBeer's log-log procedure was used.

The static load test results were subsequently compared for all EDC methods: Fixed J_c Method; UF Method; and the methods of Tran et al. (2012A and 2012B). Results are presented in tabular form for each test pile.

3.2 US-331 over Choctawhatchee Bay

3.2.1 Pier 13

The test pile at pier 13 was a solid pile, and its initial drive was on 2/24/14, followed by a restrike on 2/27/14, and a static load test on 4/6/14. On the initial drive, the pile was driven to a tip elevation of -125 feet, then 23 feet of the top of the pile was cut-off in order to fit the equipment for the static load test. As a result, the wire leads to the EDC were also cut-off, making them inaccessible during the static load test. Furthermore, SKANSKA (driving contractor) drove the pile an additional 8.8 feet deeper to the proposed cut-off elevation of +3.2 feet after the static load test. Table 3.1 summarizes the nominal resistance estimates using dynamic methods and static load test (SLT) results.

Figure 3.1 shows the observed and estimated (from inversion process) particle velocities at the top and bottom of the test pile. Agreement between the estimated and observed data is evident, with most of the dominant components well matched. Figure 3.2 shows the final mobilized skin friction as a function of displacement for 5 blows at BOR. The blows estimate ultimate skin frictions from 350 kip (blow 681) to 435 kip (blow 681).

Figure 3.3 shows the total energy arriving at the pile tip, as well as the predicted components due to inertia, damping, and static resistance. The quality of the energy balance can be assessed through the error shown in Figure 3.3, which is the difference between the measured total energy and the sum of the predicted components. Evident from Figure 3.3, energy error is near zero. Figure 3.4 shows the individual forces (i.e., inertia, damping, static) and their sum versus the measured total force with time. The estimated and measured total force match well at

the time near the maximum static force (200 kip at 0.05 sec), which also shows the inertia to be negligible and the damping to be zero (i.e., total force = static force component). Figure 3.5 shows the estimated static force, damping force, total force, and measured total force versus the pile tip displacement.

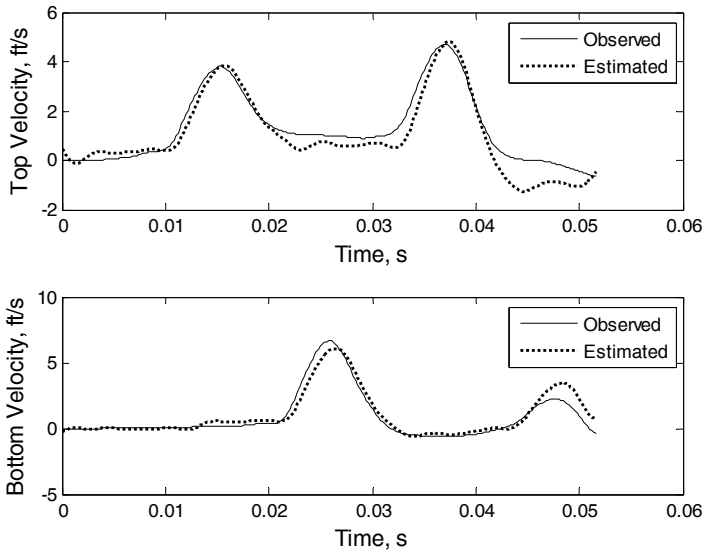

Figure 3.1 Pier 13: Comparison of the Observed and Estimated Velocities at the Top and Bottom of the Pile for Blow 688

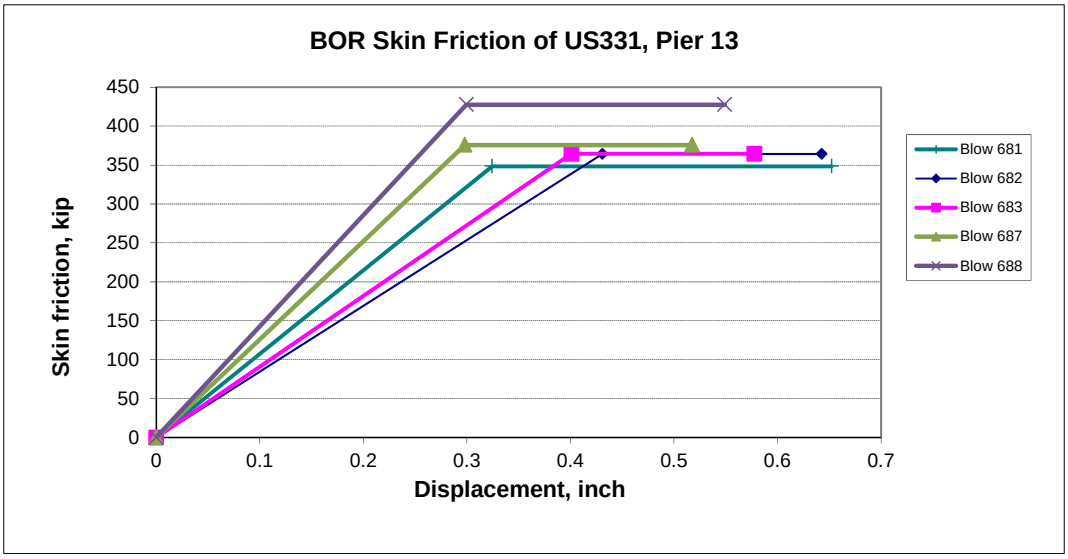

Figure 3.2 Pier 13: Skin Friction Estimates from Blows 681-683, 687, and 688

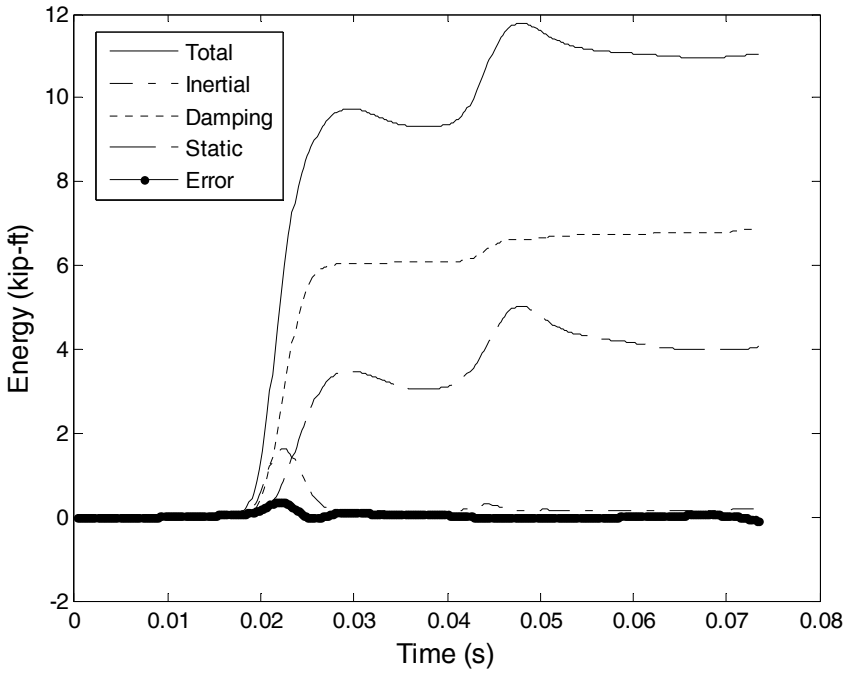

Figure 3.3 Pier 13: Energy Balancing

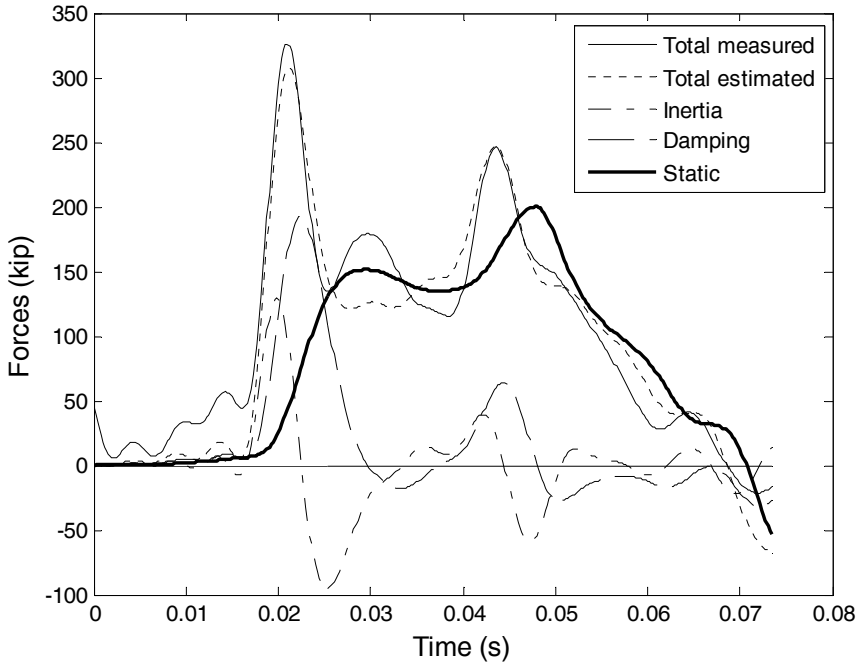

Figure 3.4 Pier 13: Forces in the Time Domain

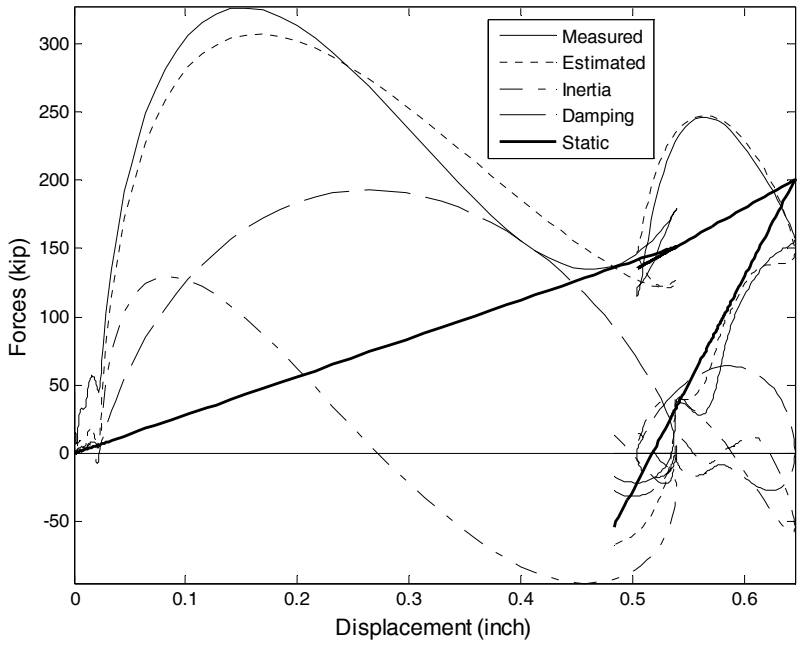

Figure 3.5 Pier 13: Forces Versus Displacement

Figure 3.6 shows the load displacement measured at the top of the pile from the static load test. Evident is that the pile begins to plunge at 1500 kip and the load is removed after a displacement of about 0.2 inches. The test pile did not reach the Davisson failure criteria shown in Figure 3.6 with a solid black line.

Table 3.2 are the Fixed J_c (total only), UF, and Tran et al. method estimates of total, skin and tip capacity for the test pile at pier 13. The tip capacity estimates are taken at the EOD and the skin capacity estimates are taken at the BOR. The estimate of total capacity is based on the Fixed J_c method, which was taken at the BOR. The estimates from the methods compare favorably well; however, the estimated total capacities don't agree with the measured from the static load test. The static load test was performed on 4/6/14, 38 days after the restrike and there were only 3 days between EOID and BOR. As a result, all methods (Fixed J_c, UF, and Tran et al.) predicted only 50% of the measured because enough time had not elapsed to capture the pile freeze.

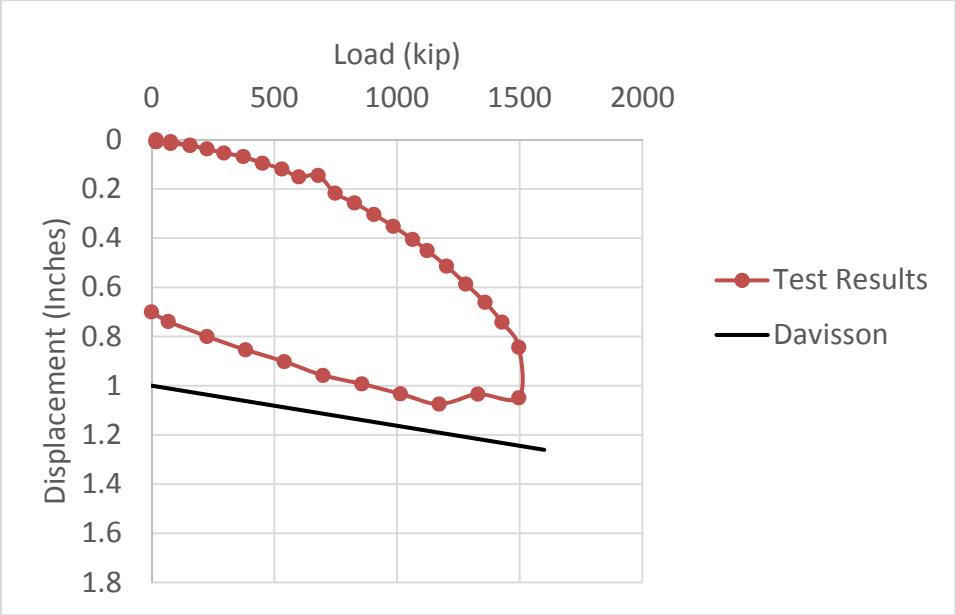

Figure 3.6 Pier 13: Load Displacement Curve from Static Load Test on Test Pile

Table 3.1 Pier 13:Summary of Nominal Pile Resistance

Date	Driving Condition	Nominal Pile Resistance Estimates (kip)		
		Fixed	UF	Tran et al.
2/24/14	EOID	289	288	NA
2/27/14	BOR - 1	593	601	NA
4/6/14	SLT**	1500		

** Pile displacement did not reach Davisson criteria

Table 3.2 Pier 13: Estimated Nominal, Side and Tip Pile Resistance Using EDC Measurements and Measured Total Capacity from Static Load Test

Fixed Method	UF Method			Tran et al. Method			Load Test
Total Capacity (kip)	Total Capacity (kip)	Skin Capacity (kip)	Tip Capacity (kip)	Total Capacity (kip)	Skin Capacity (kip)	Tip Capacity (kip)	Total Capacity (kip)
593	548	414	134	625	425	200	1500

3.2.2 Pier 25

The test pile at pier 25 was a voided pile with sets of EDC placed at the top of the pile in the solid section, on either side of the void and two sets at the tip of the pile, 5 feet, and 2.5 feet from the tip (Figure 2.1). The pile was initially driven on 3/12/14, and restrikes were performed on 3/20/14 and 3/24/14; however, AFT was not notified prior to the restrike on 3/24/14, so data for the second restrike was not collected. The pile was then driven an additional 10 feet on 3/26/14 (EOID) to a tip elevation of -125 feet, followed by a restrike on 4/1/14 (BOR3), and the static load test on 4/22/14. Note, the AFT had issues reading the EDC for the solid section gauges for phases of the installation, and the blow numbers are not number the same. The comparisons are for the same blow as verified by the date and time stamp. Table 3.3 summarizes the nominal resistance estimates using dynamic methods and static load test (SLT) results.

Figure 3.7 shows the observed and estimated (from inversion process) particle velocities at the top and bottom of the test pile at BOR3 (blow 976). Agreement between the estimated and observed data is evident, with the dominant components well matched. Figure 3.8 shows the final mobilized skin friction as a function of displacement, both total skin friction and the skin friction on the segments. Figure 3.9 shows the observed and estimated particle velocities at the top and bottom of the test pile based on the gauges in the voided section (Figure 2.1) for BOR3 (blow 2242). Figure 3.10 shows the final mobilized skin friction as a function of pile displacement, both total skin friction and the estimated skin friction on the segments. The blows estimate ultimate skin friction of about 1250 kip from the solid section gauges and 1170 kip form the voided section gauges.

Figure 3.11 shows the total energy arriving at the pile tip, as well as the predicted components due to inertia, damping, and static resistance, for blow 967. The quality of the energy balance can be assessed through the error shown in Figure 3.11, which is the difference

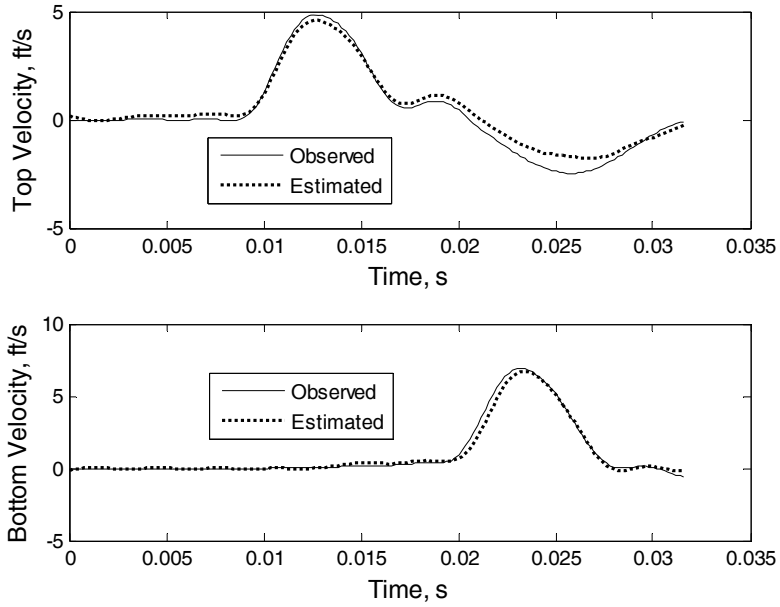

Figure 3.7 Pier 25: Comparison of Particle Velocity for BOR3 (Blow 976) From Solid Section Gauges

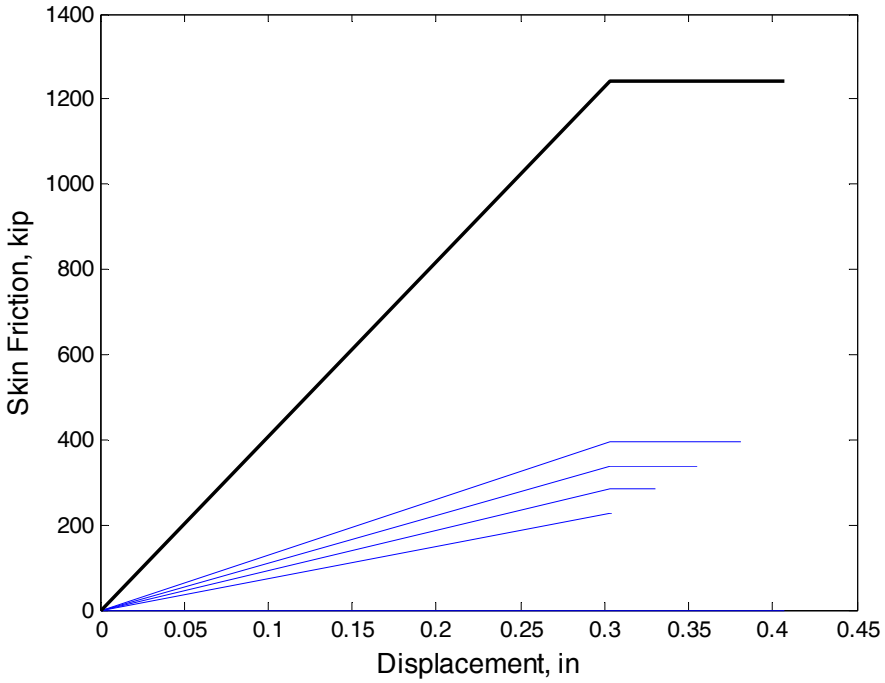

Figure 3.8 Pier 25: Estimated Skin Friction for BOR3 (Blow 976) From Solid Section Gauges (bold line = total, thin lines = segments)

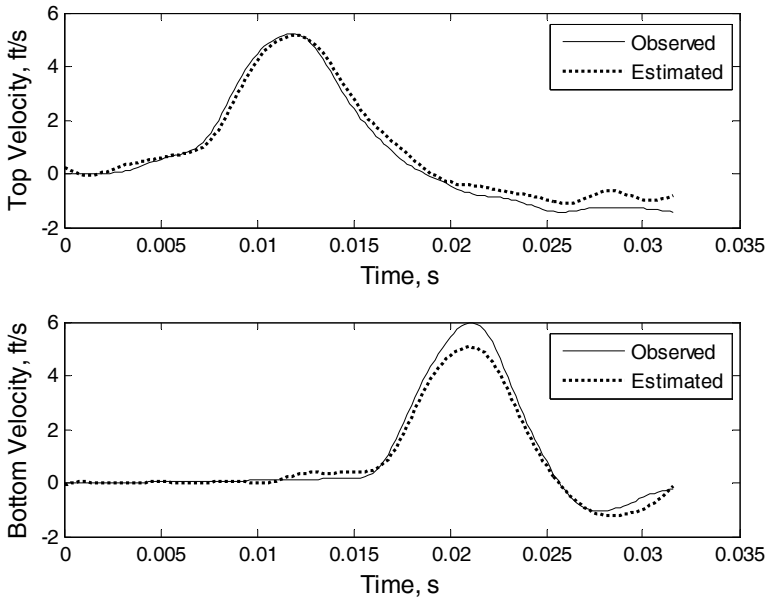

Figure 3.9 Pier 25: Comparison of Particle Velocity for BOR3 (Blow 2242) From Voided Section Gauges

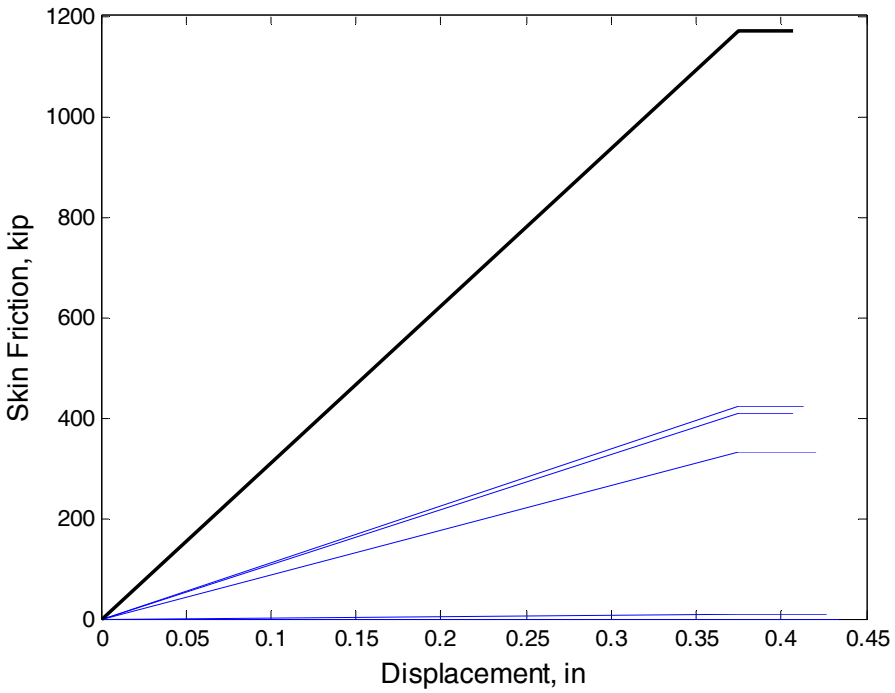

Figure 3.10 Pier 25: Estimated Skin Friction for BOR3 (Blow 2242) Voided Section Gauges (bold line = total, thin lines = segments)

between the measured total energy and the sum of the predicted components. Evident in Figure 3.11, there is a very good energy balance with near zero error. Figure 3.12 shows the individual

forces (i.e., inertia, damping, static) and their sum versus the measured total force with time. The estimated and measured total force match well at the time near the maximum static force (200 kip at 0.06 sec), which is also when the damping and inertia are zero (i.e., static force = total force). Figure 3.13 shows the estimated static force, damping force, total force, and measured total force versus the pile tip displacement.

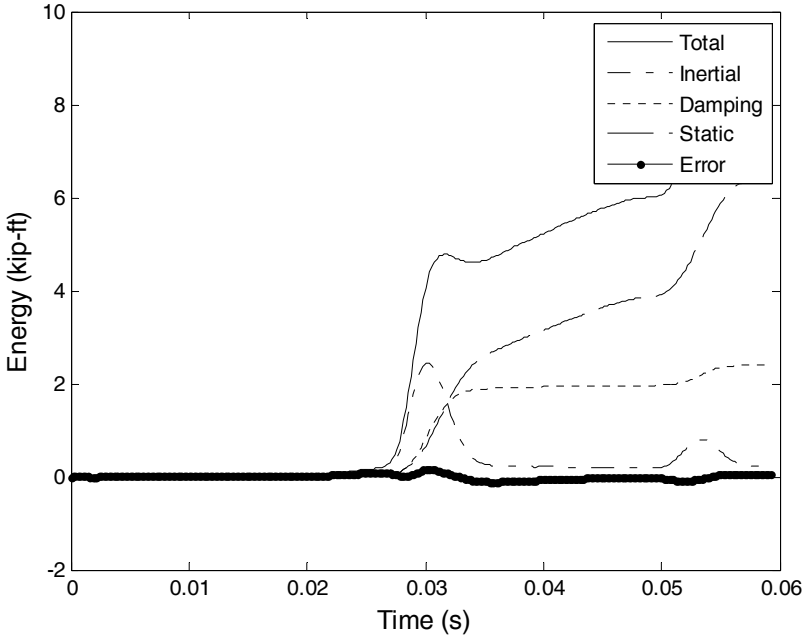

Figure 3.11 Pier 25: Energy Balancing (Blow 967)

Figure 3.14 shows the measured load displacement from the static load test plotted against the Davisson line. Evident is that the pile plunges at 1500 kip and reaches the Davisson movement at 1.4 inches. Of interest, for comparison to the estimated skin and tip capacities using the Tran et al. methods, are measured skin and tip capacities. Since the pile top was cut-off and there wasn't access to the strain gauges, an estimate of the measured skin and tip capacities was made based on the log-log plot of the load-displacement. A change in the slope of the log-log load-displacement indicates the mobilization of the skin friction. Figure 3.15 shows the log-log load-displacement with the skin friction (1220 kip) identified by the intersection of

the tangent lines. Subtracting this from the total capacity (1500 kip) gives a tip capacity of 280 kip.

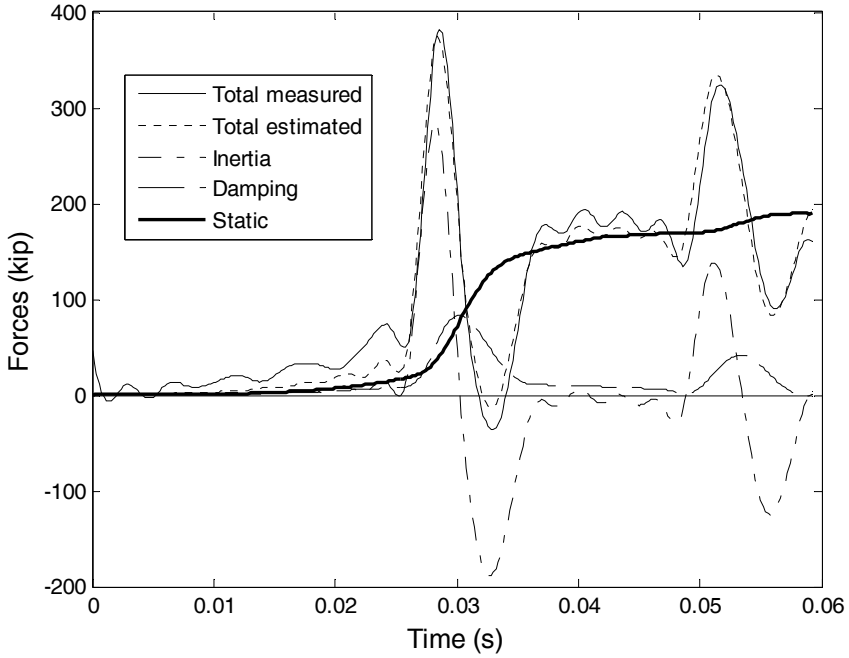

Figure 3.12 Pier 25: Forces in the Time Domain (Blow 967)

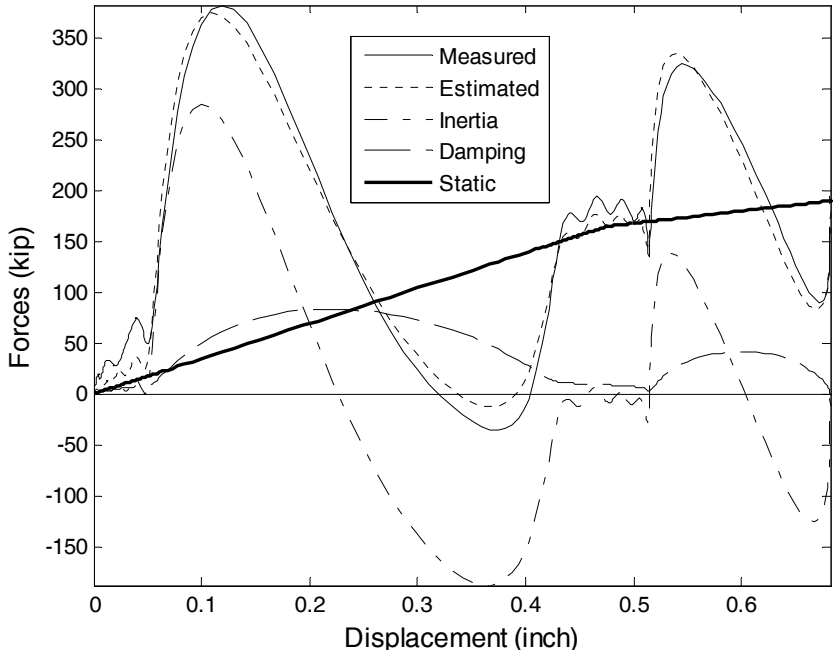

Figure 3.13 Pier 25: Forces Versus Displacement (Blow 967)

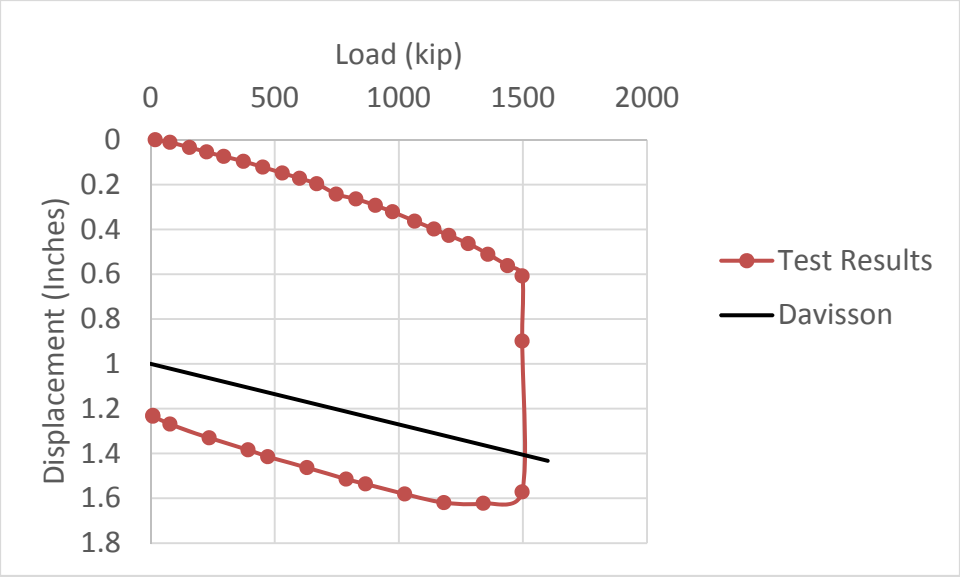

Figure 3.14 Pier 25: Load Displacement Curve From Static Load Test

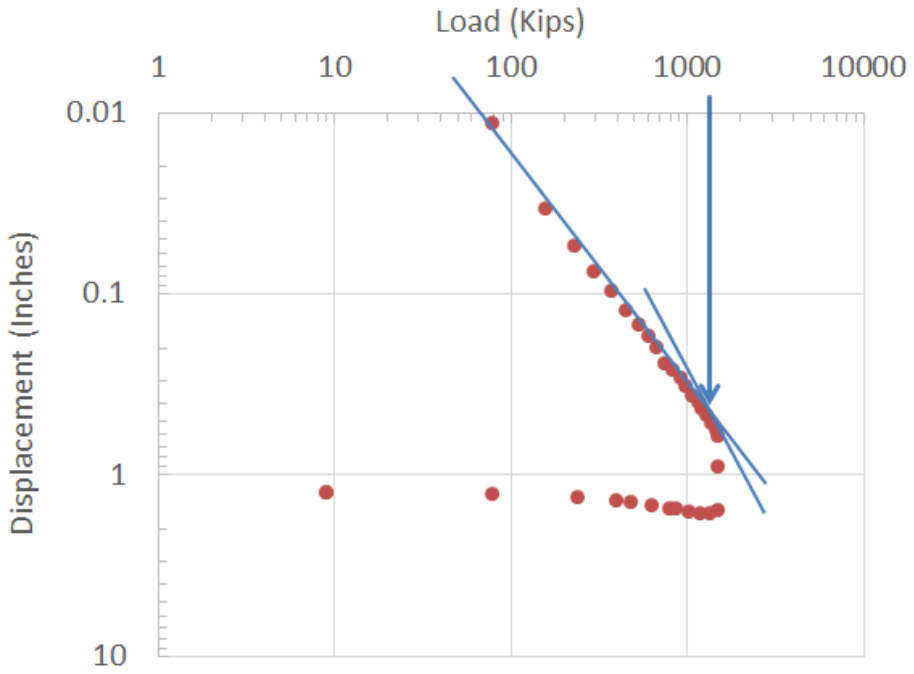

Figure 3.15 Pier 25: Log-Log Plot of Load Displacement Curve From Static Load Test

Table 3.3 are the nominal (total) resistances estimates using dynamic methods (Fixed J_c and UF methods), at EOID and BOR, and the static load test (SLT) results. The EOID-2 and BOR-3 are the only phases of install included in Table 3.3 since the pile was driven an additional

ten feet after the EOID-1 and the second BOR (BOR-2), which was before the EOID-2, was not recorded. Note, the estimates of the skin and tip resistances at both the EOID and BOR were not determined using the Tran et al. method, and therefore, the nominal (total) resistance is not available.

Table 3.3 Pier 25: Summary of Nominal Pile Resistance

Date	Driving Condition	Nominal Pile Resistance Estimates (kip)		
		Fixed	UF	Tran et al.
3/26/14	EOID - 2	NA (solid) 347 (void)	NA (solid) 365 (void)	NA
4/1/14	BOR - 3	1602 (solid) 851 (void)	1638 (solid) 1116 (void)	NA
4/22/14	SLT*	1500		

*Pile displacement reached Davisson criteria

In Table 3.4 are the estimates of total, skin and tip capacity and the total capacity measured from the static load test for the test pile at pier 13. Estimates from SmartPile Review (Fixed J_c (total only) and UF methods) are compared to the estimates using the Tran et al. methods. The tip capacity estimates are from the EOID and the skin capacity estimates are from the BOR3 records on the pile. The total capacity estimate based on the Fixed J_c method is from the BOR3.

Table 3.4 Pier 25: Estimated Nominal, Side and Tip Pile Resistance Using EDC Measurements and Measured Total Capacity from Static Load Test

Pile Gauge Locations	Fixed Method	UF Method			Tran et al. Method			Load Test		
	Total (kip)	Total (kip)	Skin (kip)	Tip (kip)	Total (kip)	Skin (kip)	Tip (kip)	Total (kip)	Skin (kip)	Tip (kip)
Top and Tip Gauges	1667	1726	1471	255	1450	1250	200	1500	1220	280
Voided Section and Tip Gauges	1008	1151	996	155	1370	1170	200			

3.2.3 Pier 33

The test pile at pier 33 was a voided pile with sets of EDC placed at the top of the pile in the solid section, on either side of the void and two sets at the tip of the pile at 5 feet and 2.5 feet from the tip (Figure 2.1). The pile was initially driven to a final tip elevation of -129.8 feet on 3/26/14 (EOID) and a restrike were performed on 4/1/14 (BOR1). All phases of installation were done with an ICE I-100 hammer. Note, the AFT had issues reading the EDC for the solid section gauges for phases of the installation and the blow numbers are not number the same. The comparisons are for the same blow as verified by the date and time stamp. Table 3.5 summarizes the nominal resistance estimates using dynamic methods and static load test (SLT) results.

Figure 3.16 shows the observed and estimated (from inversion process) particle velocities at the top and bottom of the test pile for BOR1. These are from the gauges in the solid section of the top and bottom of the pile (Figure 2.1). Agreement between the estimated and observed data is evident, with most of the dominant components well matched. Figure 3.17 shows the final mobilized skin friction as a function of displacement, both total skin friction and the skin friction

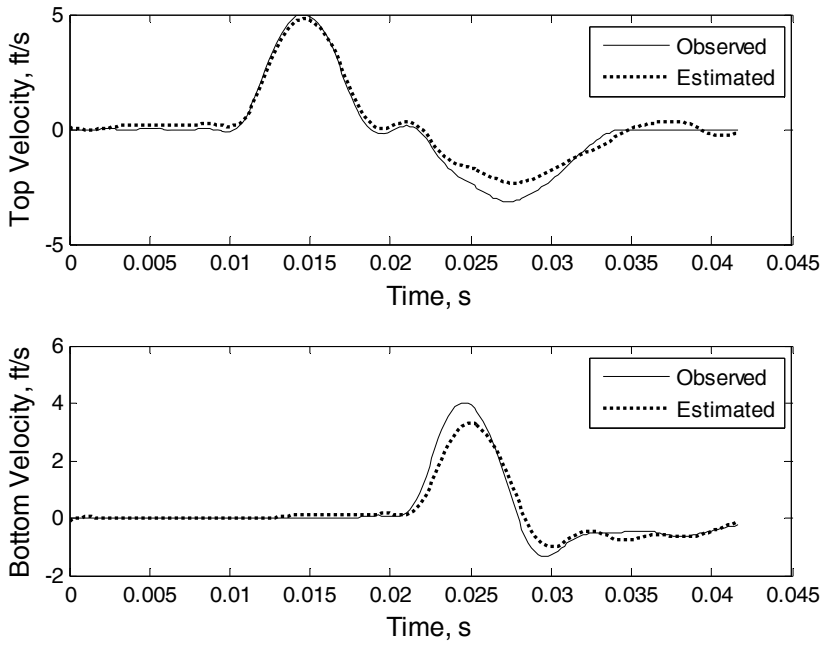

Figure 3.16 Pier 33: Comparison of Particle Velocity for BOR1 From Solid Section Gauges (Blow 2142)

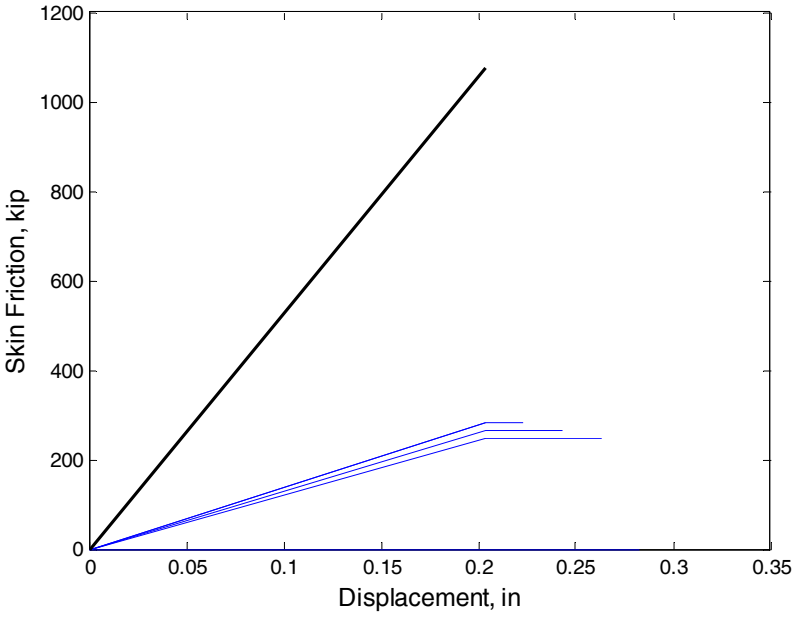

Figure 3.17 Pier 33: Estimated Skin Friction for BOR1 (Blow 2142) Solid Section Gauges (bold line = total, thin lines = segments)

on the segments. Figure 3.18 shows the observed and estimated particle velocities at the top and bottom of the test pile based on the gauges in the voided section (Figure 2.1). Figure 3.19 shows the final mobilized skin friction as a function of pile displacement, both total skin friction and the estimated skin friction on the segments. The blows estimate ultimate skin friction of about 1080 kip from the solid section gauges and 980 kip form the voided section gauges.

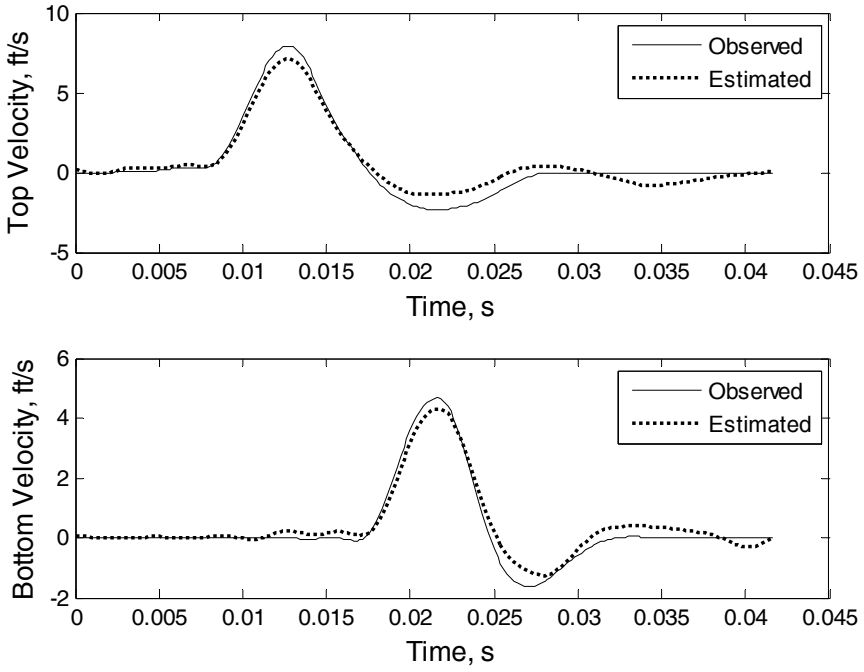

Figure 3.18 Pier 33: Comparison of Particle Velocity for BOR1 from Voided Section Gauges (Blow 2242)

Figure 3.20 shows the total energy arriving at the pile tip, as well as the predicted components due to inertia, damping, and static resistance, for blow 2141. The quality of the energy balance can be assessed through the error shown in Figure 3.20, which is the difference between the measured total energy and the sum of the predicted components. Evident in Figure 3.20 is a very good energy balance with near zero error. Figure 3.21 shows the individual forces (i.e., inertia, damping, static) and their sum versus the measured total force with time. The estimated and measured total force match well at the time near the maximum static force (330

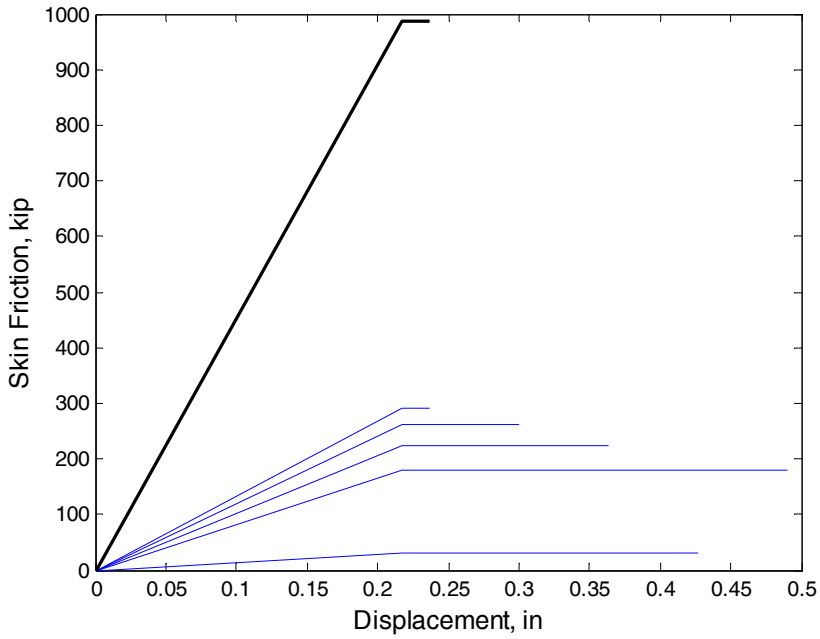

Figure 3.19 Pier 33: Estimated Skin Friction for BOR1 (Blow 2242) Voided Section Gauges (bold line = total, thin lines = segments)

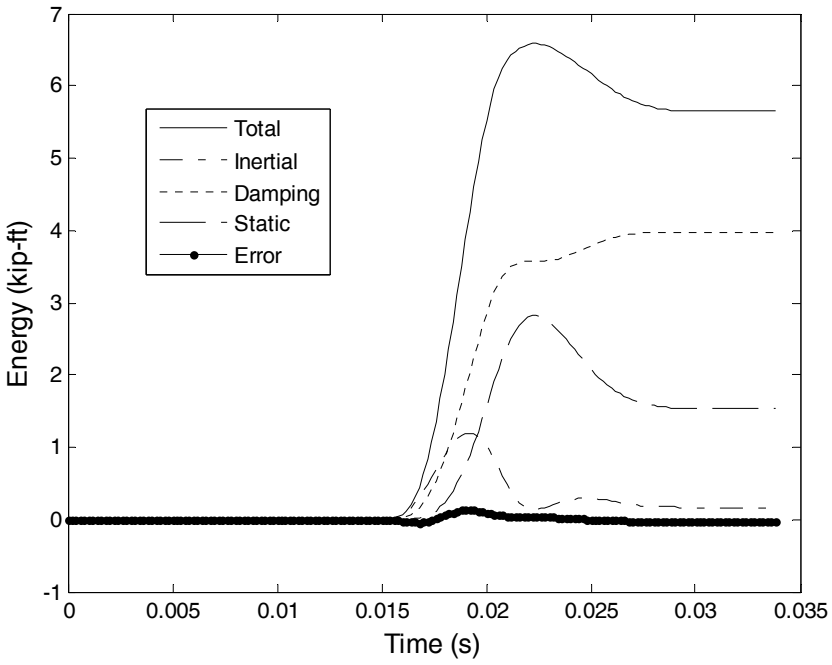

Figure 3.20 Pier 33: Energy Balancing (Blow 2141)

kip at 0.03 sec), which is also when the damping is zero (i.e., static force = total dynamic force – inertia force). Figure 3.22 shows the estimated static force, damping force, total force, and measured total force versus the pile tip displacement.

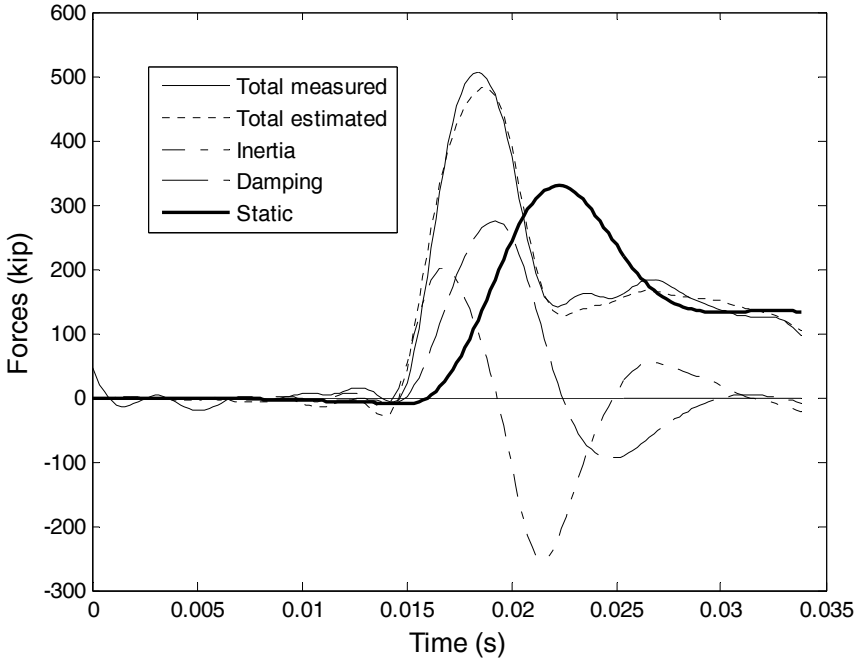

Figure 3.21 Pier 33: Forces in the Time Domain (Blow 2141)

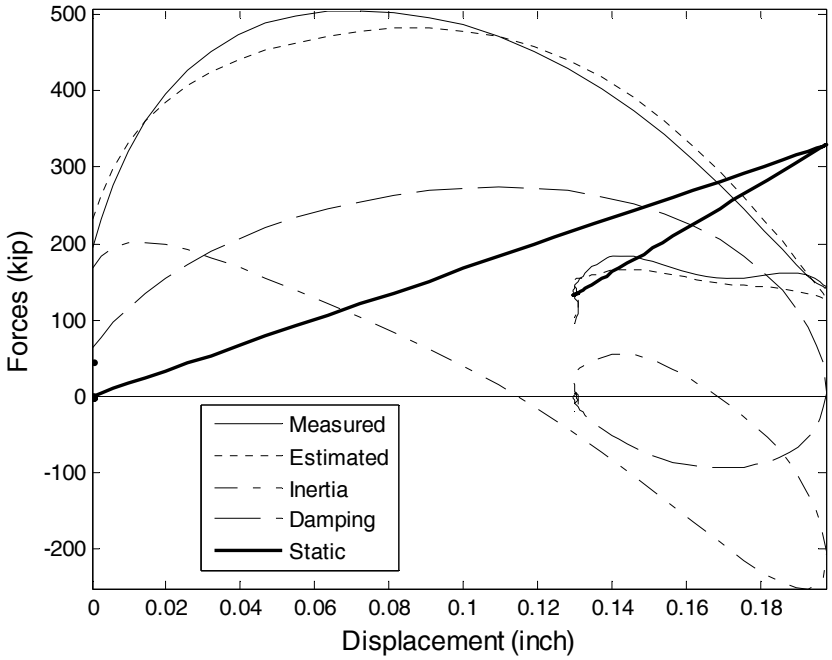

Figure 3.22 Pier 33: Forces Versus Displacement (Blow 2141)

Figure 3.23 shows the measured load displacement from the static load test plotted against the Davisson criteria line. The movement of the pile was only 0.4 inches (did not reach Davisson) and the maximum load applied of 1500 kip may not have been sufficient to mobilize the skin and tip resistances. From the log-log approach, there was no apparent change in slope of the load-displacement plot (also evident in Figure 3.23) and therefore, an estimate of the skin and tip resistance could not be made.

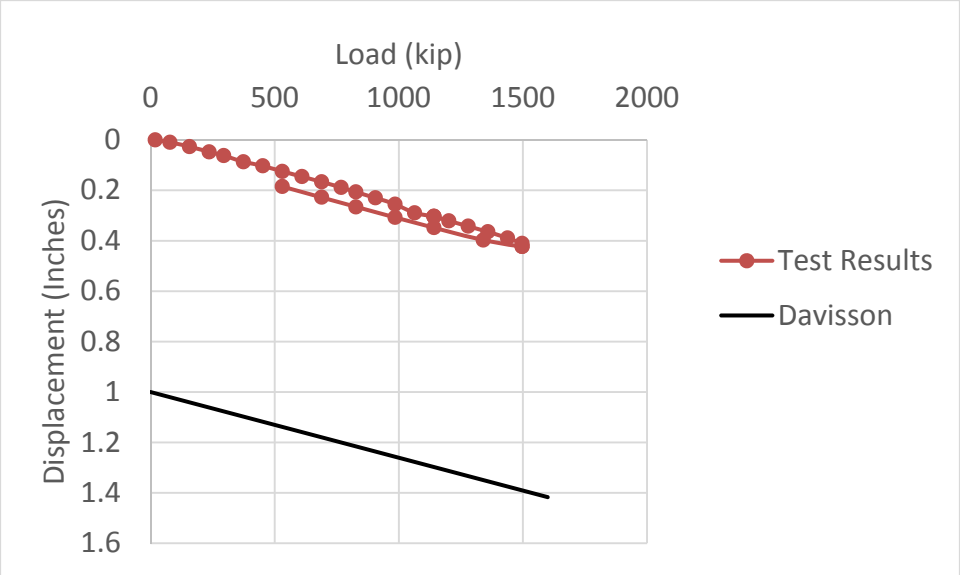

Figure 3.23 Pier 33: Load Displacement Curve from Static Load Test

The Pier 25 test pile is of very similar embedded length (125 feet) as the pile at Pier 33 (129 feet) and did exhibit plunging failure (Figure 3.14). The estimated side friction on the Pier 33 pile is similar to the Pier 25 pile (Solid section: 1080 kip versus 1250 kip, Voided section: 980 kip versus 1170 kip), however, the movement to mobilize side friction (i.e., t-z curve) is 0.22 in – Pier 33 (Figure 3.17) versus 0.35 in (Figure 3.10) – Pier 25. This would explain the smaller total movement of the Pier 33 test pile relative to the Pier 25 test pile. However, at 0.4 in of movement, both test piles exhibit full mobilization of side resistance (see Figures 3.15 and 3.19

report). It is believed that Pile 33 did not plunge due to available reserve tip resistance (Figure 3.23). It is believed that Pier 33 test pile's measured and predicted may be compared at 0.4 in of movement using a segmental approach. For instance, a simulated load test of the pile at Pier 33 was performed in FB-Multipier. The pile was modeled according to the specifications provided (cross section, length, etc.). For the soil models, the predicted skin friction (Tran et al., 2012B), Figure 3.17 and 3.19 were used for the t-z models and the predicted tip resistance (Tran et al., 2012A), Figure 3.20 was used for the Q-z model. Equal load steps were applied to the pile head until the applied load equaled that from the actual load test. Figure 3.24 shows the displacements of the first node in the pile plotted against the load for each step, for t-z and Q-z models (predictions) from the solid section and voided section assessments.

Also note, the Quick load test (ASTM 1143) was performed with the maximum load held for 1 hr. At the maximum applied load of 1500 kip there was about 0.012 in of movement. Considering all these observations and the similar total capacities of the other piles (1500 kip), at 0.4125 inch of movement the predicted resistances, Figure 3.24 were 1320 kip (solid section) and 1260 kip (voided section).

Table 3.5 are the nominal (total) resistances estimates using dynamic methods (Fixed J_c and UF methods), at EOID and BOR, and the static load test (SLT) results. Note, the estimates of the skin and tip resistances at both the EOID and BOR were not determined using the Tran et al. method, and therefore, the nominal (total) resistance is not available.

Table 3.6 are the estimates of total, skin and tip capacity and the total capacity measured from the static load test for the test pile at pier 33. Estimates from SmartPile Review (Fixed J_c (total only) and UF methods) are compared to the estimates from the Tran et al. methods. The

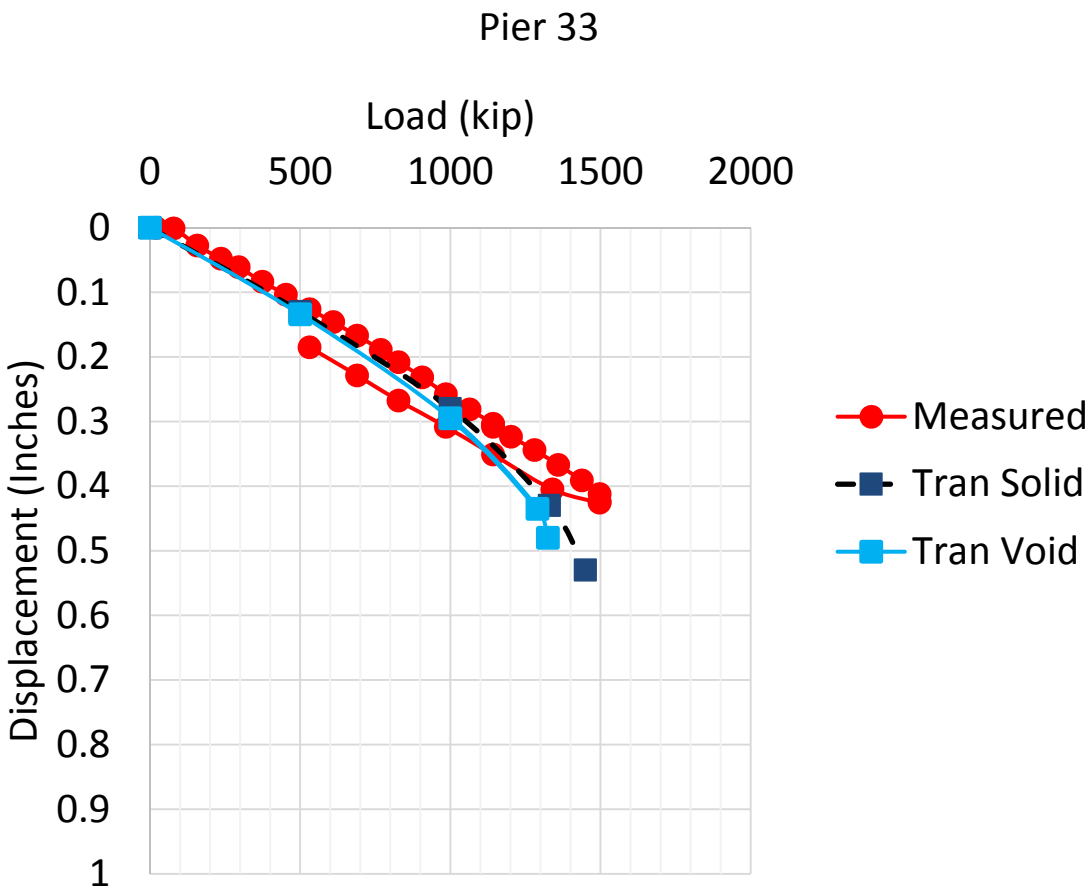

Figure 3.24 Pier 33: Measured and Simulated Load Displacement Curve

Table 3.5 Pier 33: Summary of Nominal Pile Resistance

Date	Driving Condition	Nominal Pile Resistance Estimates (kip)		
		Fixed	UF	Tran et al.
3/26/14	EOID	415 (solid) 542 (void)	557 (solid) 556 (void)	NA
4/1/14	BOR - 1	1816 (solid) 1335 (void)	1466 (solid) 1122 (void)	NA
5/3/14	SLT**	1500		

** Pile displacement did not reach Davisson criteria

tip capacity estimates are from the EOID and the skin capacity estimates are from the BOR records on the pile. The total capacity estimate based on the Fixed Jc method is from the BOR.

Table 3.6 Pier 33: Estimated Nominal, Side and Tip Pile Resistance Using EDC Measurements and Measured Total Capacity from Static Load Test

Pile Gauge Locations	Fixed Method	UF Method			Tran et al. Method			Load Test
	Total (kip)	Total (kip)	Skin (kip)	Tip (kip)	Total (kip)	Skin (kip)	Tip (kip)	Total (kip)
Top and Tip Gauges	1816	1466	1308	158	1320* 1410**	1080	330	1500
Voided Section and Tip Gauges	1335	1122	1026	96	1260* 1320**	990	330	

*Total resistance based on maximum displacement (FB-Multipier analysis)
**Total resistance = skin resistance + tip resistance

3.2.4 Pier 59

The test pile at pier 59 was a voided pile with sets of EDC placed at the top of the pile in the solid section, on either side of the void and two sets at the tip of the pile at 5 feet and 2.5 feet from the tip (Figure 2.1). The pile was driven on 4/22/14 to a final tip elevation of -106.1 feet and had restrikes done on the same day, 1.5 hours after end of drive. All phases of installation were done with an ICE I-100 hammer. Note, the AFT had issues reading the EDC for the solid section gauges for phases of the installation and the blow numbers are not number the same. The comparisons are for the same blow as verified by the date and time stamp. Table 3.7 summarizes the nominal resistance estimates using dynamic methods and static load test (SLT) results.

Figure 3.25 shows the observed and estimated (from inversion process) particle velocities at the top and bottom of the test pile for BOR1 (blow 1610). These are from the gauges in the solid section of the top and bottom of the pile (Figure 2.1). Agreement between the estimated

and observed data is evident, with the dominant components very well matched. Figure 3.26 shows the final mobilized skin friction as a function of displacement, both total skin friction and the skin friction on the segments. Figure 3.27 shows the observed and estimated particle velocities at the top and bottom of the test pile based on the gauges near the voided section (Figure 2.1) for BOR1 (blow 1550). Figure 3.28 shows the final mobilized skin friction as a function of pile displacement, both total skin friction and the estimated skin friction on the segments. The blows estimate ultimate skin friction of about 1040 kip from the solid section gauges and 920 kip from the voided section gauges.

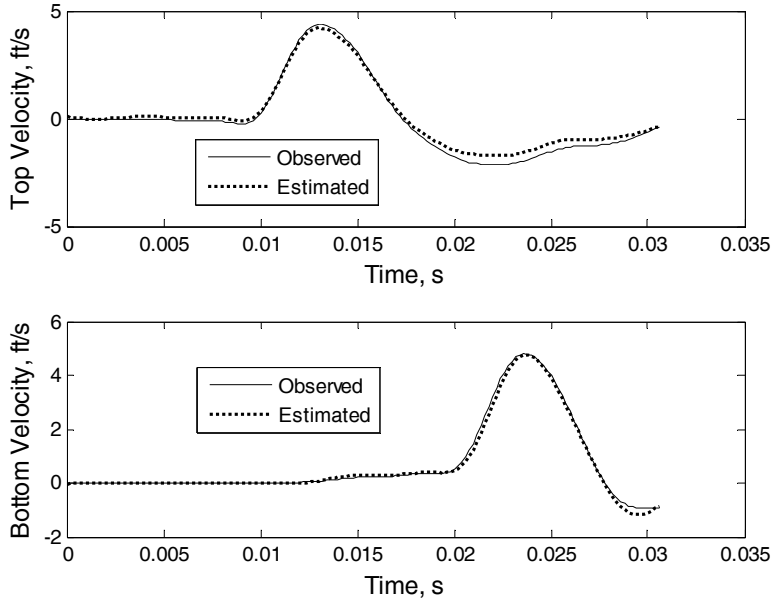

Figure 3.25 Pier 59: Comparison of Particle Velocity for BOR1 From Solid Section Gauges (Blow 1610)

Figure 3.29 shows the total energy arriving at the pile tip, as well as the predicted components due to inertia, damping, and static resistance, for blow 1610 (BOR1). The quality of the energy balance can be assessed through the error shown in Figure 3.29, which is the difference between the measured total energy and the sum of the predicted components. Evident

in Figure 3.29 is a very good energy balance with near zero error. Figure 3.30 shows the individual forces (i.e., inertia, damping, static) and their sum versus the measured total force with

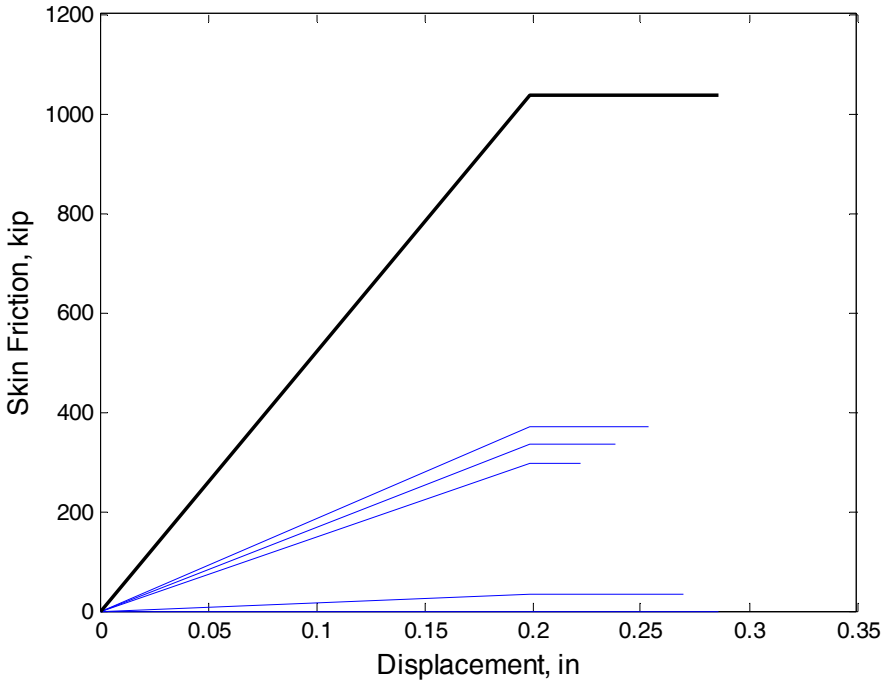

Figure 3.26 Pier 59: Estimated Skin Friction for BOR1 (Blow 1610) Solid Section Gauges (bold line = total, thin lines = segments)

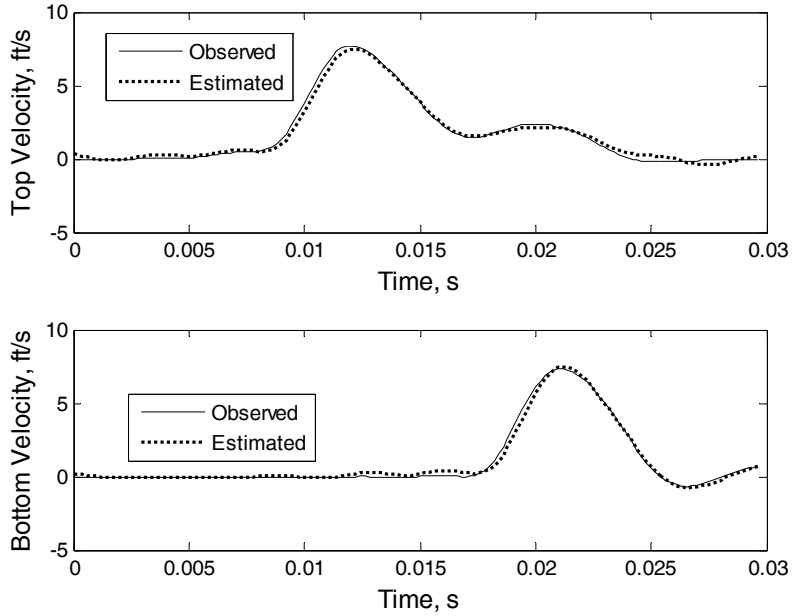

Figure 3.27 Pier 59: Comparison of Particle Velocity for BOR1 From Voided Section Gauges (Blow 1550)

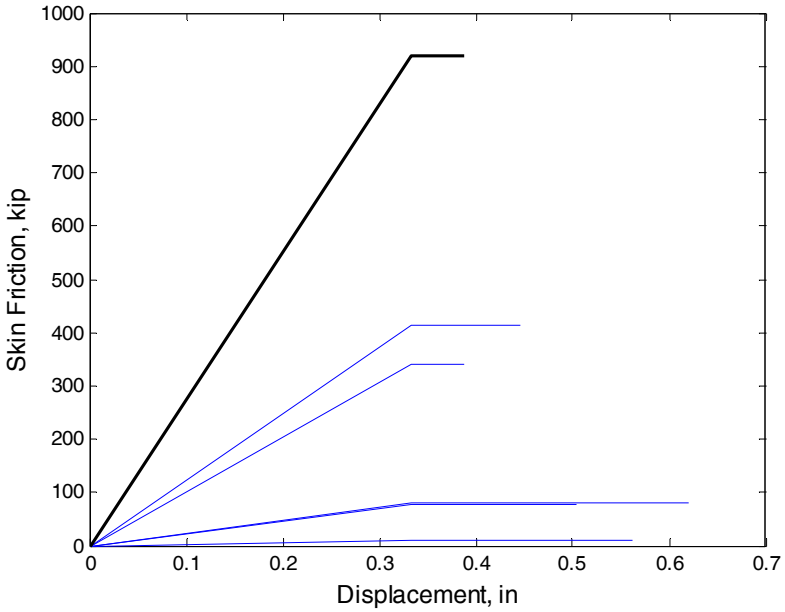

Figure 3.28 Pier 59: Estimated Skin Friction for BOR1 (Blow 1550) Voided Section Gauges (bold line = total, thin lines = segments)

time. The estimated and measured total force match well at the time near the maximum static force (280 kip at 0.025 sec), which is also when the damping is zero (i.e., static force = total dynamic force – inertia force). Figure 3.31 shows the estimated static force, damping force, total force, and measured total force versus the pile tip displacement.

Figure 3.32 shows the measured load displacement from the static load test plotted against the Davisson line. Evident is that the pile plunges at 1080 kip and reaches the Davisson movement at 1.25 inches. Of interest, for comparison to the estimated skin and tip capacities using the Tran et al. methods are measured skin and tip capacities. Since the pile top was cut-off and there wasn't access to the strain gauges, an estimate of the measured skin and tip capacities was made based on the log-log plot of the load-displacement. A change in the slope of the log-log load-displacement indicates the mobilization of the skin friction. Figure 3.33 shows the log-log load-displacement with the skin friction (900 kip) identified by the intersection of the tangent lines. Subtracting this from the total capacity (1080 kip) gives a tip capacity of 180 kip.

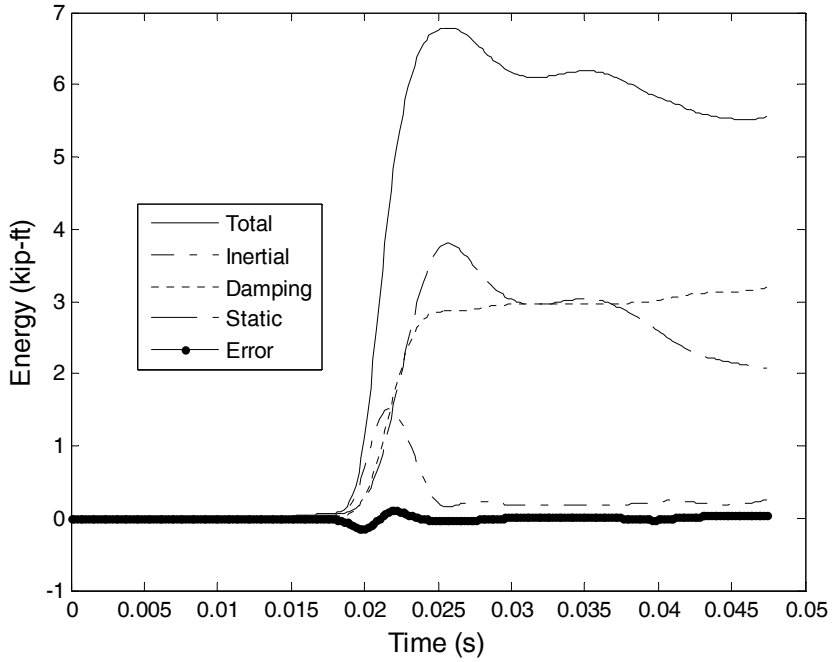

Figure 3.29 Pier 59: Energy Balancing (Blow 1610)

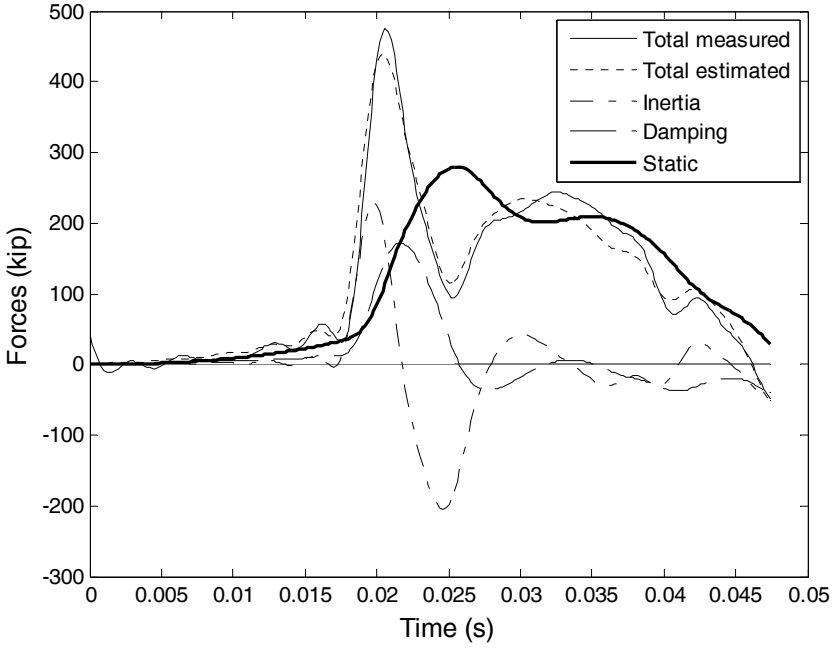

Figure 3.30 Pier 59: Forces in the Time Domain (Blow 1610)

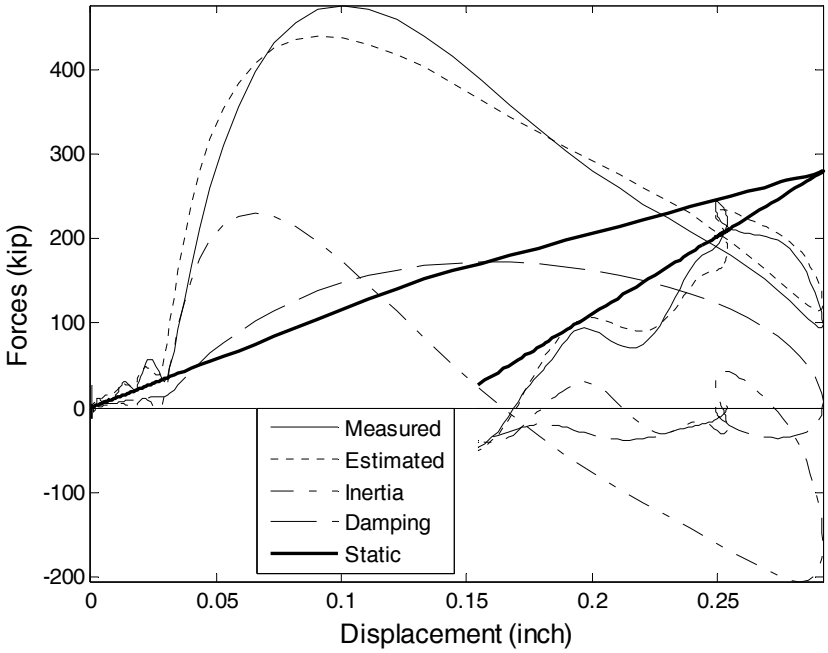

Figure 3.31 Pier 59: Forces Versus Displacement (Blow 1610)

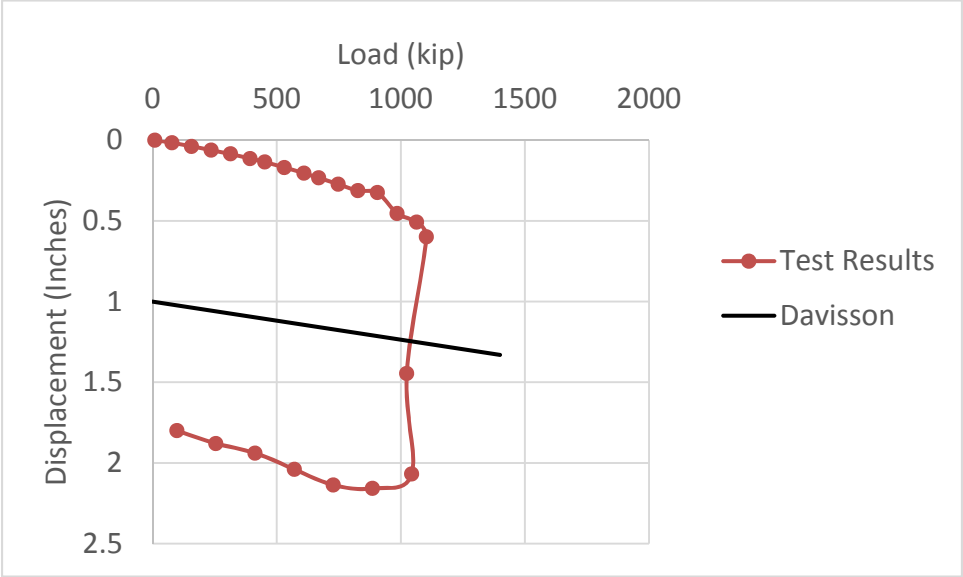

Figure 3.32 Pier 59: Load Displacement Curve from Static Load Test

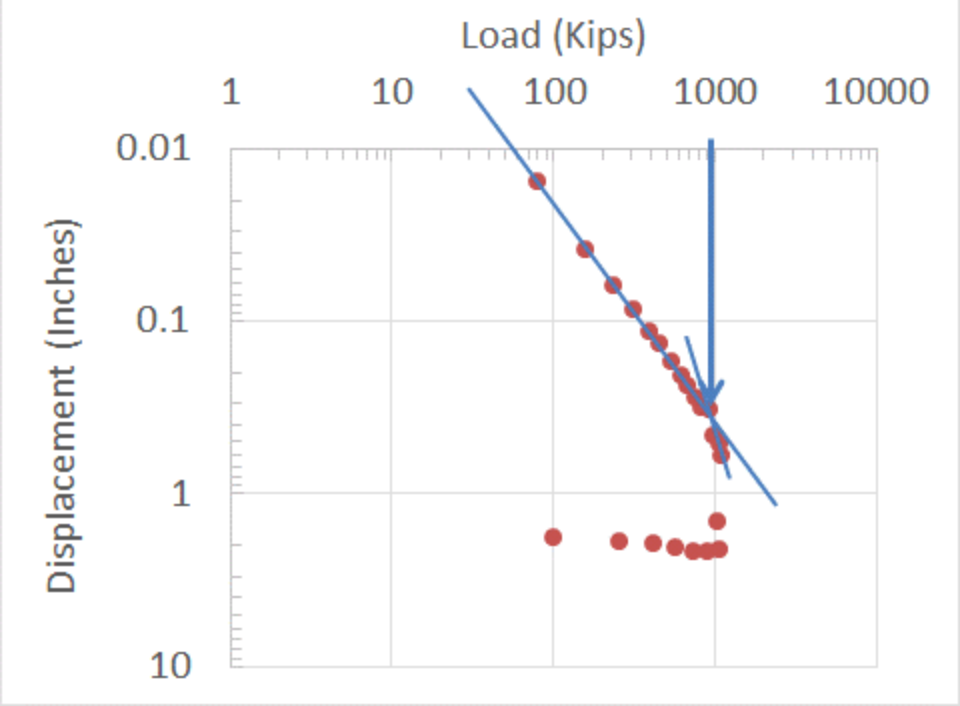

Figure 3.33 Pier 59: Log-Log Plot of Load Displacement Curve From Static Load Test

Table 3.7 are the nominal (total) resistances estimates using dynamic methods (Fixed J_c and UF methods), at EOID and BOR, and the static load test (SLT) results. Note, the estimates of the skin and tip resistances at both the EOID and BOR were not determined using the Tran et al. method, and therefore, the nominal (total) resistance is not available.

Table 3.7 Pier 59: Summary of Nominal Pile Resistance

Date	Driving Condition	Nominal Pile Resistance Estimates (kip)		
		Fixed	UF	Tran et al.
4/22/14	EOID	777 (solid) 1174 (void)	771 (solid) 1091 (void)	NA
4/22/14	BOR - 1	1312 (solid) 1127 (void)	1343 (solid) 1224 (void)	NA
5/9/14	SLT*	1080		

*Pile displacement reached Davisson criteria

Table 3.8 are the estimates of total, skin and tip capacity and the total capacity measured from the static load test for the test pile at pier 59. Estimates from SmartPile Review (Fixed J_c (total only) and UF methods) are compared to the estimates from the Tran et al. methods. The tip capacity estimates and the skin capacity estimates are from the BOR1 records on the pile. The total capacity estimate based on the Fixed J_c method is from the BOR1.

Table 3.8 Pier 59: Estimated Nominal, Side and Tip Pile Resistance Using EDC Measurements and Measured Total Capacity from Static Load Test

Pile Gauge Locations	Fixed Method	UF Method			Tran et al. Method			Load Test		
	Total (kip)	Total (kip)	Skin (kip)	Tip (kip)	Total (kip)	Skin (kip)	Tip (kip)	Total (kip)	Skin (kip)	Tip (kip)
Top and Tip Gauges	1312	1343	1092	251	1320	1040	280	1080	900	180
Voided Section and Tip Gauges	1127	1224	1018	206	1200	920	280			

3.2.5 Pier 84

The test pile at pier 84 was a voided pile with sets of EDC placed at the top of the pile in the solid section, on either side of the void and two sets at the tip of the pile at 5 feet and 2.5 feet from the tip (Figure 2.1). The pile was driven on 4 different days (5/7/14, 5/9/14, 5/13/14 and 5/15/14). The pile was initially driven to a tip elevation of -85.5 feet on 5/7/14, then driven to a tip elevation of -95.75 feet on 5/9/14, then driven to a tip elevation of -104.7 feet on 5/13/14 and finally driven to a tip elevation of -115.2 feet on 5/15/14. Restrikes were performed at the beginning of each drive phase and 32 minutes after the final driving on 5/15/14. All phases of installation were done with an ICE I-100 hammer. Note, the AFT had issues reading the EDC for the solid section gauges for phases of the installation and the blow numbers are not number

the same. The comparisons are for the same blow as verified by the date and time stamp. Table 3.9 summarizes the nominal resistance estimates using dynamic methods and static load test (SLT) results.

Figure 3.34 shows the observed and estimated (from inversion process) particle velocities at the top and bottom of the test pile for BOR3 (blow 786). These are from the gauges in the solid section of the top and bottom of the pile (Figure 2.1). Agreement between the estimated and observed data is evident, with the dominant components very well matched. Figure 3.35 shows the final mobilized skin friction as a function of displacement, both total skin friction and the skin friction on the segments. Figure 3.36 shows the observed and estimated particle velocities at the top and bottom of the test pile based on the gauges near the voided section (Figure 2.1) for BOR3 (blow 829). Figure 3.37 shows the final mobilized skin friction as a function of pile displacement, both total skin friction, and the estimated skin friction on the segments. The blows estimate ultimate skin friction of about 900 kip from the solid section gauges and 860 kip from the voided section gauges.

Figure 3.38 shows the total energy arriving at the pile tip, as well as the predicted components due to inertia, damping, and static resistance, for blow 1228 (EOID) . The quality of the energy balance can be assessed through the error shown in Figure 3.38, which is the difference between the measured total energy and the sum of the predicted components. Evident in Figure 3.38 is a very good energy balance with near zero error. Figure 3.39 shows the individual forces (i.e., inertia, damping, static) and their sum versus the measured total force with time. The estimated and measured total force match well at the time near the maximum static force (700 kip at 0.037 sec), which is also when the damping is zero and the inertia is negligible

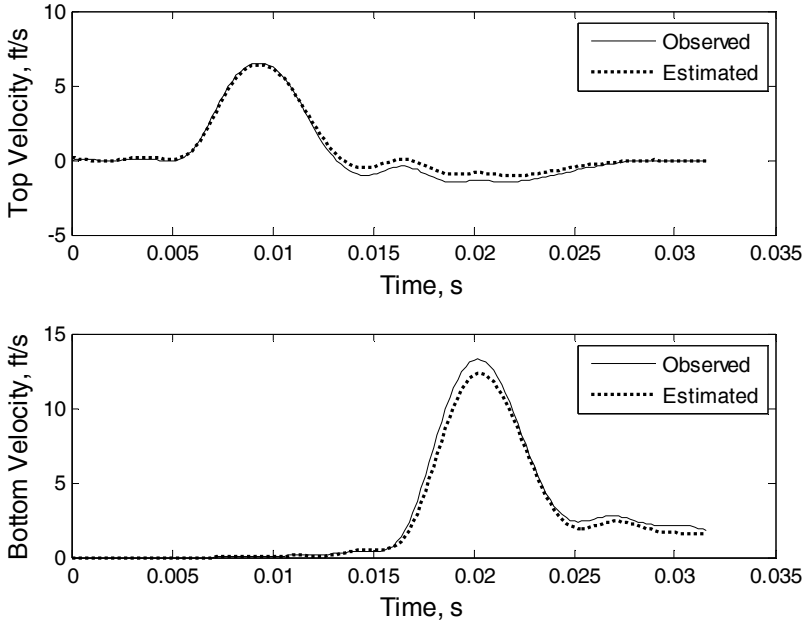

Figure 3.34 Pier 84: Comparison of Particle Velocity for BOR3 From Solid Section Gauges (Blow 786)

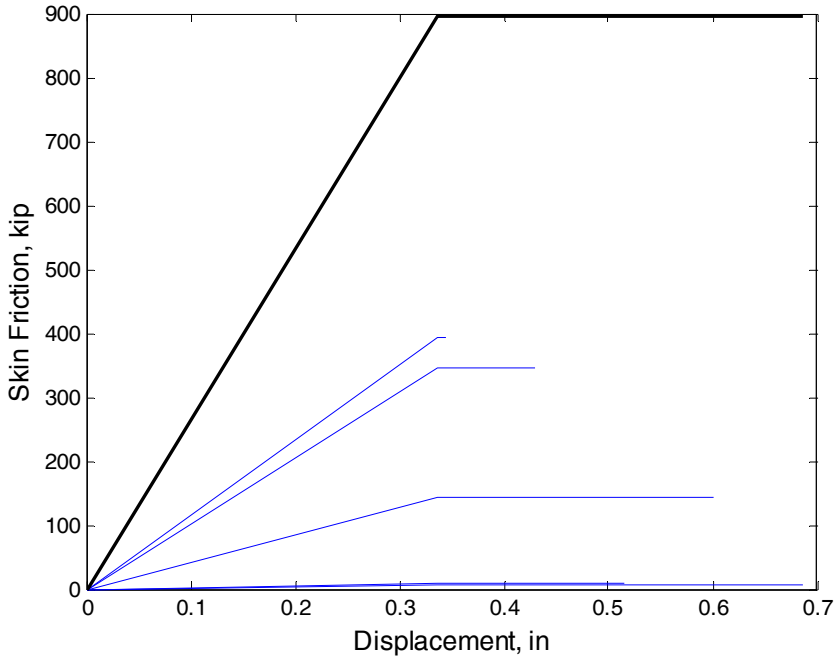

Figure 3.35 Pier 84: Estimated Skin Friction for BOR3 (Blow 786) Solid Section Gauges (bold line = total, thin lines = segments)

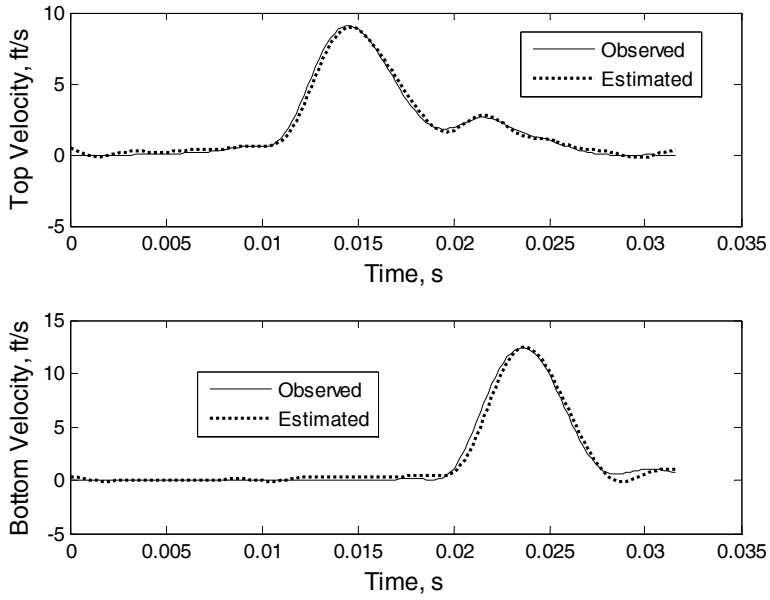

Figure 3.36 Pier 84: Comparison of Particle Velocity for BOR3 From Voided Section Gauges (Blow 829)

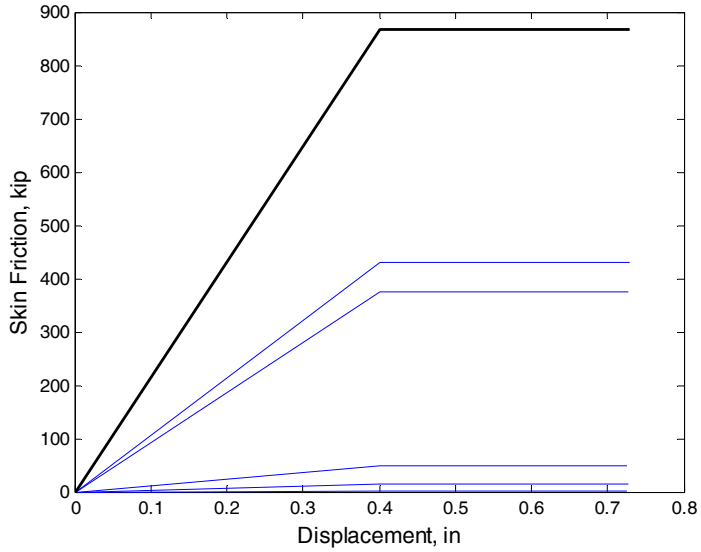

Figure 3.37 Pier 84: Estimated Skin Friction for BOR3 (Blow 829) Voided Section Gauges (bold line = total, thin lines = segments)

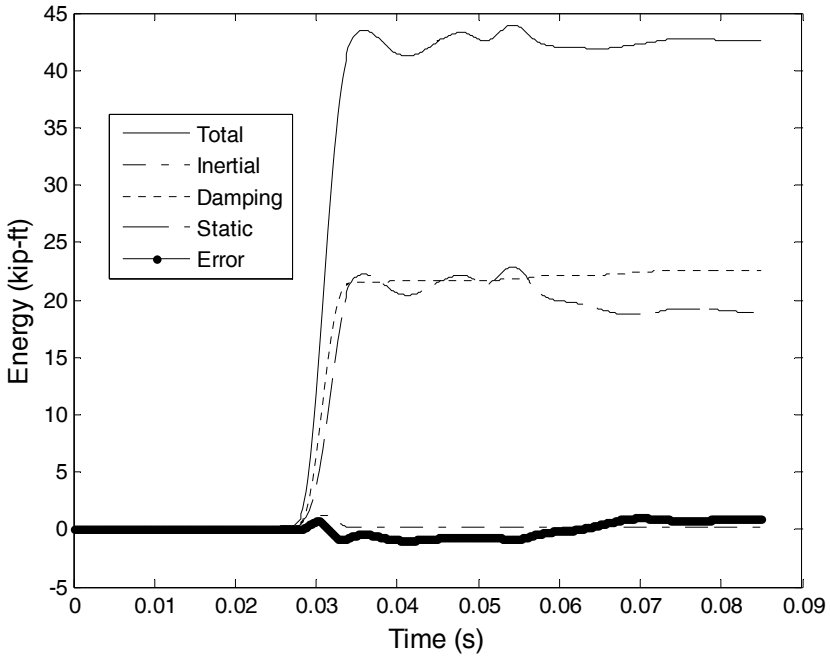

Figure 3.38 Pier 84: Energy Balancing (Blow 1228)

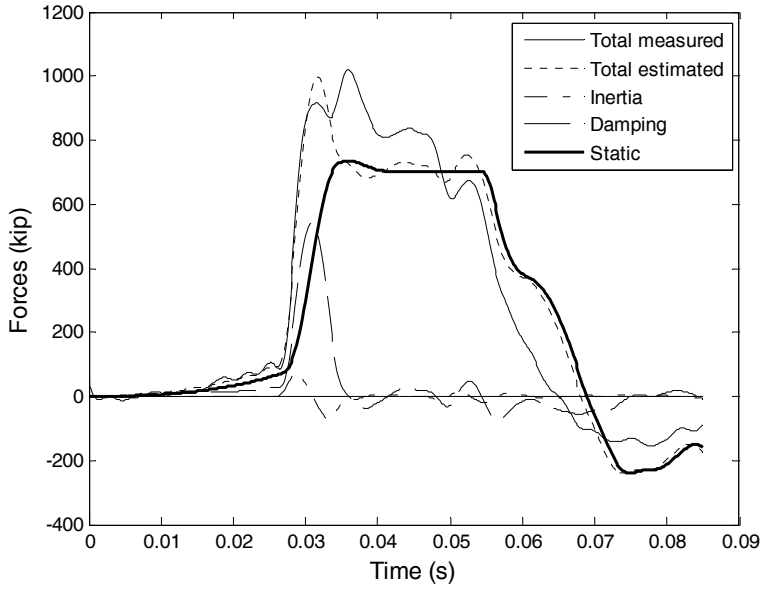

Figure 3.39 Pier 84: Forces in the Time Domain (Blow 1228)

(i.e., static force = total dynamic force). Figure 3.40 shows the estimated static force, damping force, total force, and measured total force versus the pile tip displacement.

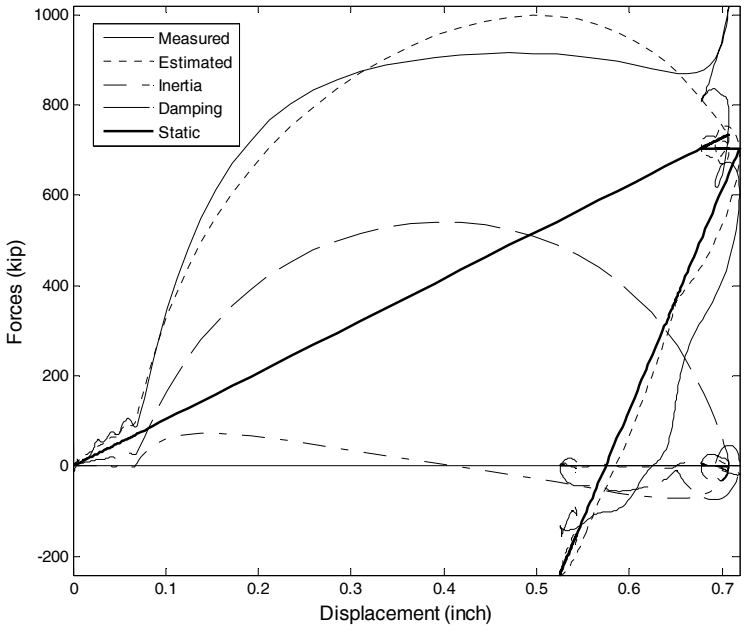

Figure 3.40 Pier 84: Forces Versus Displacement (Blow 1228)

Figure 3.41 shows the measured load displacement from the static load test plotted against the Davisson line. The movement of the pile was only 0.5 inch (did not reach Davisson) and may not have been sufficient to mobilize the skin and tip resistances. From the log-log approach, there was no apparent change in slope of the load-displacement plot (also evident in Figure 3.41) and therefore, an estimate of the skin and tip resistance could not be made.

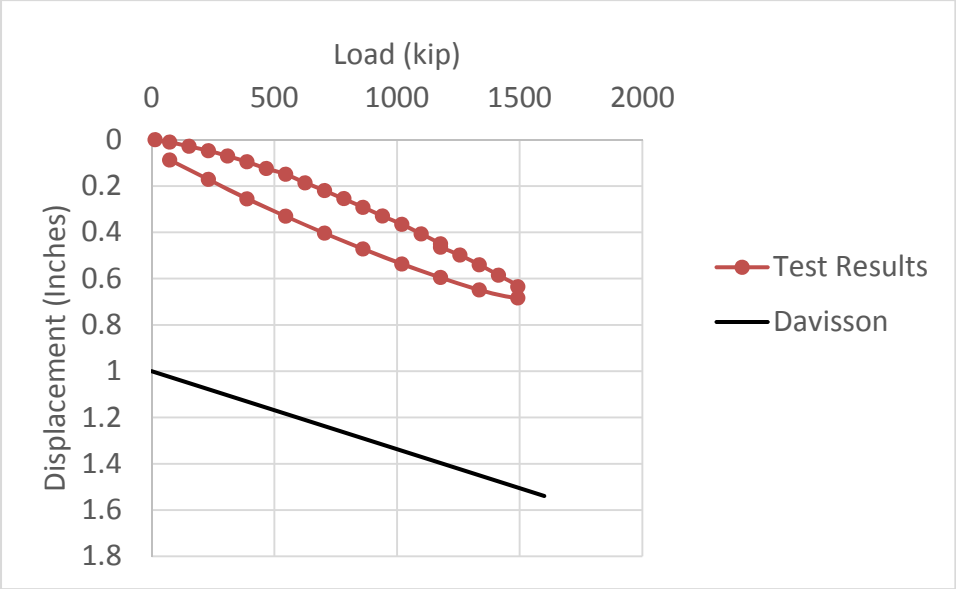

Figure 3.41 Pier 84: Load Displacement Curve from Static Load Test

It should be noted that both test piles at Piers 25 and 59 failed in plunging action at 0.6 inch and 0.53 inch of vertical movement with small tip resistance 200 kip to 300 kip. It is believed that the test pile at Pier 84 didn't fail at 0.68 inch of vertical movement because, as predicted by the Tran et al. method, this pile has twice the tip resistance (700 kip). In addition, the test pile (estimated side friction 900 kip to 1200 kip, Table 3.10) was embedded 115 feet and exhibits comparable side friction to the test pile at Pier 59 (estimated side friction 1000 kip, Figure 3.33), which was embedded 106 feet and did mobilize skin friction at 0.4 inch of movement (Figure 3.33). It is believed that Pier 84 test pile's measured and predicted may be compared at 0.68 inch of movement using a segmental approach. For instance, a simulated load test of the pile at Pier 84 was performed in FB-Multipier. The pile was modeled according to the specifications provided (cross section, length, etc.). For the soil models, the predicted skin friction (Tran et al., 2012B), Figures 3.35 and 3.37 were used for the t-z models and the predicted tip resistance (Tran et al., 2012A), Figure 3.40 was used as the Q-z model. Equal load steps were applied to the pile head until the applied load equaled that from the actual load test

(1500 kip, Figure 3.41). Figure 3.42 shows the displacements of the first node in the pile plotted against the load for each step, for t-z and Q-z models (predictions) from the solid section and voided section assessments. Based on this approach, the predicted resistances at 0.68 inch displacement are 1350 kip (solid section) and 1280 kip (voided section), Figure 3.24 were observed.

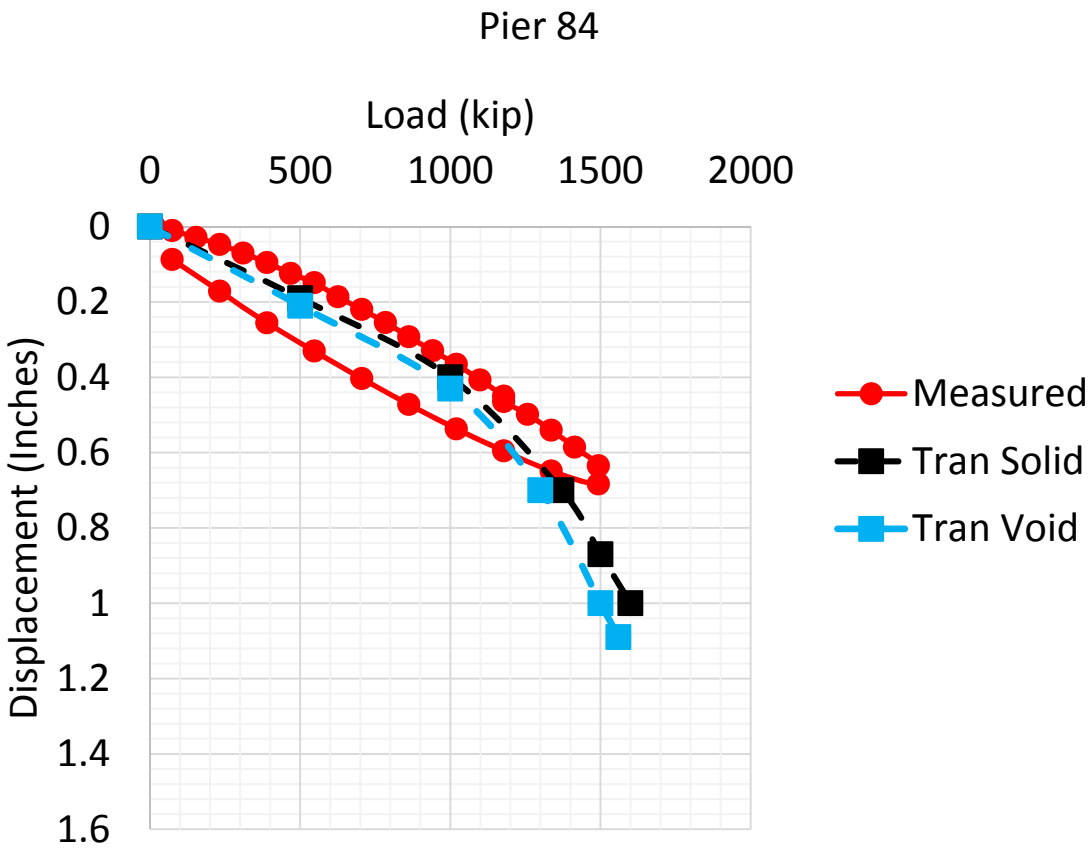

Figure 3.42 Pier 84: Measured and Simulated Load Displacement Curve

Table 3.9 are the nominal (total) resistances estimates using dynamic methods (Fixed J_c and UF methods), at EOID and BOR, and the static load test (SLT) results. The EOID-4 and subsequent BOR are the only phases of install included in Table 3.3 since the pile was driven an additional ten feet after each of the previous EOIDs (EOID -1, EOID – 2, and EOID-3). Each of the EOIDs were followed by a restrike on the same day. Note, the estimates of the skin and tip

resistances at both the EOID and BOR were not determined using the Tran et al. method, and therefore, the nominal (total) resistance is not available.

Table 3.9 Pier 84: Summary of Nominal Pile Resistance

Date	Driving Condition	Nominal Pile Resistance Estimates (kip)		
		Fixed	UF	Tran et al.
5/15/14	EOD - 4	932 (solid) 1209 (void)	1084 (solid) 1386 (void)	NA
5/15/14	BOR	761 (solid) 1096 (void)	1211 (solid) 1106 (void)	NA
5/19/14	SLT**	1500		

** Pile displacement did not reach Davisson criteria

Table 3.10 are the estimates of total, skin and tip capacity and the total capacity measured from the static load test for the test pile at pier 84. Estimates from SmartPile Review (Fixed J_c (total only) and UF methods) are compared to the estimates using the Tran et al. methods. The tip capacity estimates are from the EOID and the skin capacity estimates are from the BOR3

Table 3.10 Pier 84: Estimated Nominal, Side and Tip Pile Resistance Using EDC Measurements and Measured Total Capacity from Static Load Test

Pile Gauge Locations	Fixed Method	UF Method			Tran et al. Method			Load Test
	Total (kip)	Total (kip)	Skin (kip)	Tip (kip)	Total (kip)	Skin (kip)	Tip (kip)	Total (kip)
Top and Tip Gauges	932	1731	865	866	1350* 1600**	900	700	1500
Voided Section and Tip Gauges	1209	1424	631	793	1280* 1560**	860	700	

*Total resistance based on maximum displacement (FB-Multipier analysis)
**Total resistance = skin resistance + tip resistance

records on the pile. The total capacity estimate based on the Fixed J_c method is from the BOR3.

3.2.6 Measured Stresses in Voided Piles at US-331 Choctawhatchee Bay

Of interest are the compression and tension stresses in the solid and voided section of the piles developed during driving. To prevent damage to the pile during driving, FDOT specification 455 limits the compression and tension stresses that should be developed. Since there was a set of EDC gauges in the solid section and around the void (Figure 2.1), the stresses measured (top and tip compression) and predicted (max. tension stress) during driving could be compared for each cross section. Figures 3.43-3.46 show the pile top and tip compressive stresses and the max tension stress for the cross sections (solid and voided) of each test pile (pier 25, 33, 59, and 84). Note, the EDC gauges around the void are near the top of the pile.

Figures 3.43-3.46 show that the measured top compressive stresses in the solid section of the pile are typically about 25% smaller than the measured values in the voided section of the pile. However, if the top stresses are adjusted by area (i.e., divide by 645 $inch^2$ / 900 $inch^2$ = 0.72), then the stresses are very comparable. For all piles, the predicted max tension stress are approximately 8% lower than the mean (void and solid) for the voided section, whereas the solid section are 8% higher than the mean.

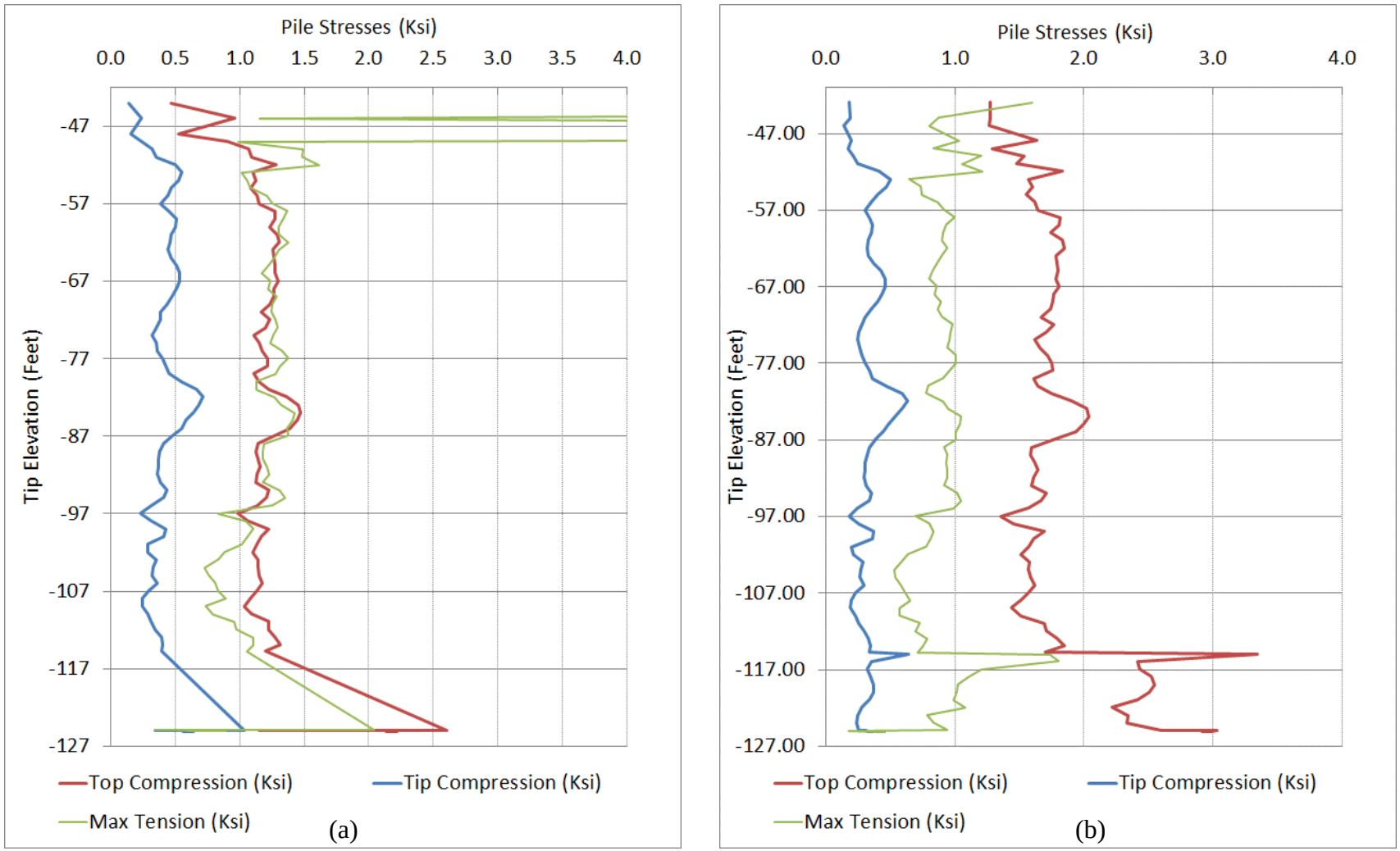

Figure 3.43 Pier 25: Measured Compression and Tension Stresses in Pile During Driving (a) Solid Section (b) Voided Section

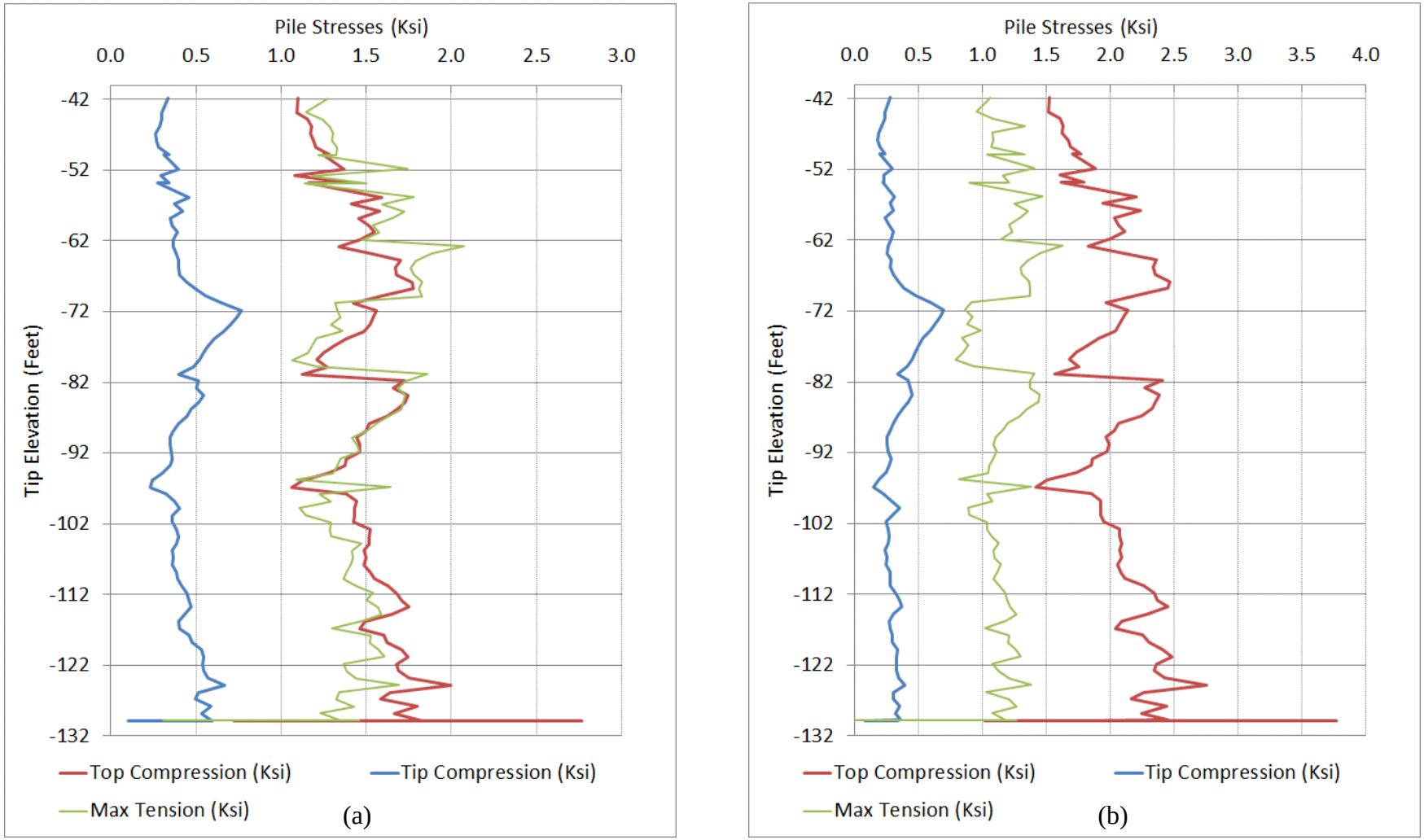

Figure 3.44 Pier 33: Measured Compression and Tension Stresses in Pile During Driving (a) Solid Section (b) Voided Section

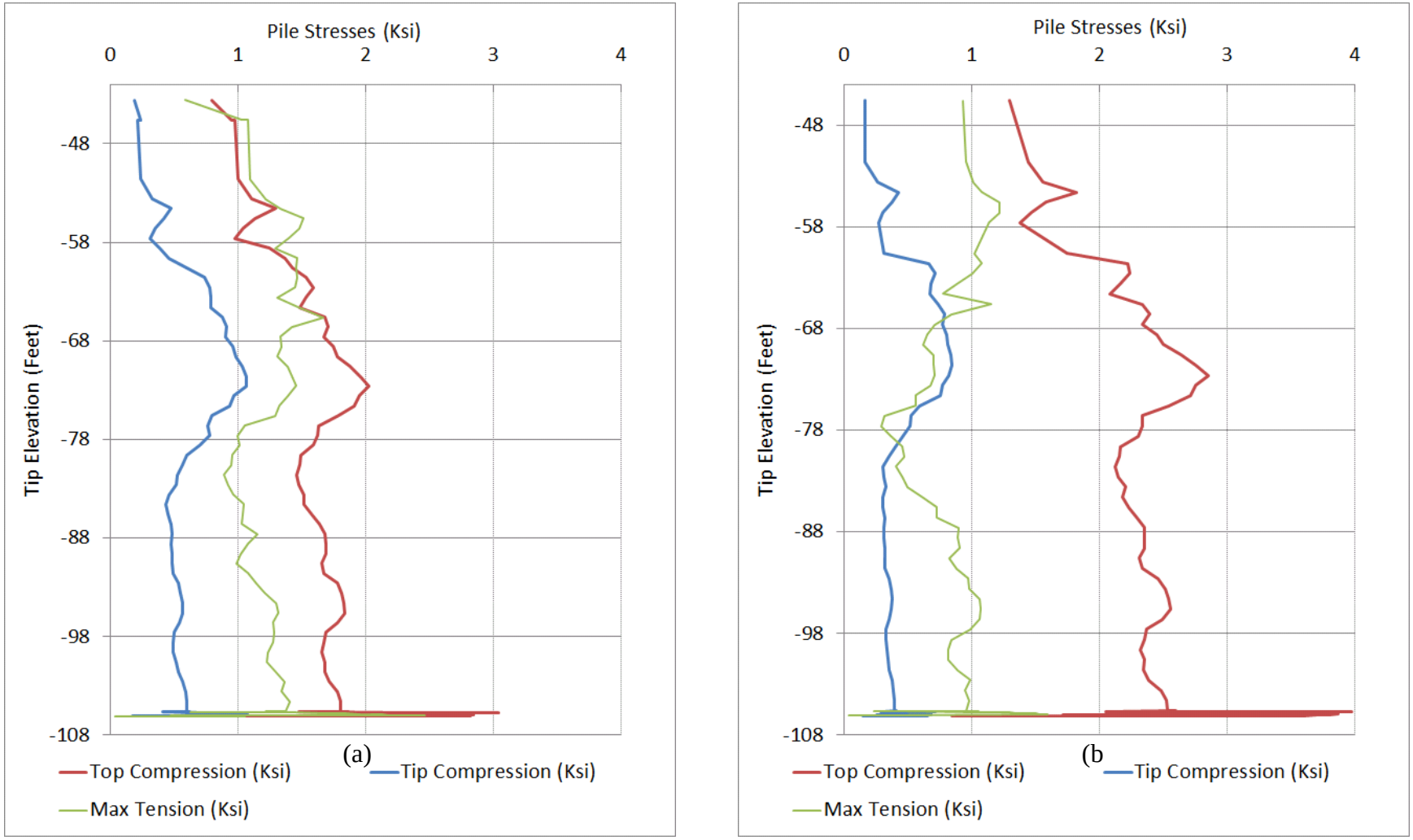

Figure 3.45 Pier 59: Measured Compression and Tension Stresses in Pile During Driving (a) Solid Section (b) Voided Section

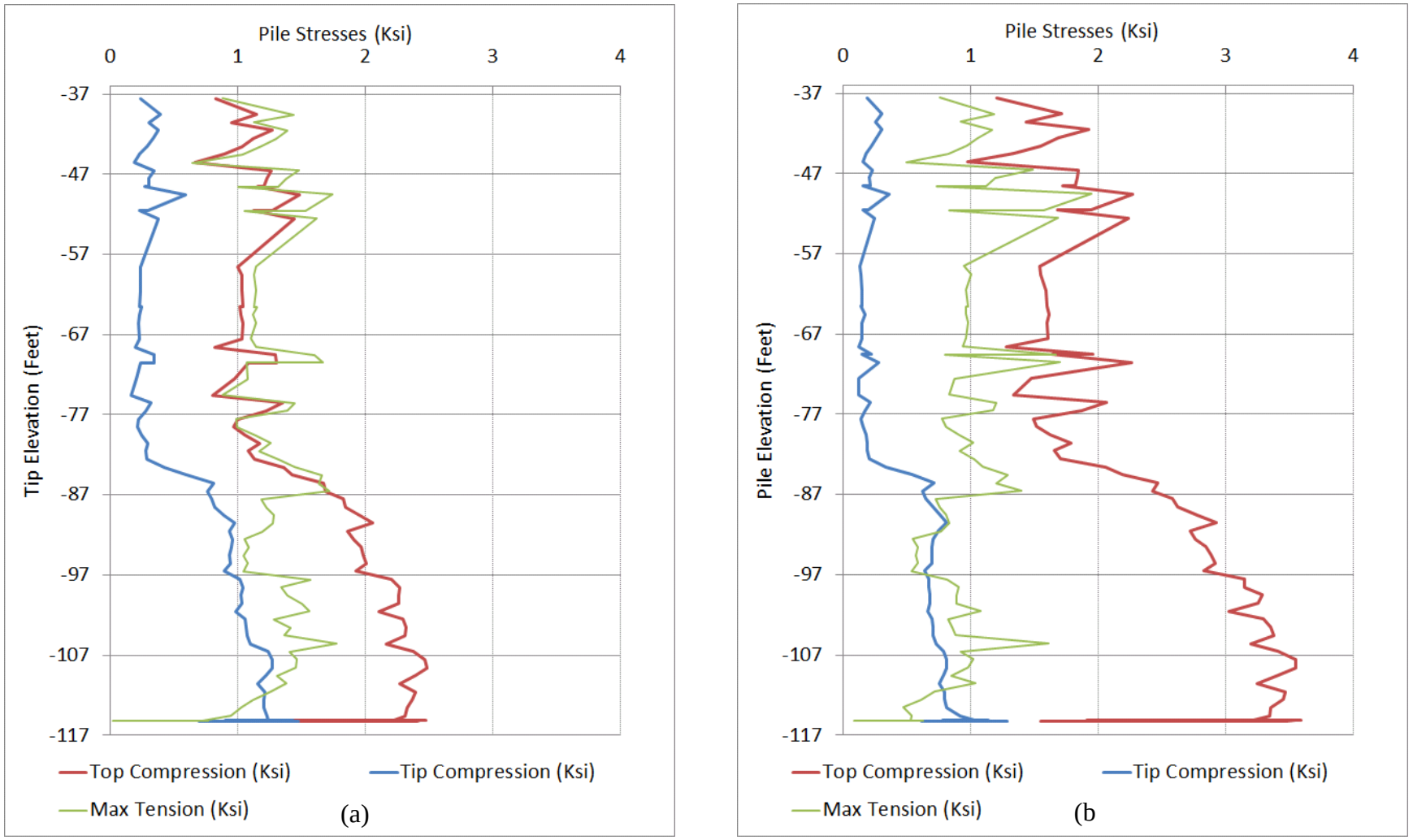

Figure 3.46 Pier 84: Measured Compression and Tension Stresses in Pile During Driving (a) Solid Section (b) Voided Section

3.2.7 Pile Resistance Estimates Using Instrumentation in Voided and Solid Sections

Five prestressed, 30-inch square concrete piles were instrumented with EDC near the top and the tip and installed at a new bridge site on US-331 near Santa Rosa Beach, Florida. Each pile was monitored during installation (EDC) and had static load tests performed to identify their capacity. Four of the piles had a circular void over 134 feet of their 160 feet lengths, (Figure 2.1) and one pile had a continuous solid cross section (160 feet in length). The four voided test piles had 2 sets of EDC in each pile. One set had a pair of EDC 30 feet from the top of pile (around pile void) and an EDC 2.5 feet from the tip of pile (Figure 2.1). The other set consisted of an EDC 5 feet from the top of pile and an EDC 5 feet from the tip of pile (Figure 2.1)

Estimates of the skin, tip, and total resistance using the Fixed J_c (total only), UF, and Tran et al. methods were made independently for each test pile, for both the voided and solid section of the piles. Shown in Table 3.11 is a summary of the comparisons for UF and Tran et al. methods for the solid and voided gauge sets. The average difference between the estimation of capacity (grey columns) for top and voided sections is larger for the UF method (23%) than the Tran et al. method (6%). Similarly, there is a larger standard deviation of the UF method (11%) compared to the Tran et al. method (3%). If the predictions are compared to the measured values (yellow and green columns), the average error is generally higher for the top solid gauges (yellow: 13% UF vs. -0.8% Tran et al.) compared to the voided gauges (green: -12% UF vs. -5% Tran et al.). However, the measurements are well within the standard deviation of the measurements, suggesting the need for separation is not necessary and given the number of test piles (i.e., 4). This is shown very clearly in the last column (green), which reports UF voided gauge predictions – 23% for first pile and +13% for third pile. For estimates of the tip resistances, the voided and solid section gauges were the same for each test pile, and the estimate based on the solid section gauge was used for comparison.

Table 3.11 Predicted and Measured Capacities in Solid and Voided Sections

Pile	Gage Locations	Predicted NEW (kips)	Predicted UF Method (kips)	Measured (kips)	NEW Diff Top with Voided (%)	UF Diff Top with Voided (%)	NEW Error with Measured (%)	UF Error with Measured (%)	NEW Top Error with Measured (%)	NEW Voided Error with Measured (%)	UF Top Error with Measured (%)	UF Voided Error with Measured (%)
25	top&tip	1450	1726	1500	5.3	38.3	-3.3	15.1	-3.3		15.1	
	void&tip	1370	1151				-8.7	-23.3		-8.7		-23.3
33	top&tip	1320	1466	1500	4.0	22.9	-12.0	-2.3	-12.0		-2.3	
	void&tip	1260	1122				-16.0	-25.2		-16.0		-25.2
59	top&tip	1320	1343	1080	11.1	11.0	22.2	24.4	22.2		24.4	
	void&tip	1200	1224				11.1	13.3		11.1		13.3
84	top&tip	1350	1731	1500	4.7	20.5	-10.0	15.4	-10.0		15.4	
	void&tip	1280	1424				-14.7	-5.1		-14.7		-5.1
				Mean	6.3	23.2	-2.4	2.5	-0.8	-4.5	13.1	-11.7
				Std. Dev.	3.3	11.3	13.6	18.6	15.8	12.5	11.1	18.0

3.3 Bayou Lacassine

The 3rd site in the Phase I study (FDOT BDK75 977-24, 2013) was Bayou Lacassine at Jefferson Davis Parish, Louisiana. The site consists of interbedded layers of sandy-silt overlying clay. Two test piles, 30 in square and 75 feet long, had EDC gauges at the top (5 feet from the top of pile) and tip (2.5 feet from the tip of pile). Each was installed with an ICE I-62 diesel hammer with a rated energy of 165 kip-feet. Applied Foundation Testing monitored both piles.

3.3.1 Bent 1 Pile 1

Pile 1 was driven on 10/4/2012 (EOID), followed by a restrike on 10/5/2012 (BOR), and a static load test on 10/17/2012. Table 3.12 summarizes the nominal resistance estimates using dynamic methods and static load test (SLT) results.

Figure 3.47 shows the observed and estimated (from inversion process) particle velocities at the top and bottom of the test pile for blow 1126 (BOR). Agreement between the estimated and observed data is evident, with the dominant components very well matched. Figure 3.48 shows the final mobilized skin friction as a function of displacement, both total skin friction and the skin friction on the segments. The blows estimate ultimate skin friction of about 505 kip.

Figure 3.49 shows the total energy arriving at the pile tip, as well as the predicted components due to inertia, damping, and static resistance, also for blow 1126. The quality of the energy balance can be assessed through the error shown in Figure 3.49, which is the difference between the measured total energy and the sum of the predicted components. Evident in Figure 3.49 is a very good energy balance with near zero error. Figure 3.50 shows the individual forces (i.e., inertia, damping, static) and their sum versus the measured total force with time. The estimated and measured total force match well at the time near the maximum static force (53 kip at 0.0225 sec), which is also when the inertia is zero and the damping is negligible (i.e., static

force = total dynamic force). Figure 3.51 shows the estimated static force, damping force, total force, and measured total force versus the pile tip displacement.

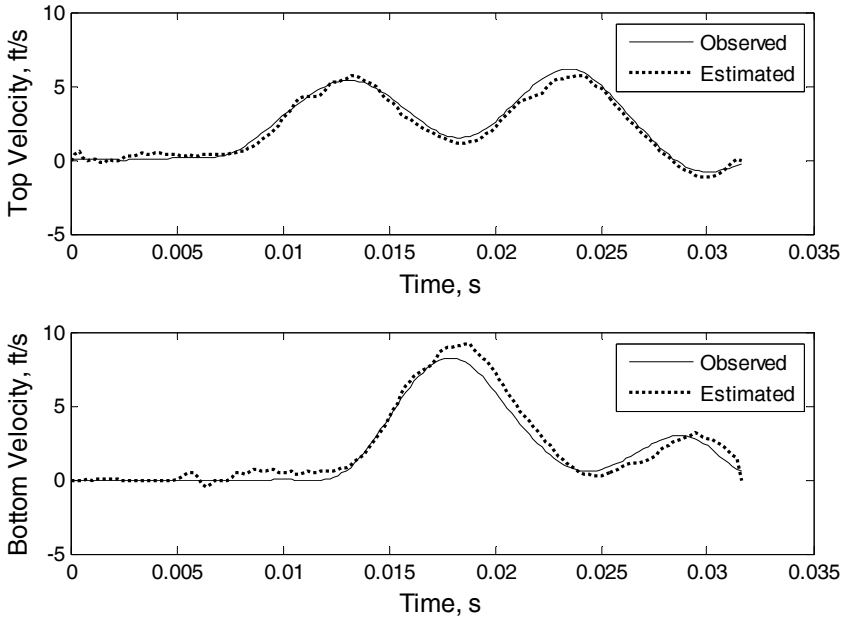

Figure 3.47 Bent 1 Pile 1: Comparison of Particle Velocity for BOR (Blow 1126)

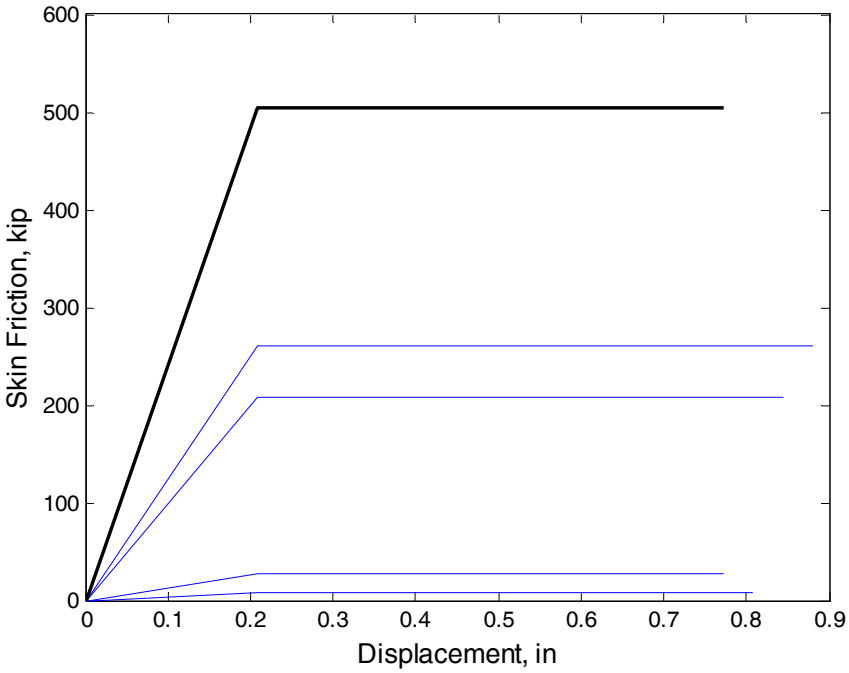

Figure 3.48 Bent 1 Pile 1: Estimated Skin Friction for BOR (Blow 1126) (bold line = total, thin lines = segments)

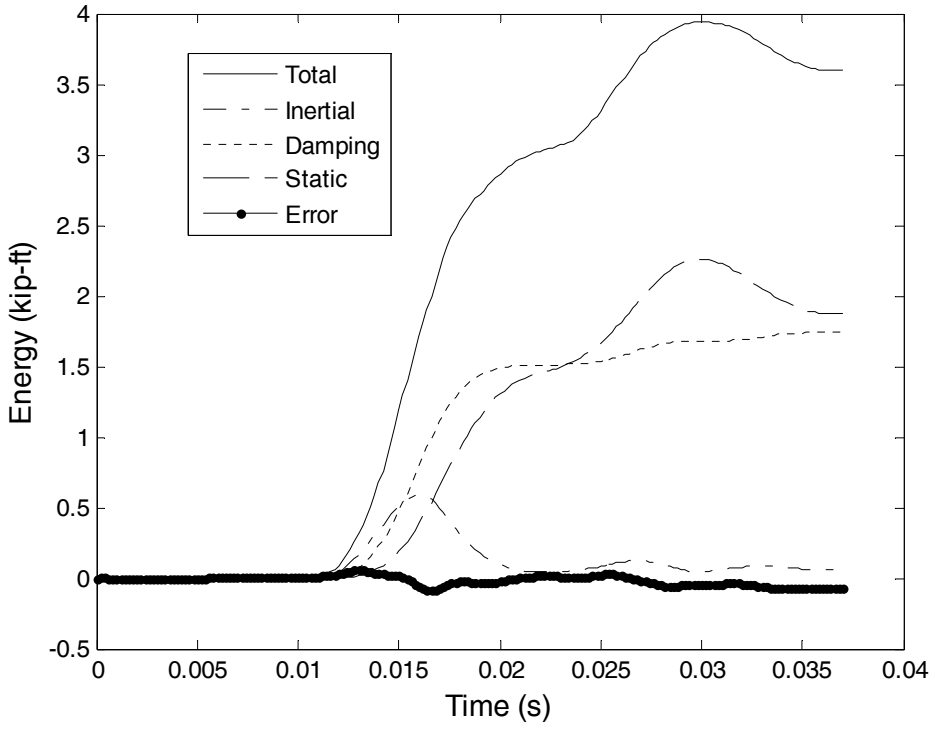

Figure 3.49 Bent 1 Pile 1: Energy Balancing (Blow 1126)

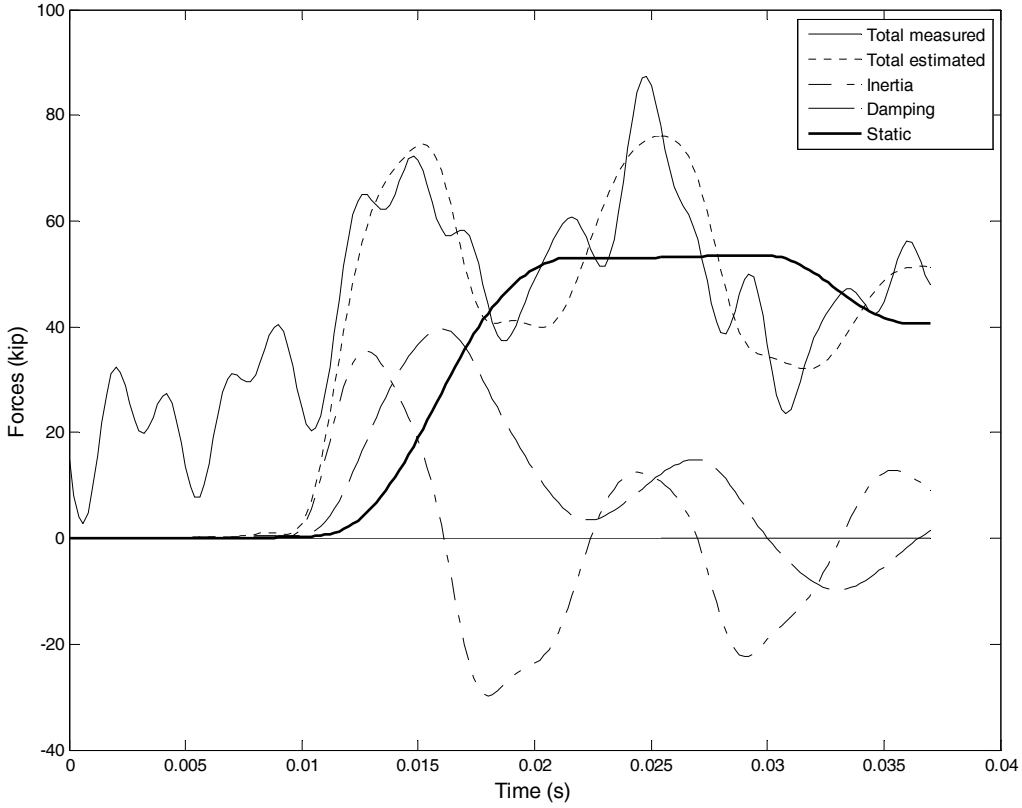

Figure 3.50 Bent 1 Pile 1: Forces in the Time Domain (Blow 1126)

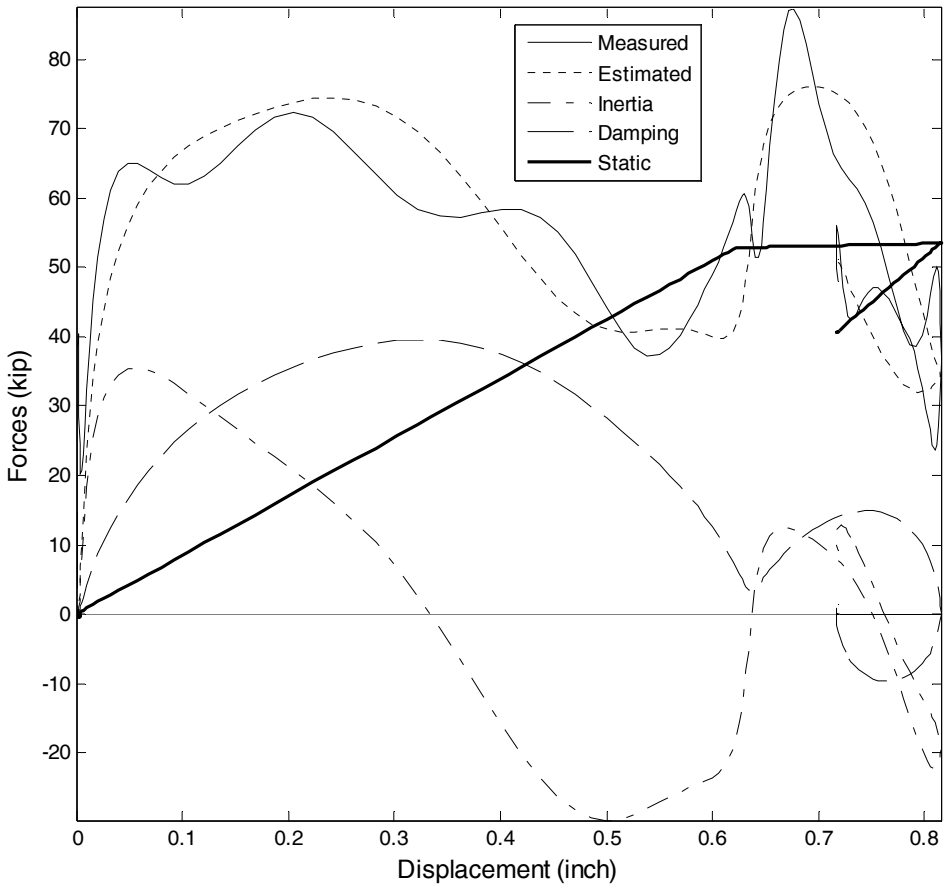

Figure 3.51 Bent 1 Pile 1: Forces Versus Displacement (Blow 1126)

Shown in Figure 3.52 is the static load response for Bent 1 Pile 1. Evident, the Davisson and ultimate capacities are quite similar. Haque et al (2014) reported on the measured skin friction and tip capacities from the static load tests performed.

Table 3.12 are the nominal (total) resistances estimates using dynamic methods (Fixed J_c and UF methods), at EOID and BOR, and the static load test (SLT) results. Note, the estimates of the skin and tip resistances at both the EOID and BOR were not determined using the Tran et al. method, and therefore, the nominal (total) resistance is not available. Table 3.13 lists the predicted capacities using the UF methods and the Tran et al. methods together with the measured total, skin, and tip capacities.

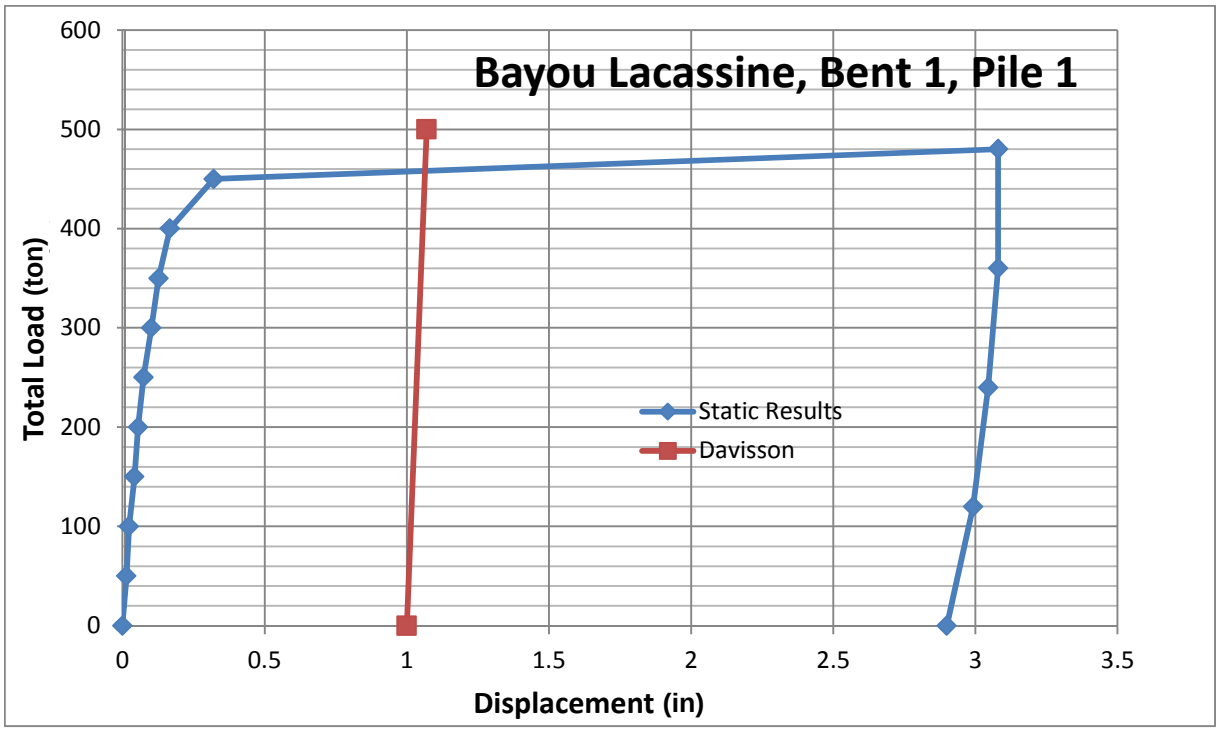

Figure 3.52 Static Load Test Results and Davisson Capacity for Bayou Lacassine, Bent 1 Pile 1

Table 3.12 Bent 1 Pile 1: Summary of Nominal Pile Resistance

Date	Driving Condition	Nominal Pile Resistance Estimates (kip)		
		Fixed	UF	Tran et al.
10/4/12	EOID	280	288	NA
10/5/12	BOR - 1	411	432	NA
10/17/12	SLT*	460		

* Pile displacement did reach Davisson criteria

Table 3.13 Bent 1 Pile 1: Estimated Nominal, Side and Tip Pile Resistance using EDC Measurements and Measured Total Capacity From Static Load Test

Fixed Method	UF Method			Tran et al. Method			Load Test		
Total (kip)	Total (kip)	Skin (kip)	Tip (kip)	Total (kip)	Skin (kip)	Tip (kip)	Total (kip)	Skin (kip)	Tip (kip)
411	432	341	91	558	505	53	460	381	71

3.3.2 Bent 1 Pile 3

Pile 3 was driven on 9/18/2012 (EOID), followed by a restrike on 9/19/2012 (BOR), and a static load test on 10/3/2012. Table 3.14 summarizes the nominal resistance estimates using dynamic methods and static load test (SLT) results.

Figure 3.53 shows the observed and estimated (from inversion process) particle velocities at the top and bottom of the test pile for blow 1951 (BOR). Agreement between the estimated and observed data is evident, with the dominant components very well matched. Figure 3.54 shows the final mobilized skin friction as a function of displacement, both total skin friction and the skin friction on the segments. The blows estimate ultimate skin friction of about 759 kip.

Figure 3.55 shows the total energy arriving at the pile tip, as well as the predicted components due to inertia, damping, and static resistance, also for blow 1951. The quality of the energy balance can be assessed through the error shown in Figure 3.55, which is the difference between the measured total energy and the sum of the predicted components. Evident in Figure 3.55 is a very good energy balance with near zero error. Figure 3.56 shows the individual forces (i.e., inertia, damping, static) and their sum versus the measured total force with time. The estimated and measured total force match well at the time near the maximum static force (86 kip at 0.02 sec), which is also when the inertia is zero and the damping is negligible (i.e., static force = total dynamic force). Figure 3.57 shows the estimated static force, damping force, total force, and measured total force versus the pile tip displacement.

Shown in Figure 3.58 is the static load response for Bent 1, Pile 3. Evident, the Davisson and ultimate capacities are quite similar. Haque et al (2014) reported on the measured skin friction and tip capacities from the static load tests performed.

Table 3.13 are the nominal (total) resistances estimates using dynamic methods (Fixed J_c and UF methods), at EOID and BOR, and the static load test (SLT) results. Note, the estimates of the

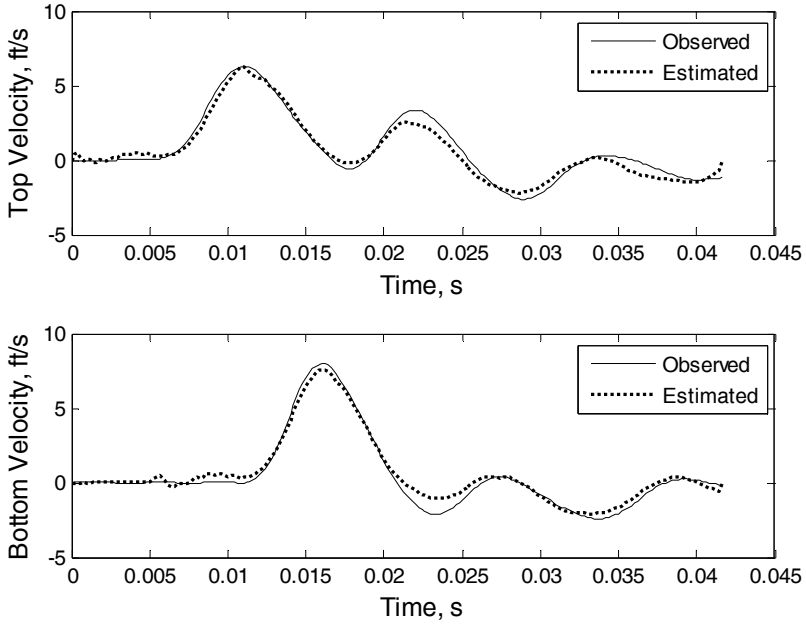

Figure 3.53 Bent 1 Pile 3: Comparison of Particle Velocity for BOR (Blow 1951)

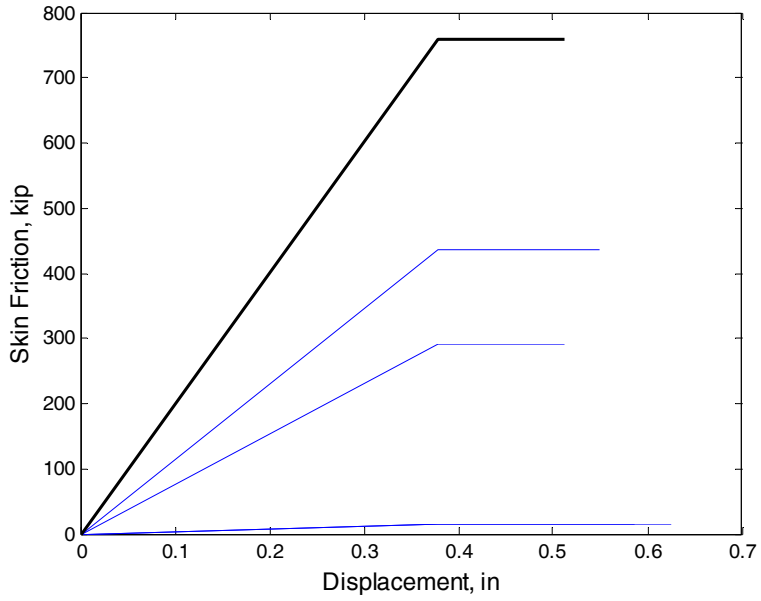

Figure 3.54 Bent 1 Pile 3: Estimated Skin Friction for BOR (Blow 1951) (bold line = total, thin lines = segments)

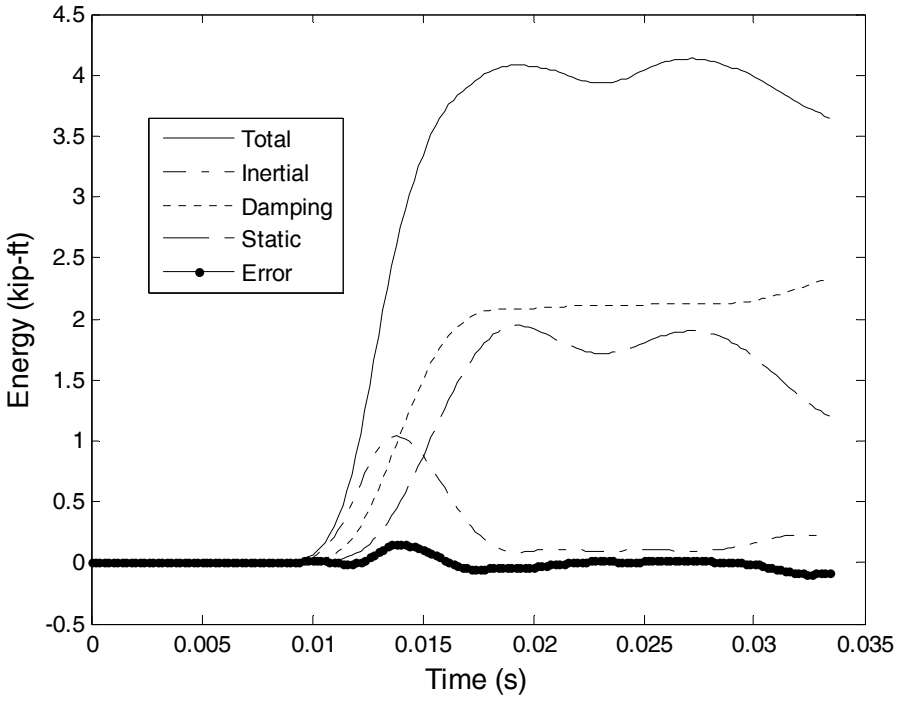

Figure 3.55 Bent 1 Pile 3: Energy Balancing (Blow 1951)

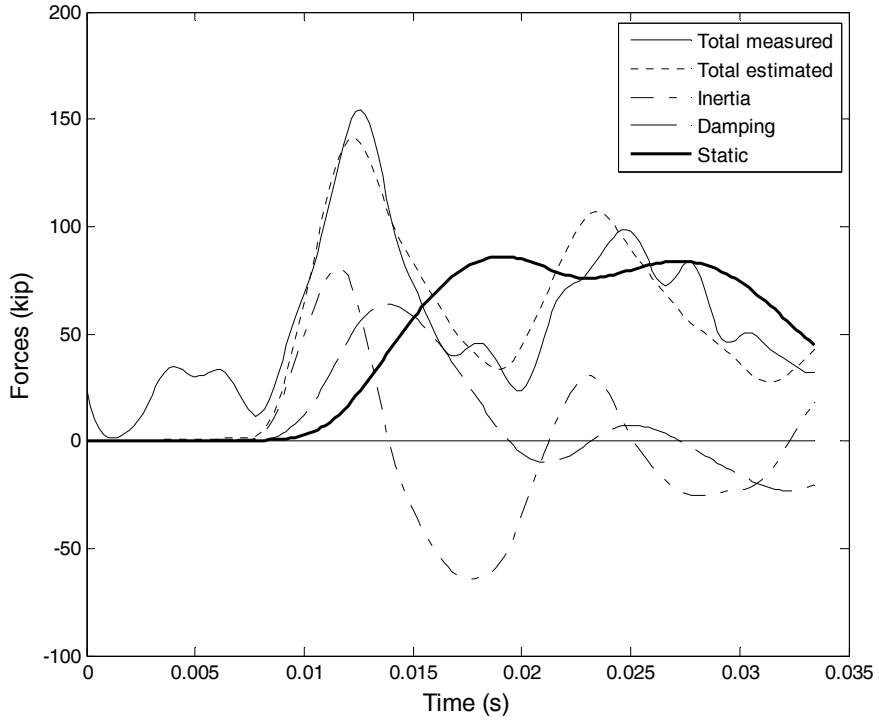

Figure 3.56 Bent 1 Pile 3: Forces in the Time Domain (Blow 1951)

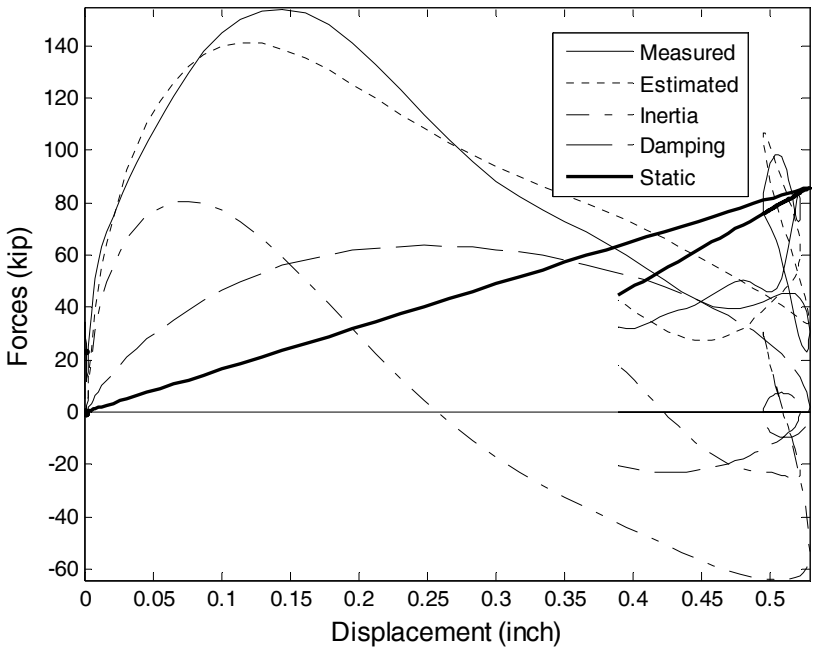

Figure 3.57 Bent 1 Pile 3: Forces Versus Displacement (Blow 1951)

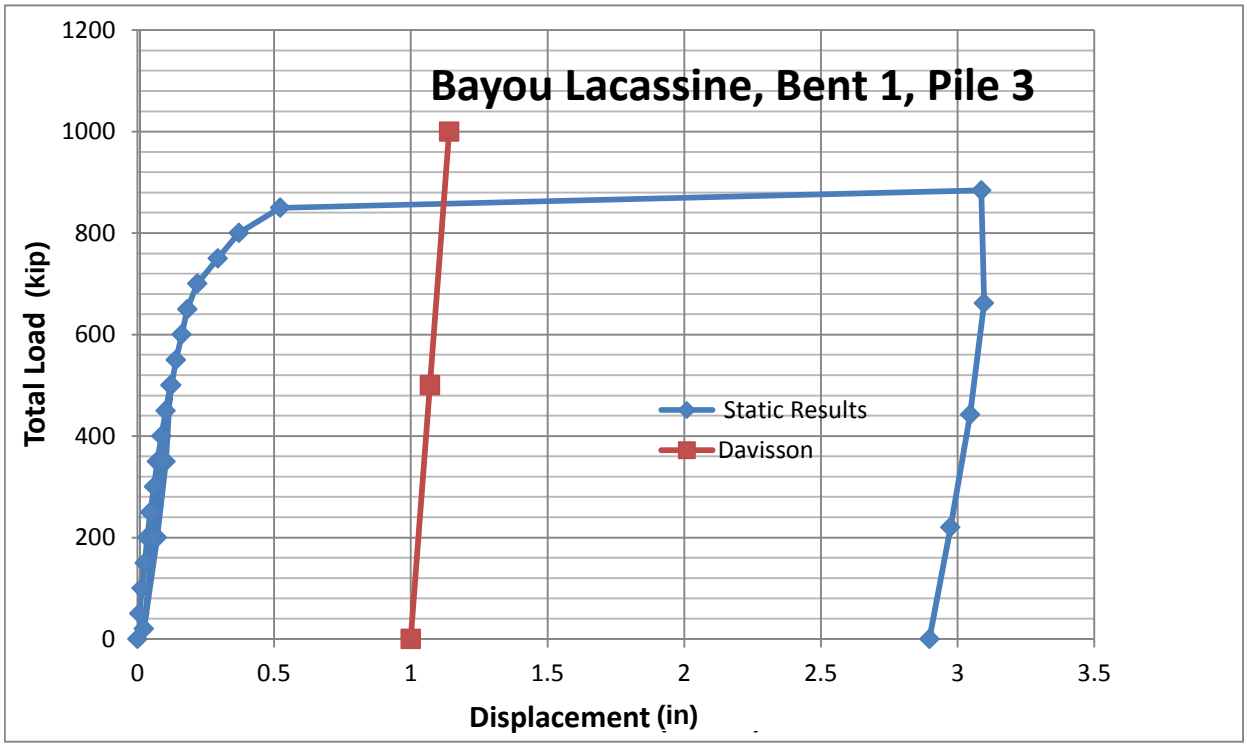

Figure 3.58 Static Load Test Results and Davisson Capacity for Bayou Lacassine, Bent 1 Pile 3

skin and tip resistances at both the EOID and BOR were not determined using the Tran et al. method, and therefore, the nominal (total) resistance is not available. Table 3.14 lists the predicted capacities using the UF methods and the Tran et al. methods together with the measured total, skin, and tip capacities.

Table 3.14 Bent 1 Pile 3: Summary of Nominal Pile Resistance

Date	Driving Condition	Nominal Pile Resistance Estimates (kip)		
		Fixed	UF	Tran et al.
9/18/12	EOID	722	659	NA
9/19/12	BOR	804	745	NA
10/3/12	SLT*	850		

* Pile displacement did reach Davisson criteria

Table 3.15 Bent 1 Pile 3: Estimated Nominal, Side and Tip Pile Resistance using EDC Measurements and Measured Total Capacity From Static Load Test

Fixed Method	UF Method			Tran et al. Method			Load Test		
Total (kip)	Total (kip)	Skin (kip)	Tip (kip)	Total (kip)	Skin (kip)	Tip (kip)	Total (kip)	Skin (kip)	Tip (kip)
804	745	671	74	846	759	87	850	697	153

3.4 Results for 5th Street Bascule

The 5th site in the Phase I study (FDOT BDK75 977-24, 2013) was the 5th Street bascule Bridge in Miami-Dade County, Florida. The site consists of interbedded sand, sandstone, and limestone. Four piles with EDC gauges installed at the top (4 feet from the top of pile) and tip (2 feet from the tip of pile) were tested in tension. Each of the test piles were driven using a Delmag 46-32 open end diesel hammer.

3.4.1 Pier 2 Pile 37

Pile 37 was driven on 8/1/208 (EOID), followed by a static load test on 8/11/2008. Figure 3.59 shows the observed and estimated (from inversion process) particle velocities at the top and bottom of the test pile for EOID (blow 2375). Agreement between the estimated and observed data is evident, with the dominant components very well matched. Figure 3.60 shows the final mobilized skin friction as a function of displacement, both total skin friction and the skin friction on the segments. The blows estimate ultimate skin friction of about 158 kip. Table 3.16 shows the estimated skin friction capacity from the UF and Tran et al. methods compared to the measured skin friction capacity.

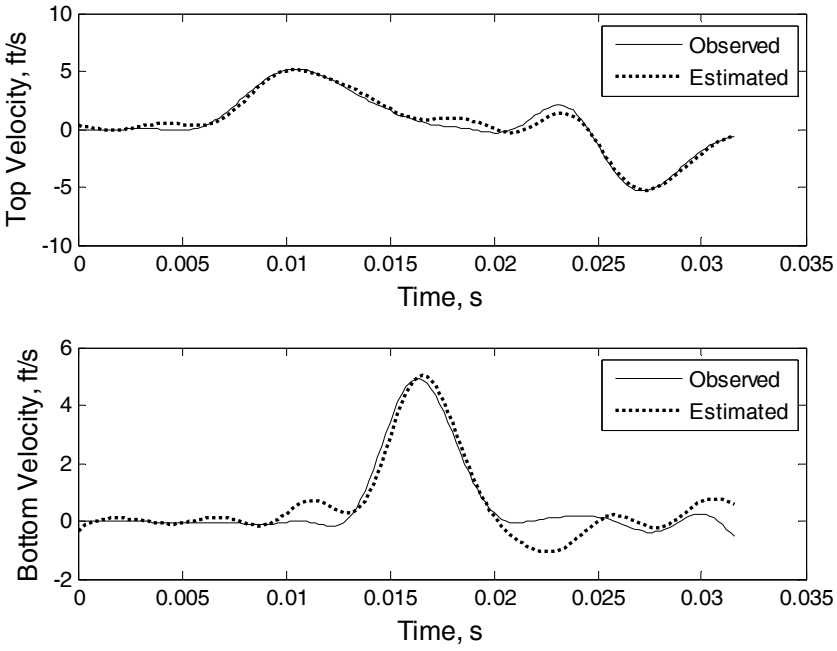

Figure 3.59 Pier 2 Pile 37: Comparison of Particle Velocity for EOID (Blow 2375)

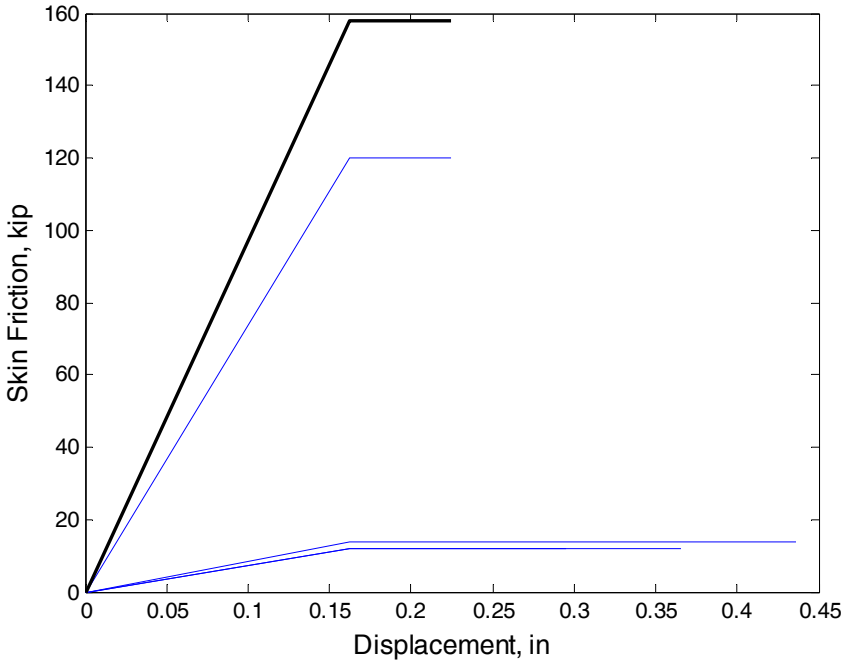

Figure 3.60 Pier 2 Pile 37: Forces Versus Displacement (Blow 2375)

Table 3.16 Pier 2 Pile 37: Estimated Side Resistance using EDC Measurements and Measured Side Capacity From Tension Load Test

UF Method	Tran et al. Method	Load Test
Skin Capacity (kip)		
220	158	185

3.4.2 Pier 2 Pile 53

Pile 53 was driven on 7/28/2008 (EOID), followed by a static load test on 8/10/2008. Figure 3.61 shows the observed and estimated (from inversion process) particle velocities at the top and bottom of the test pile for EOID (blow 3382). Agreement between the estimated and observed data is evident, with the dominant components very well matched. Figure 3.62 shows the final mobilized skin friction as a function of displacement, both total skin friction and the skin friction on the segments. The blows estimate ultimate skin friction of about 194 kip. Table

3.17 shows the estimated skin friction capacity from the UF and Tran et al. methods compared to the measured skin friction capacity.

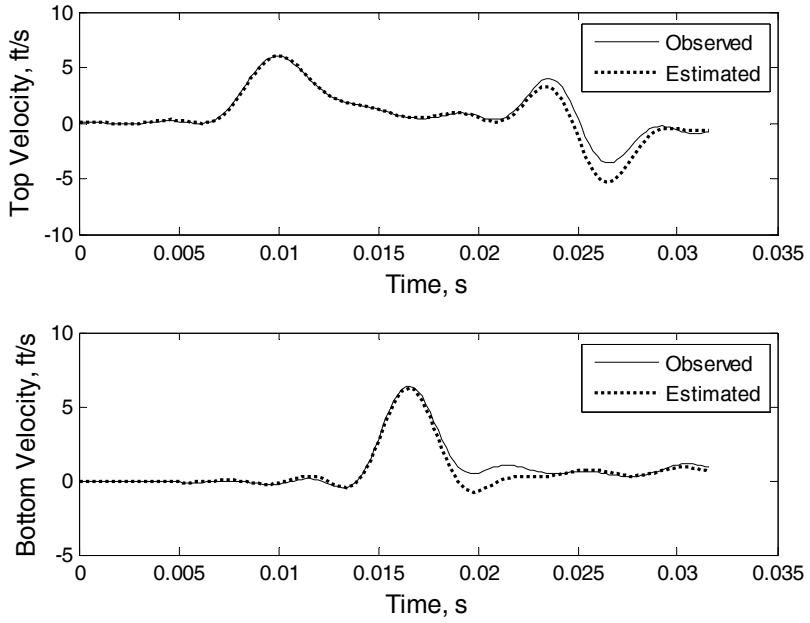

Figure 3.61 Pier 2 Pile 53: Comparison of Particle Velocity for EOID (Blow 3382)

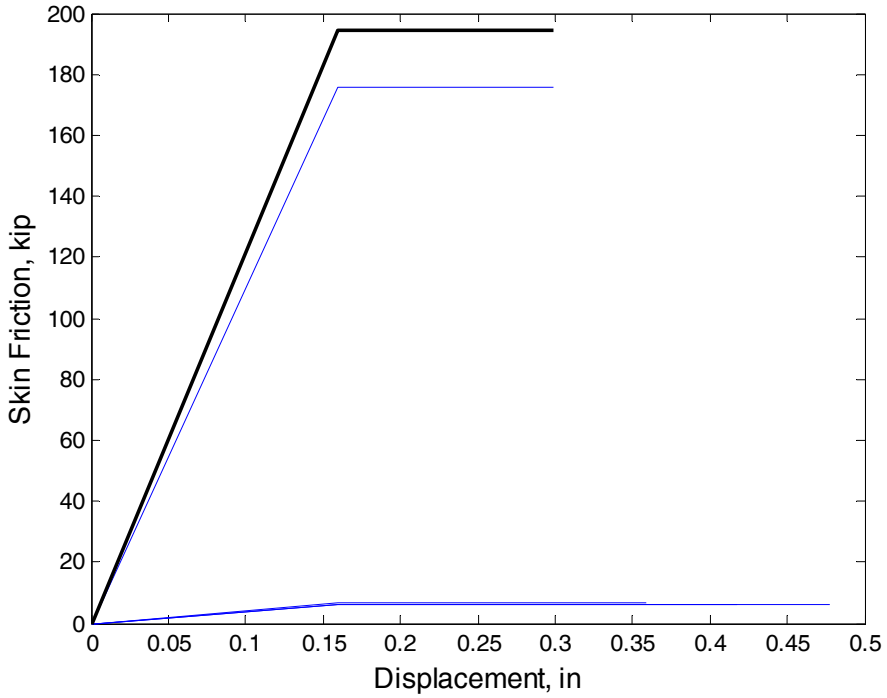

Figure 3.62 Pier 2 Pile 53: Forces Versus Displacement (Blow 3382)

Table 3.17 Pier 2 Pile 53: Estimated Side Resistance using EDC Measurements and Measured Side Capacity From Tension Load Test

UF Method	Tran et al. Method	Load Test
Skin Capacity (kip)		
200	194	180

3.4.3 Pier 3 Pile 9

Pile 9 was driven on 8/21/2008 (EOID), followed by a static load test on 8/24/2008. Figure 3.63 shows the observed and estimated (from inversion process) particle velocities at the top and bottom of the test pile for EOID (blow 2184). Agreement between the estimated and observed data is evident, with the dominant components very well matched. Figure 3.64 shows the final mobilized skin friction as a function of displacement, both total skin friction and the skin friction on the segments. The blows estimate ultimate skin friction of about 216 kip.

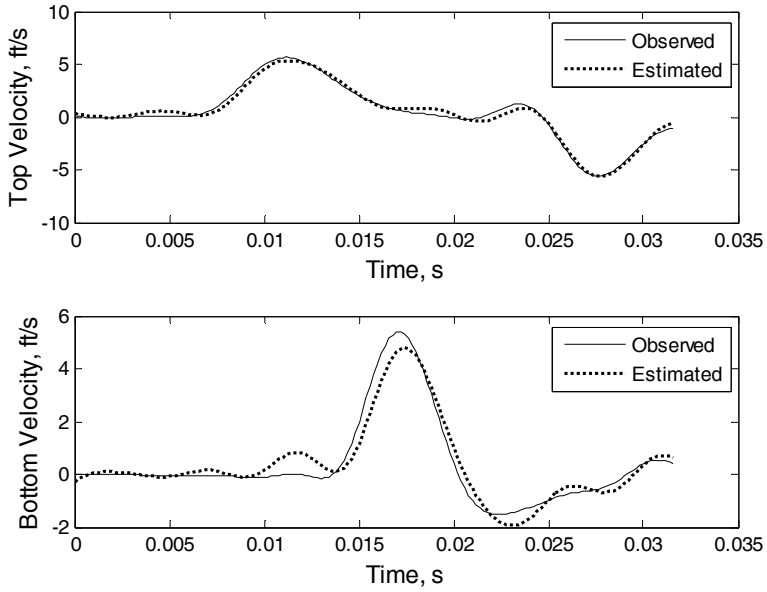

Figure 3.63 Pier 3 Pile 9: Comparison of Particle Velocity for EOID (Blow 2184)

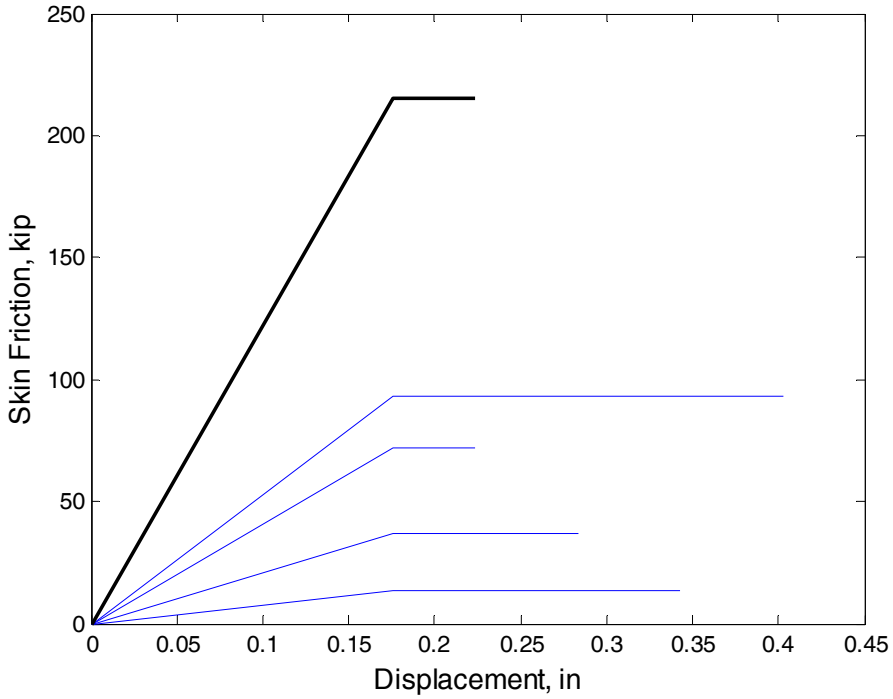

Figure 3.64 Pier 3 Pile 9: Forces Versus Displacement (Blow 2184)

Table 3.18 Pier 3 Pile 9: Estimated Side Resistance using EDC Measurements and Measured Side Capacity From Tension Load Test

UF Method	Tran et al. Method	Load Test
Skin Capacity (kip)		
150	216	68

3.4.4 Pier 3 Pile 42

Pile 42 was driven on 8/26/2008 (EOID), followed by a static load test on 8/29/2008. As reported in the Phase I final report, the UF method predicted 215 kip of skin friction (tension) capacity (Table 3.19). The accelerometer at the tip of the pile may have been damaged and good data was not available for an estimate based on the Tran et al. method.

Table 3.19 Pier 3 Pile 42: Estimated Side Resistance using EDC Measurements and Measured Side Capacity From Tension Load Test

UF Method	Load Test
Skin Capacity (kip)	
215	153

CHAPTER 4
CALIBRATION OF LRFD RESISTANCE FACTORS

4.1 Introduction

The purpose of Task 3 was to collect all static load test results and develop LRFD resistance factors for total, skin and tip resistance for the UF methods and the methods by Tran et al. (2012A and 2012B). As part of EDC II (FDOT BDK-75-977-24), static load test data from six sites, 12 piles with EDC (17 independent values: skin, tip and total) had been collected. With the addition of the US-331 Choctawhatchee Bay site, five static load tests and ten independent measurements (skin, tip and total) were to be collected in Florida. The Bayou Lacassine (LDOT) site with measured side and tip resistance data became available (Haque et. al, 2014). Additionally, the EDC drive data from piles at the 5th Street Bascule Bridge, in Miami-Dade County, Florida, also became available. The piles in these new sites had to be analyzed with the recent methods (Tran et al, 2012A and 2012B) by the sub-contractor (Dr. Khiem Tran, Clarkson University). This chapter presents the data sets collected to date, a blind prediction study (1. estimates of pile capacity were made before each static load test and 2. estimates by AFT and static load test results were not released to Dr. Tran), analyses of resistance bias for the UF method and the Tran et al. method, and calibration of the LRFD resistance factor for the Fixed J_c, UF, and Tran et al. method using the First Order Second Moment method (FOSM) and the First Order Reliability Method (FORM).

4.2 Load Test Results and Pile Capacity Estimates

The data set now includes the measured static load test results on 16 test piles that were monitored with EDC instrumentation. With the data from the instrumentation, estimates, or predictions, of skin, tip and total pile capacity were made using the Fixed J_c (total only), UF

method (current option in SmartPile Review) and the Tran et al. method. The data set (up to 42 estimates of skin, tip, and total capacity) developed from the 16 tests piles is analyzed for sufficiency in number of samples and the method bias (Fixed J_c, UF, and Tran et al. methods) and bias summary statistics are calculated.

4.2.1 Static Load Test Results

The total data set now includes 11 test piles which had top-down static load tests performed to measure the skin, tip, and total (Davisson) capacity, and 5 uplift (tension) tests, for a total of 16 test piles. Table 4.1 lists the test pile locations, pile dimensions, and measured capacities. Of the 16 piles tested, the results include measurements of 11 total pile resistance, 14 skin resistance and 9 tip resistances. Of the 11 compression tests that were monitored with EDC during pile driving, EDC data was collected on only 7 of them during the static load test. Out of the 4 piles where data was not collected during static load testing, the mobilized skin friction for 2 test piles was estimated based on log-log load displacement plots (analysis in Chapter 3). This permitted the tip capacity to be assessed as well (i.e., tip capacity = total capacity – skin capacity). For the other 2 test piles, the total capacity was estimated based on pile head movement as the piles did not reach Davisson failure. A total of 5 tension tests were performed on tests piles in Broward County, FL (Dixie Highway) and in Miami-Dade County, FL (5^{th} Street Bascule Bridge). A total of 34 data points consisting of total, skin, and tip capacity were collected with EDC.

Table 4.1 Static Load Test Results

Site and Pile	Location	Pile Dimensions		Measured Capacity		
		Width (in)	Length (ft)	Skin (kip)	Tip (kip)	Davisson (kip)
Dixie Highway End Bent 1	Broward County, FL	24	50	134	296	430
Dixie Highway Pier 8	Broward County, FL	24	49	180	200	380
Caminada Bay Bent 1	Louisiana	30	69*	395.2	144.8	540
Caminada Bay Bent 7	Louisiana	30	69*	545	80	625
Bayou Lacassine Bent 1 Pile 1	Louisiana	30	75	381	71	460
Bayou Lacassine Bent 1 Pile 3	Louisiana	30	75	697	153	850
I-95 Eau Gallie Bridge Bent 1 Pile 1	Jacksonville, FL	17.7	78.7*	180	200	380
Dixie Highway Pier 4	Broward County, FL	24	74	212		
5th St Bascule Pier 2 Pile 37	Miami-Dade County, FL	24	95*	185		
5th St Bascule Pier 2 Pile 53	Miami-Dade County, FL	24	95*	180		
5th St Bascule Pier 3 Pile 9	Miami-Dade County, FL	24	95*	68		
5th St Bascule Pier 3 Pile 42	Miami-Dade County, FL	24	95*	153		
US-331 Choctawhatchee Bay Pier 25	Walton County, FL	30	160	1220	280	1500
US-331 Choctawhatchee Bay Pier 33	Walton County, FL	30	160			1500
US-331 Choctawhatchee Bay Pier 59	Walton County, FL	30	160	900	180	1080
US-331 Choctawhatchee Bay Pier 84	Walton County, FL	30	160			1500

* Embedded pile length

4.2.2 Assessing Quality of Data

To accommodate the differences in the level of quality of the measured pile capacities in the data set, a Bayesian updating method is selected for use in calculating the mean, μ, and variance, σ^2, of the bias for the prediction methods. The level of quality is defined as "better" or "good" according to the following criteria:

- Better Data
    - Pile tested to failure
    - Pile EDC observed during load test (i.e., measured skin and tip capacity)
    - Pile compression tests
- Good Data
    - Pile not loaded to failure
    - Predictions used based on pile movement (pile not loaded to failure)
    - Estimated measured skin and tip pile capacity (i.e., application of DeBeer's method)
    - Pile tension tests

Bayesian updating is a useful technique for accounting for the quality of data subsets. The technique has been applied in other pile capacity predictions and analysis (Kwak et al, 2010; Yu, 2006; Zhang and Tang, 2002). Equations 4.1 and 4.2 are used to calculate the updated mean, μ_U, and variance, σ^2_U

$$\mu_U = \frac{\mu_B \cdot \sigma_G^2 + \mu_G \cdot \sigma_B^2}{\sigma_G^2 + \sigma_B^2} \quad \text{Eq. 4-1}$$

$$\sigma_U^2 = \frac{\sigma_G^2 \cdot \sigma_B^2}{\sigma_G^2 + \sigma_B^2} \quad \text{Eq. 4-2}$$

where μ_B is the mean of the better quality data, μ_G is the mean of the good quality data, σ^2_B is the variance of the better quality data, and σ^2_G is the variance of the good quality data (Ang and

Tang, 1975). The data set of bias for the prediction methods in this study will be divided into sub sets based on the "better" or "good" quality criteria and the updated summary statistics will be presented and used in the assessment of the LRFD resistance factors, Φ.

4.2.3 UF Method for Skin, Tip, and Total Resistance

The UF method used in the current version of SmartPile Review estimates the total capacity using Case equation (Likens and Hussein, 1988) with a dynamic J_c (estimated using top and tip instrumentation in real time for every blow) and tip capacity using the unloading point method (Middendorp et al, 1992). The skin capacity is taken as the difference between the total and the tip (e.g., skin capacity = total capacity – tip capacity). Table 4.2 lists the predicted skin, tip and total capacities for the piles in Table 4.1 which the UF method was applied. In four of the test piles (US-331 Choctawhatchee Bay) where 30-inch pre-stressed concrete piles with voids along the middle third of the pile were driven, estimates of total capacity are based on gauges (i.e., strain transducers and accelerometers) near the top of the pile. In cases where top instrumentation was located in the voided section of the pile, the results were identified in italics in Table 4.2. A comparison of estimates based on the EDC in the top solid and voided sections (bottom set of gauges in solid sections) was presented in Chapter 3. The comparison showed, on average, 23% difference in resistances. Method bias determined from the solid and voided section data will be used to for the LRFD resistance, Φ, assessment.

Figure 4.2 shows the measured versus predicted (n = 42) where estimates for the US-331 Choctawhatchee Bay test piles are based on the instrumentation in the solid section as well as top voided section. Table 4.3 lists the summary statistics for the better, good, and updated data sets. Note, the 42 values are the combined values of skin (compression and tension), tip and total capacity.

Table 4.2 Predicted Pile Capacities – UF Methods

Site and Pile	Predicted Capacity		
	Skin (kip)	Tip (kip)	Davisson (kip)
Dixie Highway End Bent 1	99	349	448
Dixie Highway Pier 8	220	250	470
Caminada Bay Bent 1	480	94	574
Caminada Bay Bent 7	520	67	587
Bayou Lacassine Bent 1 Pile 1	341	91	432
Bayou Lacassine Bent 1 Pile 3	671	74	745
I-95 Eau Gallie Bridge Bent 1 Pile 1	106	263	369
Dixie Highway Pier 4	171		
5th St Bascule Pier 2 Pile 37	220		
5th St Bascule Pier 2 Pile 53	200		
5th St Bascule Pier 3 Pile 9	150		
5th St Bascule Pier 3 Pile 42	215		
US-331 Choctawhatchee Bay Pier 25	1471	255	1726
US-331 Choctawhatchee Bay Pier 33	1308	158	1466
US-331 Choctawhatchee Bay Pier 59	1092	251	1343
US-331 Choctawhatchee Bay Pier 84	865	866	1731
US-331 Choctawhatchee Bay Pier 25	*996*	*155*	*1151*
US-331 Choctawhatchee Bay Pier 33	*1026*	*96*	*1122*
US-331 Choctawhatchee Bay Pier 59	*1018*	*206*	*1224*
US-331 Choctawhatchee Bay Pier 84	*631*	*793*	*1424*

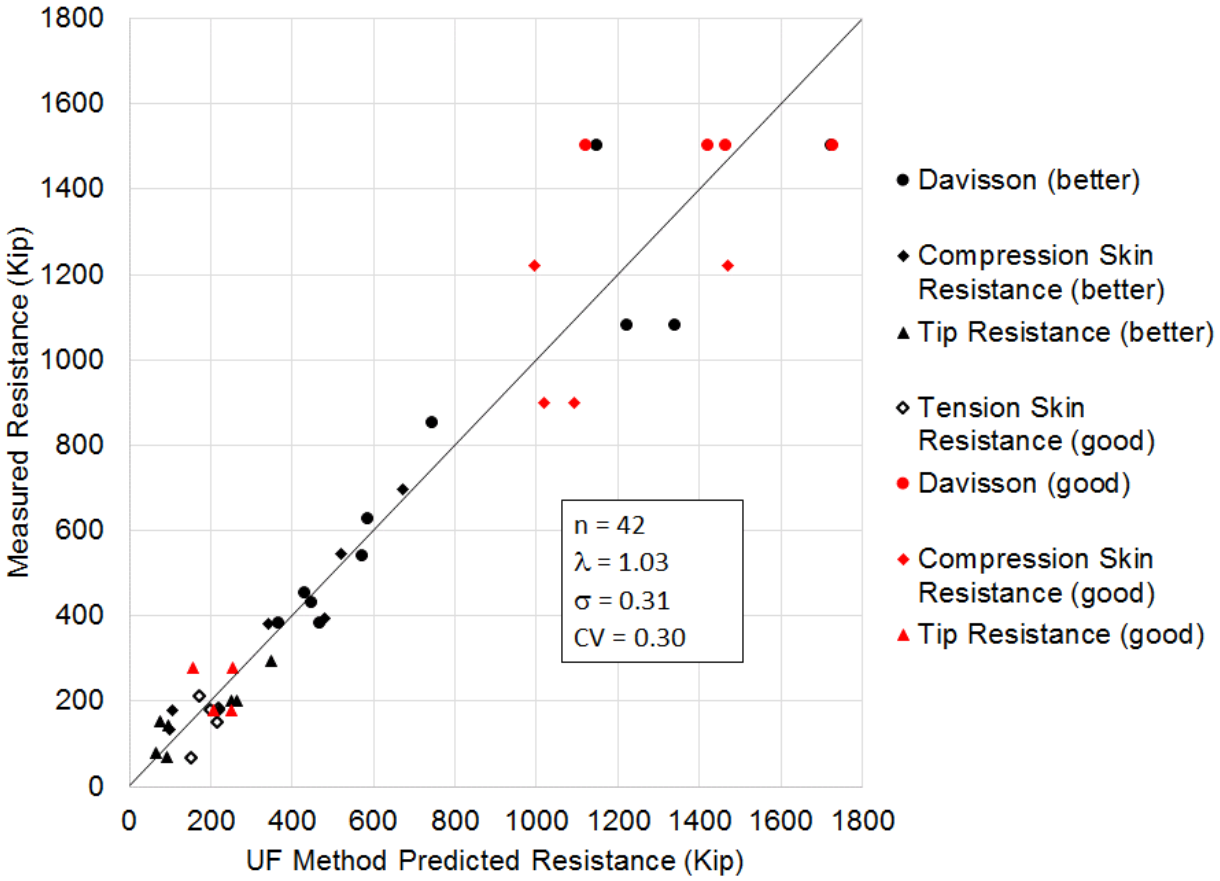

Figure 4.1 Measured and Predicted (UF Methods) Total, Skin, and Tip resistances

Table 4.3 Summary Statistics of Resistance Bias for UF Methods

Better	Good	Updated
$\mu_B = 1.06$ $\sigma_B = 0.318$ $CV_B = 0.298$ n = 25	$\mu_G = 0.981$ $\sigma_G = 0.304$ $CV_G = 0.310$ n = 17	$\mu_U = 0.998$ $\sigma_U = 0.212$ $CV_U = 0.212$ n = 42

To test the sample size of the data set (i.e., n) for being representative of the larger population, bootstrapping of the data was performed. Bootstrapping is a procedure where original data is randomly sampled and replaced to create a data set of equal size to the original data set (Navidi, 2006). Many realizations are made such that properties of the estimators (i.e.,

mean of the variance, variance of the mean, variance of the variance) are determined for error analyses. For the analysis, 10,000 realizations (i.e., bootstraps) were made of the resistance bias values. Agreement between the mean of the bootstrap variance and the variance of the sample population suggested the data set is representative of the population (sufficient number of samples). For the data set in Figure 4.1, the mean of the bootstrap variance, 0.095, compared to the variance of the data set, $\sigma^2 = 0.097$, indicates good agreement. Comparison of the variance of the bootstrap variance and the mean of the bootstrap variance ($0.0008 << 0.097$) indicates a high order of accuracy in variance determination and population representation.

Figure 4.2 shows the UF method data from Figure 4.1 plotted against lognormal and normal models based on the data's summary statistics. It is evident that the data is well described by the lognormal model with the exception of one value in the lower tail ($\lambda = 0.45$). An inspection of the value shows it is the resistance bias for a tension test (i.e., skin capacity) on pile 9, pier 3 5th Street Bascule. Note, the lower tail of the resistance distribution is of greater interest than the upper tail in terms of guaranteeing a resistance factor (i.e., resistance > load). There are also three values in the upper tail which could be considered outliers according to values outlying $\mu \pm 2\sigma$ (Paikowsky et al., 2004 and Kwak et al., 2010). The values correspond to two under predicted tip capacities (Bayou Lacassine, Bent 1 Pile 3, US-331 Choctawhatchee Bay Pier 25) and an under predicted skin friction capacity (I-95). For purposes of utilizing all the data collected and until more data becomes available, outliers were not removed for subsequent analysis. A K-S (Kolmogorov-Smirnov) goodness of fit test shows that the lognormal model could not be rejected at a level of significance of 5%, with a probability of 60% that the lognormal model describes the distribution of the data set.

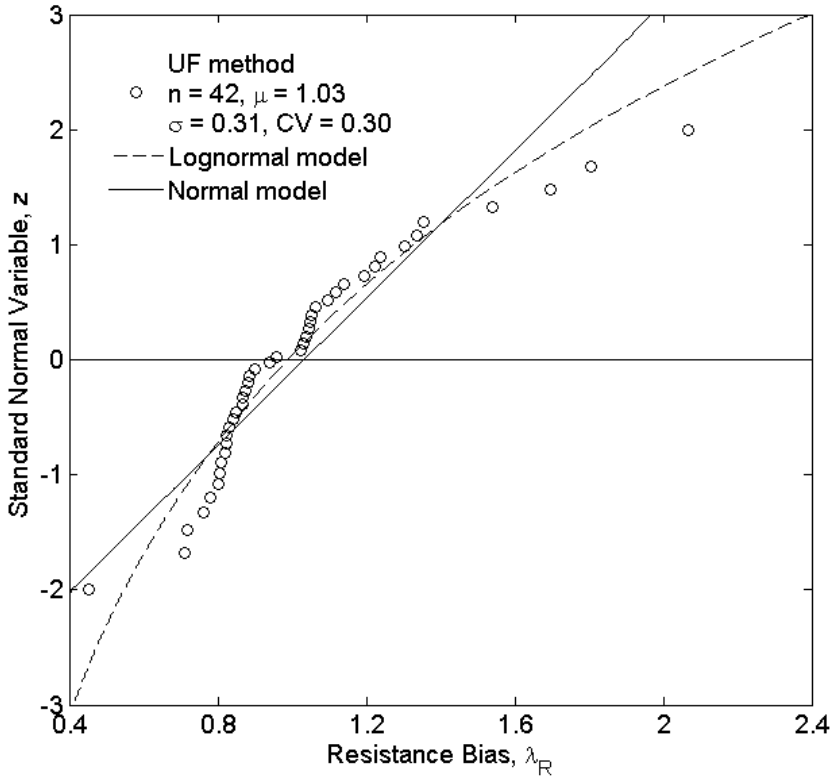

Figure 4.2 Cumulative Distribution Plots of Resistance Bias for the UF Methods Predicted Capacities and Fitted models

4.2.4 Tran et al. Methods for Skin and Tip Resistance

The methods by Tran et al. (2012A and 2012B) provide independent estimates of skin and tip resistance based on EDCs measured strain and accelerations at the top and bottom of a driven pile. Table 4.4 lists the predicted skin, tip and total capacities for the piles in Table 4.1 using the Tran et al. methods. Estimates for the 5th St Bascule Pier 3 Pile 42 could not be obtained due to poor signal (i.e., noise) data and is not included in Table 4.4. Estimates of skin and tip capacity for the US-331 Choctawhatchee Bay test piles based on EDCs around the void in each pile (Figure 2.1) are identified with italics. Note, the analysis of the EDC readings from 5 feet and 2.5 feet from the pile tip showed the same results. As a result, the EDC located 5 feet from the pile tip was used for the estimates. Subsequently, the tip estimates for the Pier 25 and 59 test piles (Table 4.4) are the same and the bias values are only counted once. Further, the skin

Table 4.4 Predicted Pile Capacities – Tran et al. Methods

Site and Pile	Predicted Capacity		
	Skin (kip)	Tip (kip)	Total (kip)
Dixie Highway End Bent 1	155	225	380
Dixie Highway Pier 8	184	174	358
Caminada Bay Bent 1	405	180	585
Caminada Bay Bent 7	450	90	540
Bayou Lacassine Bent 1 Pile 1	505	53	558
Bayou Lacassine Bent 1 Pile 3	759	87	846
I-95 Eau Gallie Bridge Bent 1 Pile 1	200	280	480
Dixie Highway Pier 4	180		
5th St Bascule Pier 2 Pile 37	158		
5th St Bascule Pier 2 Pile 53	194		
5th St Bascule Pier 3 Pile 9	216		
US-331 Choctawhatchee Bay Pier 25	1250	200	1450
US-331 Choctawhatchee Bay Pier 33			1320
US-331 Choctawhatchee Bay Pier 59	1040	280	1320
US-331 Choctawhatchee Bay Pier 84			1350
US-331 Choctawhatchee Bay Pier 25	*1170*	*200*	*1370*
US-331 Choctawhatchee Bay Pier 33			*1260*
US-331 Choctawhatchee Bay Pier 59	*920*	*280*	*1200*
US-331 Choctawhatchee Bay Pier 84			*1280*

and tip capacity estimates for US-331 Choctawhatchee Bay Pier 33 and 84 test piles from Chapter 3 are not included in Table 4.4, as there isn't measured values to calculate a bias for each.

Figure 4.3 shows the measured versus predicted (n = 39) where estimates for the US-331 Choctawhatchee Bay test piles are based on the instrumentation in the solid section as well as top voided section. Table 4.5 lists the summary statistics for the better, good, and updated data sets.

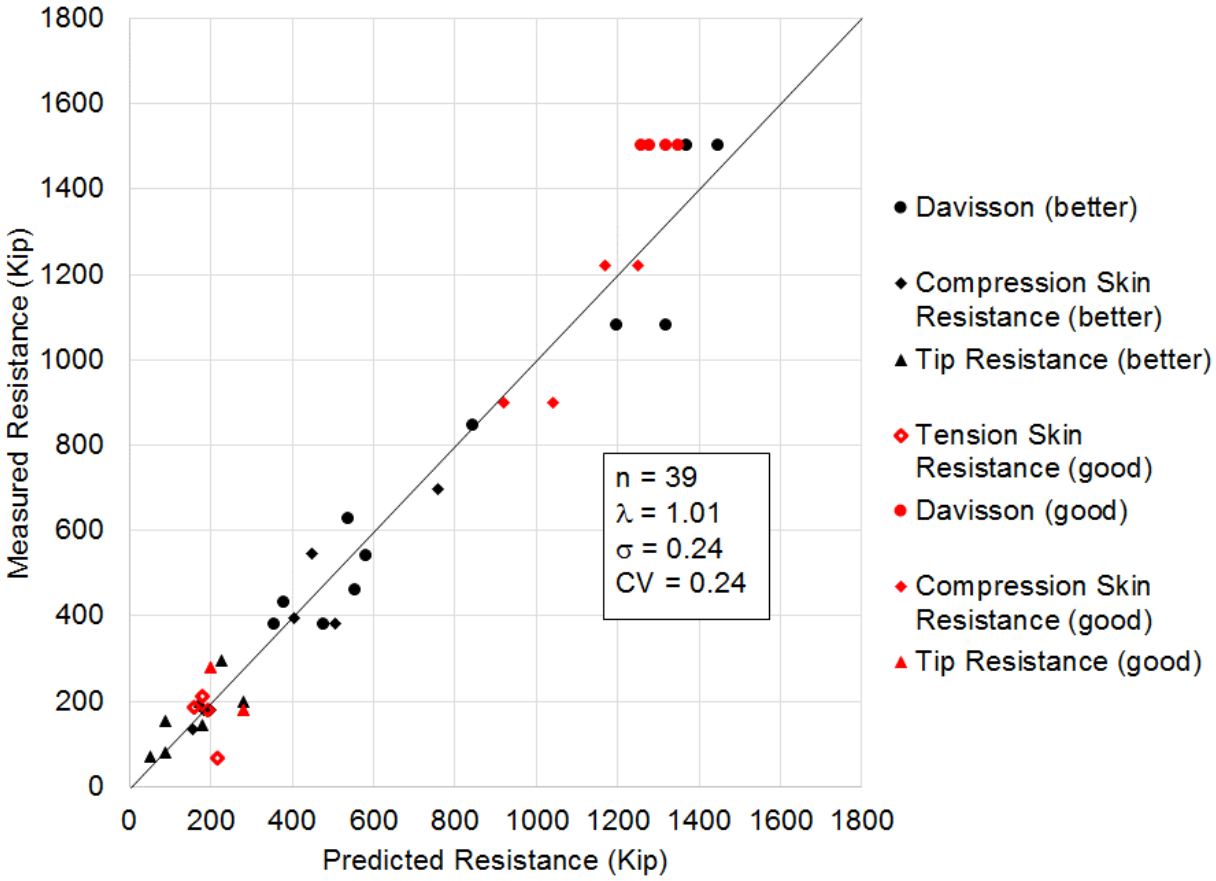

Figure 4.3 Measured and Predicted (Tran et al. Methods) Total, Skin, and Tip Resistances

Table 4.5 Summary Statistics of Resistance Bias for Tran et al. Methods

Better	Good	Updated
$\mu_B = 1.01$ $\sigma_B = 0.229$ $CV_B = 0.226$ n = 25	$\mu_G = 1.0$ $\sigma_G = 0.268$ $CV_G = 0.266$ n = 14	$\mu_U = 0.991$ $\sigma_U = 0.169$ $CV_U = 0.17$ n = 39

Note, the 39 values are the combined values of skin (compression and tension), tip and total capacity.

To test the sample size of the data set (i.e., n) for being representative of the larger population, bootstrapping of the data was performed. For the data set shown in Figure 4.3, the mean of the bootstrap variance, 0.056, compared to the variance of the data set, $\sigma^2 = 0.057$,

indicates good agreement. Comparison of the variance of the bootstrap variance and the mean of the bootstrap variance (0.00034 << 0.056) indicates a high order of accuracy in determination of the variance and provides confidence there is sufficient number of samples.

Figure 4.4 shows the Tran et al. method data from Figure 4.3 plotted against lognormal and normal models based on the data's summary statistics. It is evident that the data is well described by the lognormal model with the exception of a value in the lower tail ($\lambda = 0.34$) and a value in the upper tail ($\lambda = 1.75$). An inspection of the lower tail value shows it is the resistance bias for a tension test (i.e., skin capacity) on pile 9, pier 3 5th Street Bascule. Note, the lower tail of the resistance distribution is of greater interest than the upper tail in terms of guaranteeing a resistance factor (i.e., resistance > load). The upper tail value is from an under predicted tip

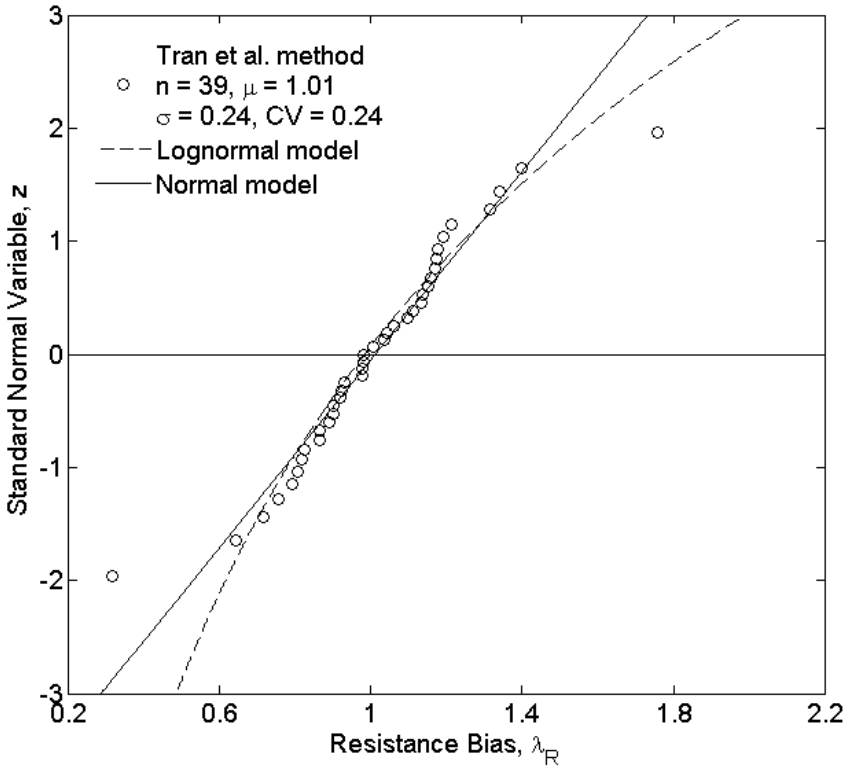

Figure 4.4 Cumulative Distribution Plots of Resistance Bias for the Tran et al. Method Predicted Capacities and Fitted Models

capacity on Bayou Lacassine, Bent 1 Pile 3. Both values could be considered outliers according to values outlying $\mu \pm 2\sigma$ (Paikowsky et al., 2004 and Kwak et al., 2010). For purposes of utilizing all the data collected and until more data becomes available, outliers were not removed for subsequent analysis. A K-S (Kolmogorov-Smirnov) goodness of fit test shows that the lognormal model could not be rejected at a level of significance of 5%, with a probability of 60% that the lognormal model describes the distribution of the data set.

4.2.5 Fixed J_c Method for Total Resistance

The total pile resistance predictions using the Fixed J_c method are shown in Table 4.6. Only the piles that were load tested in compression were included in the data set. As a result, there are 11 piles and 15 predictions of total resistance (four piles from US-331 Choctawhatchee Bay contribute two estimates due to two sets of EDC). Table 4.7 are the summary statistics of the method bias for the Fixed J_c method.

4.3 Calibration of LRFD Resistance Factor

Resistance factors for each of the methods (Fixed J_c, UF, and Tran et al.) were calibrated using the First Order Reliability Method (FORM) as developed by Hasofer and Lind (1974) and described in detail in Paikowsky et al. (2004) and Styler (2005). The FORM is an iterative method, where the reliability index, β, is converged upon for a given resistance factor, Φ. As a result, the approach gives a unique solution and is more robust over the First Order Second Moment (FOSM) approach. While the FOSM method is a closed form method, it gives results which are non-unique and works appropriately when the load and resistance are lognormally distributed (tested in section 4.2), while FORM only requires an assumption on the type of distribution. Paikowsky et al. (2004) showed in an NCHRP 507 study of LRFD for deep foundations that Φ's developed using the FORM were 10% - 15% greater than those developed

Table 4.6 Predicted Pile Total Capacities – Fixed J_c Method

Site and Pile	Total (kip)
Dixie Highway End Bent 1	526
Dixie Highway Pier 8	457
Caminada Bay Bent 1	534
Caminada Bay Bent 7	471
Bayou Lacassine Bent 1 Pile 1	411
Bayou Lacassine Bent 1 Pile 3	804
I-95 Eau Gallie Bridge Bent 1 Pile 1	460
US-331 Choctawhatchee Bay Pier 25	1667
US-331 Choctawhatchee Bay Pier 33	1816
US-331 Choctawhatchee Bay Pier 59	1312
US-331 Choctawhatchee Bay Pier 84	932
US-331 Choctawhatchee Bay Pier 25	*1170*
US-331 Choctawhatchee Bay Pier 33	*1335*
US-331 Choctawhatchee Bay Pier 59	*1127*
US-331 Choctawhatchee Bay Pier 84	*1209*

Table 4.7 Summary Statistics of Resistance Bias for Fixed J_c Method

Fixed J_c
$\lambda = 1.05$ $\sigma = 0.235$ CV = 0.224 n = 15

using the FOSM method. For comparison, Φ's using the FOSM method are included.

For validation of the Matlab code written for this task, resistance factors determined with the code (Φ_{herein}) are compared with published Φs by others that used FORM (Kwak et al., 2010 and Paikowsky et al., 2004). Table 4.8 shows the Φs and Φ_{herein} for different μ and CV of

resistance methods for driven piles determined for $\beta = 2.0$. There is good agreement between the reported Φs and the Φ_{herein} determined using the FORM code.

For the calibration, the following load parameters according to the AASHTO (2014) recommendation for load cases, I, II, and IV, and used by Paikowsky et al. (2004) in the NCHRP 507 study, were used: dead to live load ratio $q_D/q_L = 2$, dead load factor $\gamma_D = 1.25$, live load factor $\gamma_L = 1.75$, dead load bias factor $\lambda_D = 1.05$, live load bias factor $\lambda_L = 1.15$, dead load coefficient of variation $CV_D = 0.10$, and live load coefficient of variation $CV_L = 0.20$.

Table 4.8 Comparison of Resistance Factors From FORM for Driven Piles

Reference	Load Statistics	Resistance Statistics		For $\beta = 2.0$	
		μ	CV_R	Φ	Φ_{herein}
Kwak et al. (2010)	$\lambda_D = 1.05$ $CV_D = 0.10$ $\lambda_L = 1.15$ $CV_L = 0.20$ $q_D/q_L = 1.72$ $\gamma_D = 1.25$ $\gamma_L = 1.75$	1.01	0.515	0.445	0.442
		1.782	0.773	0.472	0.468
		0.73	0.423	0.391	0.388
		1.341	0.754	0.369	0.369
Paikowsky et al. (2004)	$\lambda_D = 1.05$ $CV_D = 0.10$ $\lambda_L = 1.15$ $CV_L = 0.20$ $q_D/q_L = 2.0$ $\gamma_D = 1.25$ $\gamma_L = 1.75$	0.96	0.49	0.46	0.44
		0.87	0.48	0.42	0.41
		0.81	0.38	0.47	0.46
		0.84	0.31	0.57	0.56

Table 4.9 are the resulting β's of the FOSM method and the FORM iterations for Φ's ranging from 0.5 to 0.9 (incremented by 0.5) for the data sets of the UF and Tran et al. methods. The calibrated resistance factors are for driven concrete piles with EDC. Figure 4.5 illustrates the relationships between Φ and β, which have similar trends between the FOSM and FORM for

the range of β investigated. Solutions of the relationships for a β = 2.33 show that Φ_{FORM} = 0.75 and Φ_{FOSM} = 0.64 for the UF method, Φ_{FORM} = 0.81 and Φ_{FOSM} = 0.68 for the Tran et al. method.

Figure 4.6 are the relationships between for β's and Φ's from the FORM and the FOSM method for the Fixed J_c method. Solutions of the relationships for a β = 2.33 show that Φ_{FORM} = 0.76 and Φ_{FOSM} = 0.66.

Table 4.9 Resistance Factors and Reliability Indices for the Fixed J_c, UF, and Tran et al. Methods

Method	Φ_{FORM}	Φ_{FOSM}	β	P_f
Fixed J_c	0.50	0.38	4.17	1.5E-05
	0.55	0.43	3.77	8.1E-05
	0.60	0.48	3.41	3.3E-04
	0.65	0.53	3.07	1.1E-03
	0.70	0.58	2.76	2.9E-03
	0.75	0.64	2.47	6.8E-03
	0.80	0.70	2.19	1.4E-02
	0.85	0.75	1.94	2.6E-02
	0.90	0.81	1.70	4.5E-02
UF	0.50	0.37	4.09	2.2E-05
	0.55	0.42	3.67	1.2E-04
	0.60	0.47	3.30	4.9E-04
	0.65	0.52	2.95	1.6E-03
	0.70	0.58	2.63	4.3E-03
	0.75	0.63	2.33	9.9E-03
	0.80	0.69	2.05	2.0E-02
	0.85	0.75	1.79	3.7E-02
	0.90	0.81	1.54	6.2E-02
Tran et al.	0.50	0.34	4.86	5.9E-07
	0.55	0.39	4.37	6.3E-06
	0.60	0.44	3.92	4.4E-05
	0.65	0.49	3.51	2.3E-04
	0.70	0.55	3.13	8.9E-04
	0.75	0.61	2.77	2.8E-03
	0.80	0.66	2.44	7.4E-03
	0.85	0.73	2.12	1.7E-02
	0.90	0.79	1.83	3.4E-02

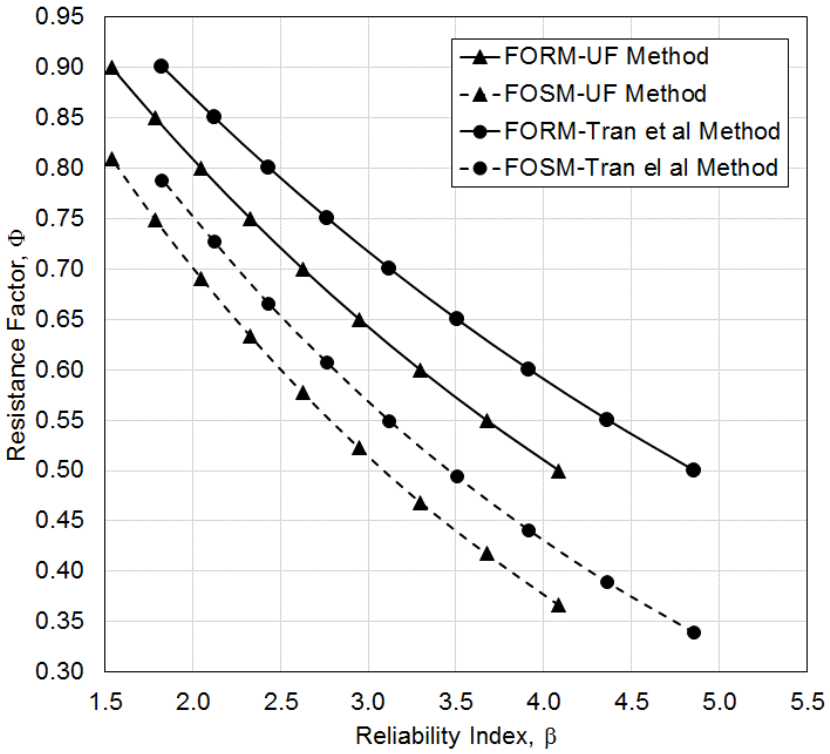

Figure 4.5 LRFD Resistance Factor Versus Reliability Index for the UF and Tran et al. Methods

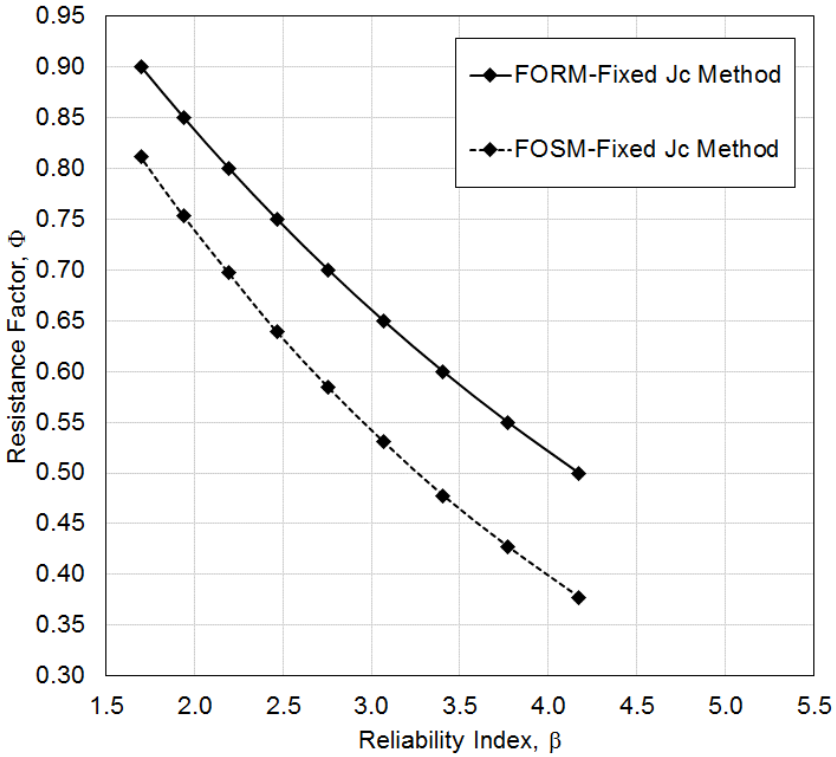

Figure 4.6 LRFD Resistance Factor Versus Reliability Index for the Fixed J_c Method

Current FDOT design standard index number 20602 specifies that the EDC instrumentation be embedded at 2D (D = pile diameter) from the top of the pile and 3 feet from the tip of the pile. Considering this specification on the use of EDC in concrete piles driven in Florida, new data sets that exclude the skin, tip, and total resistance predictions based on the EDC in the voided section of the test piles (four test piles from the US-331 Choctawhatchee Bay) were considered. The estimates which were excluded are identified in italics in Table 4.2 (UF method), Table 4.4 (Tran et al. method), and Table 4.6 (Fixed J_c method). For the UF method, Table 4.10 lists the summary statistics for the better, good, and updated data sets. For the Tran et al. method, Table 4.11 lists the summary statistics for the better, good, and updated data sets. For the Fixed J_c method, Table 4.12 lists the summary statistics based on the very limited data set of 11 bias values for nominal (total) resistance.

Table 4.10 Summary Statistics of Resistance Bias for UF Methods for Dataset Excluding Voided Section Estimates

Better	Good	Updated
$\mu_B = 1.07$ $\sigma_B = 0.33$ $CV_B = 0.31$ n = 23	$\mu_G = 0.86$ $\sigma_G = 0.21$ $CV_G = 0.24$ n = 11	$\mu_U = 0.918$ $\sigma_U = 0.172$ $CV_U = 0.188$ n = 34

Table 4.11 Summary Statistics of Resistance Bias for Tran et al. Methods for Dataset Excluding Voided Section Estimates

Better	Good	Updated
$\mu_B = 1.01$ $\sigma_B = 0.237$ $CV_B = 0.234$ n = 23	$\mu_G = 0.972$ $\sigma_G = 0.31$ $CV_G = 0.318$ n = 10	$\mu_U = 0.979$ $\sigma_U = 0.182$ $CV_U = 0.186$ n = 33

Table 4.12 Summary Statistics of Resistance Bias for Fixed J_c Method for Dataset Excluding Voided Section Estimates

Fixed J_c
$\lambda = 1.01$ $\sigma = 0.256$ CV = 0.253 n = 11

Similarly, the FOSM method and the FORM were used to calculate the resistance factors for driven concrete piles with EDC based on the data sets described in Tables 4.10 through 4.12. The solutions for a $\beta = 2.33$ show that $\Phi_{FORM} = 0.73$ and $\Phi_{FOSM} = 0.62$ for the UF method, $\Phi_{FORM} = 0.78$ and $\Phi_{FOSM} = 0.66$ for the Tran et al. method. The solution for a $\beta = 2.33$ shows that $\Phi_{FORM} = 0.76$ and $\Phi_{FOSM} = 0.66$ for the Fixed J_c method.

4.4 Conclusions from Task 4

In conclusion, 16 test piles instrumented with EDCs had static load tests performed to measure the skin, tip, and total (Davisson) capacity. Capacity estimates using the Fixed J_c, UF, and Tran et al. methods were evaluated for method bias. The data sets were evaluated for sufficiency in number of samples (n) and evaluated against normal and lognormal CDF models. Based on AASHTO's recommended load combinations for LRFD, Φs for each method were calculated using the FOSM method and the FORM. Table 4.13 shows the Φs for driven concrete piles with EDC that correspond to a $\beta = 2.33$. Additionally, smaller data sets that exclude the estimates based on EDC in the voided section of the test piles (four test piles from the US-331 Choctawhatchee Bay) were considered. For the same methods, the Φs for driven concrete piles with EDC that correspond to a $\beta = 2.33$ are shown in Table 4.14.

An evaluation of method efficiency based on Φ/λ (%) (McVay et al., 2000) for Φ_{FORM} and Φ_{FOSM} is shown in Tables 4.13 and 4.14. The UF method's efficiency is 64% to 67% for the FOSM method and 75% to 79% for the FORM. The Tran et al. method's efficiency is 67% to 69% for the FOSM method and 80% to 82% for the FORM.

Table 4.13 FORM and FOSM resistance factors ($\beta = 2.33$) and Efficiency Factors for the UF and Tran et al. Methods

Prediction Method	Φ_{FORM}	Φ/λ (%)	Φ_{FOSM}	Φ/λ (%)
UF $\lambda = 0.998$ $\sigma_\lambda = 0.212$ $CV_\lambda = 0.212$ n = 42	0.75	75	0.64	64
Tran et al. $\lambda = 0.991$ $\sigma_\lambda = 0.169$ $CV_\lambda = 0.17$ n = 39	0.81	82	0.68	69

Table 4.14 FORM and FOSM resistance factors ($\beta = 2.33$) and Efficiency Factors for the UF and Tran et al. Methods for Dataset Excluding Voided Section Estimates

Prediction Method	Φ_{FORM}	Φ/λ (%)	Φ_{FOSM}	Φ/λ (%)
UF $\lambda = 0.918$ $\sigma_\lambda = 0.172$ $CV_\lambda = 0.188$ n = 34	0.73	79	0.62	67
Tran et al. $\lambda = 0.979$ $\sigma_\lambda = 0.182$ $CV_\lambda = 0.186$ n = 33	0.78	80	0.66	67

Tables 4.15 and 4.16 are the Φs for the Fixed J_c method for driven concrete piles with EDC that correspond to a $\beta = 2.33$, for the data set that includes the estimates based on the EDC in the voided section and the data set that excludes these, respectively. Note, these are presented separately from the UF and Tran et al. methods because the summary statistics of the data set were not calculated to account for the quality of the data (only 15 and 11 values of bias). Furthermore, the efficiency factor is not calculated since the method is not being compared to others.

Table 4.15 FORM and FOSM resistance factors ($\beta = 2.33$) for the Fixed J_c Method

Prediction Method	Φ_{FORM}	Φ_{FOSM}
Fixed J_c $\lambda = 1.05$ $\sigma_\lambda = 0.235$ $CV_\lambda = 0.224$ n = 15	0.76	0.66

Table 4.16 FORM and FOSM resistance factors ($\beta = 2.33$) for the Fixed J_c Method for Dataset Excluding Voided Section Estimates

Prediction Method	Φ_{FORM}	Φ_{FOSM}
Fixed J_c $\lambda = 1.01$ $\sigma = 0.256$ CV = 0.253 n = 11	0.69	0.60

CHAPTER 5
SUMMARY, CONCLUSIONS, AND RECOMMENDATIONS

5.1 Background

Monitoring the installation of driven pile foundations is of critical importance for ensuring adequate safety of pile-supported structures (e.g., bridges). Dynamic load testing of driven test piles is currently the preferred alternative used by industry on the grounds that it is a cost-effective and a reliable method for assessing total capacity. EDC, a new system developed to monitor piles during driving, employs instrumentation at the pile top and tip and provides direct measurements of stresses and motions at both locations. The EDC software (SmartPile Review) assess stresses (top and bottom), total pile capacity, as well as end bearing and skin friction in "real time" for every blow of the hammer.

In an effort to evaluate the effectiveness of the EDC system the FDOT engaged in an evaluation program (Phase I) of comparison with dynamic load testing methods and wave matching software (i.e., CAPWAP), which is used by industry. Phase I yielded promising results, prompting the FDOT central office's geotechnical team to pursue the implementation of EDC as well as a Phase II to evaluate its reliability by comparing the recorded results with static load tests. To adopt the EDC technology as an alternate to current pile driving monitoring practice, the FDOT requires LRFD resistance factors for the technology. Resistance factors should be calibrated based on a sufficiently large database of instrumented static load test results. The purpose of the current work (continued Phase II efforts) was to develop a large enough database that would suffice for a Phase II LRFD resistance factor assessment.

In order to develop the necessary database, the FDOT funded the monitoring and testing of 5 test piles at a new bridge on US-331 crossing Choctawhatchee Bay in Walton County,

Florida. The test piles were instrumented with the EDCs and monitored during installation by Applied Foundation Testing out of Green Cove Springs, Florida. Four of the test piles had 18-inch diameter voids, 134 feet in length. In addition to EDCs at the top and tip of these piles, EDCs were also included on either side of the void near the top of the pile and at a second location in the tip (Figure 5.1). Static load tests performed on each of the test piles resulted in 8 new values of total, skin and tip capacity to compare with predictions based on the EDC instrumentation.

In all, 16 tests are reported on, five of which have only skin friction capacity reported. With the capacities, the bias, λ, and CV of resistance are reported for the UF methods (currently available option in SmartPile Review) and recent methods by Tran et al. (2012A) and (2012B), which estimate independent values of skin and tip resistance. This is followed by calibration of the LRFD resistance factor (Φ) for skin friction, end bearing and total static capacity, for each method.

5.2 Summary of Comparisons of EDC Used in Voided Piles

Four prestressed, 30-inch square concrete piles with a 18-inch diameter, 134 feet long void were instrumented with EDC near the top and the tip and installed at a new bridge site on US-331 in Walton County, Florida. Each pile was monitored during installation (EDC) and had static load tests performed to identify their capacity. The voided test piles had 2 pair of EDC gauges in each pile. One set of EDC had a pair of gauges in the top voided section (Figure 5.1) and another gauge in the solid section at the bottom of the pile. The other set of EDC had a pair of gauges in both solid sections (Figure 2.1), i.e., top and bottom of the pile.

The measured top compressive stresses in the solid section of the pile are typically about 25% smaller than the measured values in the voided section of the pile. However, if the top

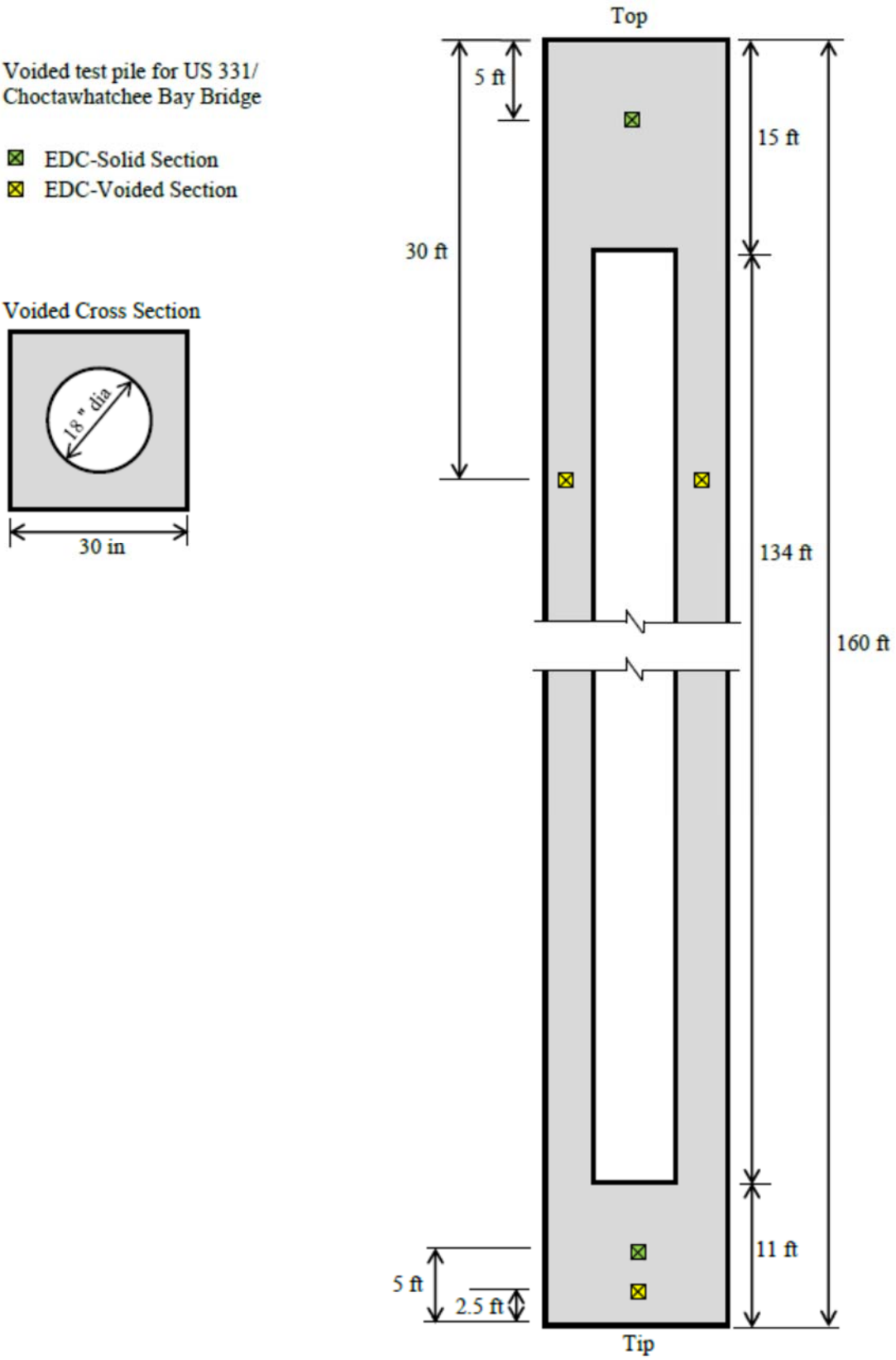

Figure 5.1 Voided 30-inch Square Prestressed Concrete Test Pile

stresses are adjusted by area (i.e., divide by 645 inch^2 / 900 inch^2 = 0.72), then the stresses are very comparable. For all piles, the predicted max tension stress are approximately 8% lower than the mean (void and solid) for the voided section, whereas the solid section are 8% higher than the mean.

Estimates of the skin and tip resistance using the Fixed J_c, UF, and Tran et al. methods were made independently for each test pile for both the voided and solid section of the piles. Shown in Table 5.1 are the comparisons of the UF and Tran et al. methods for the solid and voided gauge sets. The average difference between the estimation of capacity (grey columns) for the top and voided sections is larger for the UF method (23%) than the Tran et al. method (6%). Similarly, there is a lager standard deviation of the UF method (11%) compared to the Tran et al. method (3%). If the predictions are compared to the measured values (yellow and green columns), the average error is generally higher for the top solid gauges (yellow: 13% UF vs. -0.8% Tran et al) compared to the voided gauges (green: -12% UF vs. -5% Tran et al.). However, the measurements are well within the standard deviation of the measurements, suggesting the need for separation is not necessary and given the number of test piles (i.e., 4). This is shown very clearly in the last column (green) which reports UF voided gauge predictions – 23% for first pile, and +13% for third pile.

For estimates of the tip resistances, the voided and solid section sets both used tip gauges in the solid tip section. Consequently, only one solid tip set gauges was used in estimating static tip response.

Table 5.1 Predicted and Measured Capacities in Solid and Voided Sections

Pile	Gage Locations	Predicted NEW (kips)	Predicted UF Method (kips)	Measured (kips)	NEW Diff Top with Voided (%)	UF Diff Top with Voided (%)	NEW Error with Measured (%)	UF Error with Measured (%)	NEW Top Error with Measured (%)	NEW Voided Error with Measured (%)	UF Top Error with Measured (%)	UF Voided Error with Measured (%)
25	top&tip	1450	1726	1500	5.3	38.3	-3.3	15.1	-3.3		15.1	
	void&tip	1370	1151				-8.7	-23.3		-8.7		-23.3
33	top&tip	1320	1466	1500	4.0	22.9	-12.0	-2.3	-12.0		-2.3	
	void&tip	1260	1122				-16.0	-25.2		-16.0		-25.2
59	top&tip	1320	1343	1080	11.1	11.0	22.2	24.4	22.2		24.4	
	void&tip	1200	1224				11.1	13.3		11.1		13.3
84	top&tip	1350	1731	1500	4.7	20.5	-10.0	15.4	-10.0		15.4	
	void&tip	1280	1424				-14.7	-5.1		-14.7		-5.1
				Mean	6.3	23.2	-2.4	2.5	-0.8	-4.5	13.1	-11.7
				Std. Dev.	3.3	11.3	13.6	18.6	15.8	12.5	11.1	18.0

5.3 Summary of Bias for Skin, Tip, and Total Capacities Using EDC Methods

In all, 16 test piles instrumented with EDCs had static load tests performed to measure the skin, tip, and total (Davisson) capacity. Capacity estimates using the UF and Tran et al. methods were evaluated for method bias (measured/predicted). Figure 5.2 shows the measured versus UF method predicted for 42 estimates of skin, tip and total resistance. Figure 5.3 shows the measured versus Tran et al. method predicted for 39 estimates of skin, tip and total resistance. In comparison, the Tran et al. method's CV was 0.24 versus the UF method value of 0.30. Note, the data shown in Figures 5.2 and 5.3 include the US-331 Choctawhatchee Bay test pile estimates based on the instrumentation in the solid section and top voided section of the piles and in the solid section at the bottom of the piles (Figure 5.1). Each data set was evaluated using the bootstrapping technique for sufficiency in number of samples (n). Goodness of fit tests showed the resistance bias for each method's data set could most well be described as lognormally distributed, at the level of significance of 5%.

5.4 Summary of Calibrated LRFD Resistance Factors for Driven Concrete Piles with EDC

In this study, the LRFD Φs for each method (Fixed J_c, UF, and Tran et al.) were calculated using the FOSM method and the FORM. Based on AASHTO's recommended load for load cases, I, II, and IV, and that used by Paikowsky et al. (2004) in the NCHRP 507 study, the following were used: dead to live load ratio $q_D/q_L = 2$, dead load factor $\gamma_D = 1.25$, live load factor $\gamma_L = 1.75$, dead load bias factor $\lambda_D = 1.05$, live load bias factor $\lambda_L = 1.15$, dead load coefficient of variation $CV_D = 0.10$, live load coefficient of variation $CV_L = 0.20$, and summary statistics from Figures 5.2 and 5.3. Figure 5.4 shows the relationships between Φ and β for each the UF and Tran et al. methods using the FOSM method and the FORM. Table 5.2 shows the Φs

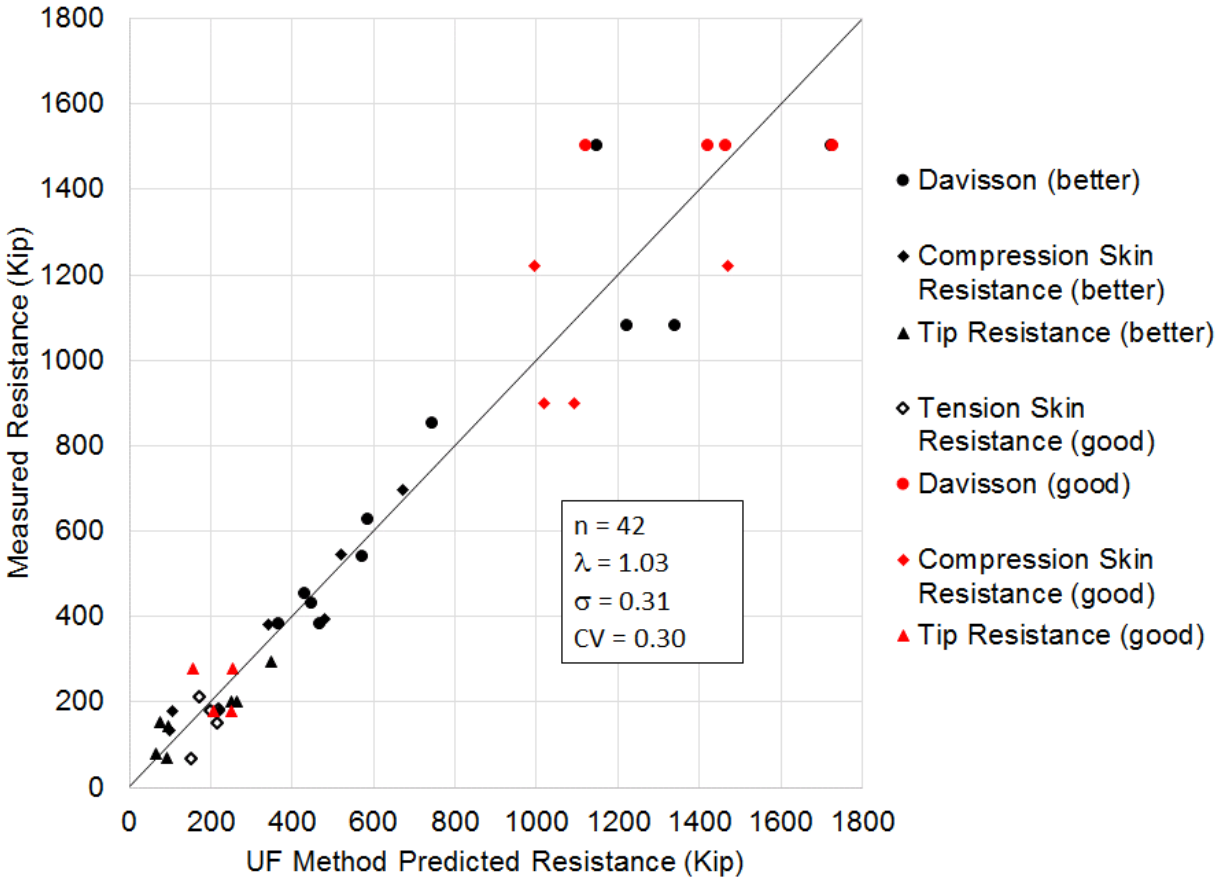

Figure 5.2 Measured and predicted (UF method) total, skin and tip resistances for filtered data set

for driven concrete piles with EDC that correspond to a $\beta = 2.33$. Solutions of the relationships for a $\beta = 2.33$ show that $\Phi_{FORM} = 0.75$ and $\Phi_{FOSM} = 0.64$ for the UF method, $\Phi_{FORM} = 0.81$ and $\Phi_{FOSM} = 0.68$ for the Tran et al. method.

An evaluation of method efficiency based on Φ/λ (%) (McVay et al., 2000) for Φ_{FORM} and Φ_{FOSM} is shown in Table 5.2. The UF method's efficiency is 64% for the FOSM method and 75% for the FORM. The Tran et al. method efficiency is 69% for the FOSM method and 82% for the FORM.

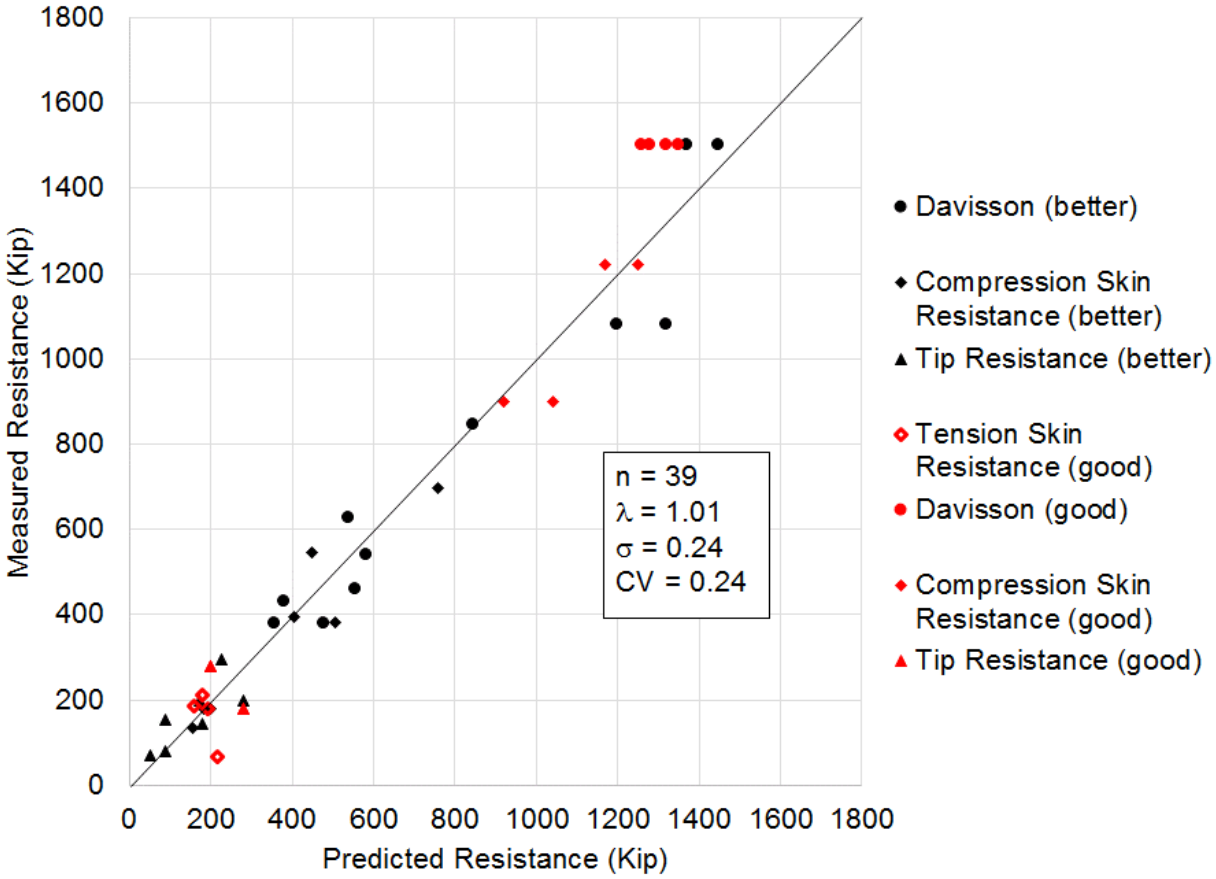

Figure 5.3 Measured and Predicted (Tran et al. Methods) Total, Skin and Tip Resistances

Figure 5.5 are the relationships between for β's and Φ's from the FORM and the FOSM method for the Fixed J_c method. Table 5.3 shows the Φs for the Fixed J_c method for driven concrete piles with EDC that correspond to a β = 2.33. Solutions of the relationships for a β = 2.33 show that $\Phi_{FORM} = 0.76$ and $\Phi_{FOSM} = 0.66$. Note, these are presented separately from the UF and Tran et al. methods because the summary statistics of the data set were not calculated to account for the quality of the data (only 15 values of bias). Furthermore, the efficiency factor is not calculated since the method is not being compared to others.

Current FDOT design standard index number 20602 specifies that the EDC instrumentation be embedded at 2D (D = pile diameter) from the top of the pile and 3 feet from the tip of the pile. Considering this specification on the use of EDC in concrete piles driven in

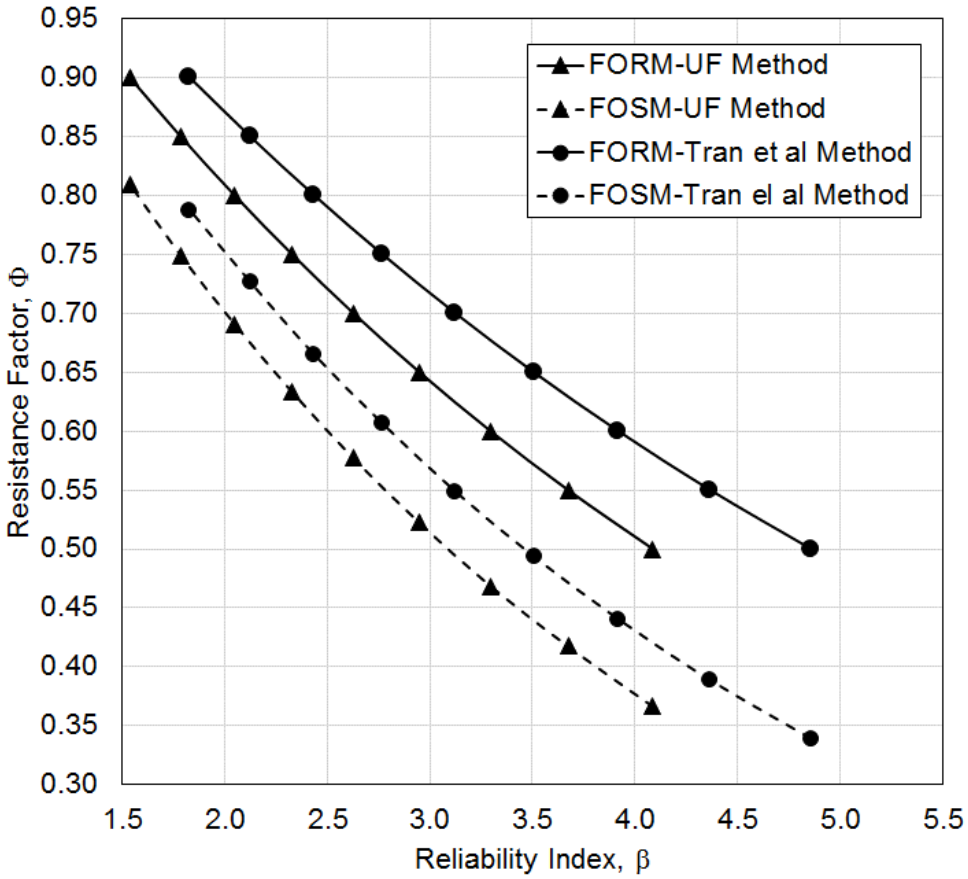

Figure 5.4 LRFD Resistance Factor Versus Reliability Index for the UF and Tran et al. Methods

Table 5.2 FORM and FOSM resistance factors (β = 2.33) and Efficiency Factors for the UF and Tran et al. Methods

Prediction Method	Φ_{FORM}	Φ/λ (%)	Φ_{FOSM}	Φ/λ (%)
UF $\lambda = 0.998$ $\sigma_\lambda = 0.212$ $CV_\lambda = 0.212$ n = 42	0.75	75	0.64	64
Tran et al. $\lambda = 0.991$ $\sigma_\lambda = 0.169$ $CV_\lambda = 0.17$ n = 39	0.81	82	0.68	69

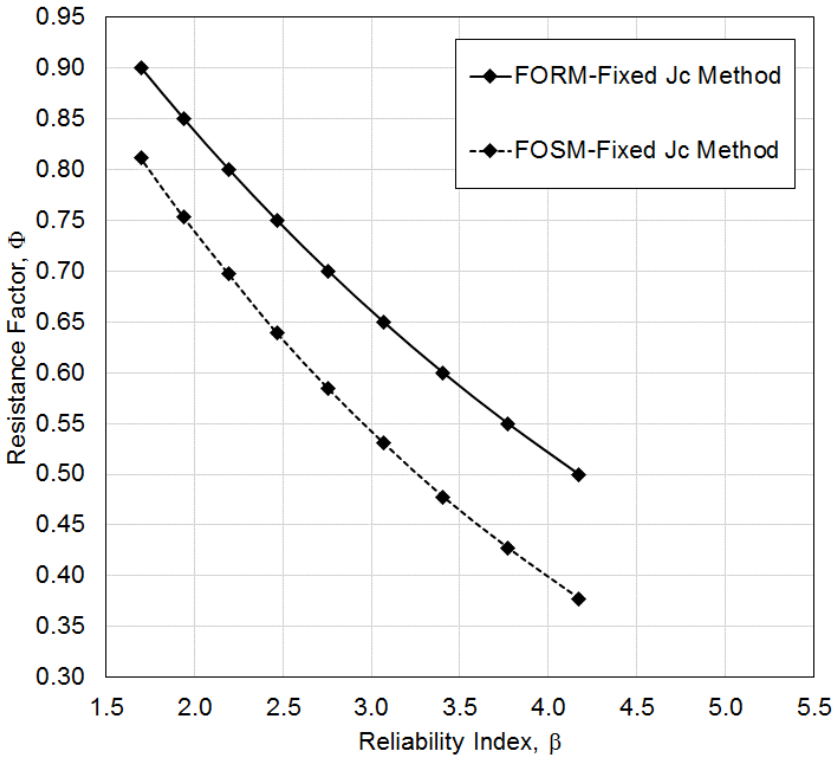

Figure 5.5 LRFD resistance factor versus reliability index for the Fixed J_c method

Table 5.3 FORM and FOSM resistance factors ($\beta = 2.33$) for the Fixed J_c Method

Prediction Method	Φ_{FORM}	Φ_{FOSM}
Fixed J_c $\lambda = 1.05$ $\sigma_\lambda = 0.235$ $CV_\lambda = 0.224$ $n = 15$	0.76	0.66

Florida, new data sets that exclude the skin, tip, and total resistance predictions based on the EDC in the voided section of the test piles (four test piles from the US-331 Choctawhatchee Bay) were considered. The estimates which were excluded are identified in italics in Table 4.2 (UF method), Table 4.4 (Tran et al. method), and Table 4.6 (Fixed J_c method). For the UF method,

Table 5.4 lists the summary statistics for the better, good, and updated data sets. For the Tran et al. method, Table 5.5 lists the summary statistics for the better, good, and updated data

Table 5.4 Summary Statistics of Resistance Bias for UF Methods for Dataset Excluding Voided Section Estimates

Better	Good	Updated
$\mu_B = 1.07$ $\sigma_B = 0.33$ $CV_B = 0.31$ n = 23	$\mu_G = 0.86$ $\sigma_G = 0.21$ $CV_G = 0.24$ n = 11	$\mu_U = 0.918$ $\sigma_U = 0.172$ $CV_U = 0.188$ n = 34

Table 5.5 Summary Statistics of Resistance Bias for Tran et al. Methods for Dataset Excluding Voided Section Estimates

Better	Good	Updated
$\mu_B = 1.01$ $\sigma_B = 0.237$ $CV_B = 0.234$ n = 23	$\mu_G = 0.972$ $\sigma_G = 0.31$ $CV_G = 0.318$ n = 10	$\mu_U = 0.979$ $\sigma_U = 0.182$ $CV_U = 0.186$ n = 33

Table 5.6 Summary Statistics of Resistance Bias for Fixed J_c Method for Dataset Excluding Voided Section Estimates

Fixed J_c
$\lambda = 1.01$ $\sigma = 0.256$ CV = 0.253 n = 11

sets. For the Fixed J_c method, Table 5.6 lists the summary statistics based on the very limited data set of 11 bias values for nominal (total) resistance.

Similarly, the FOSM method and the FORM were used to calculate the resistance factors are for driven concrete piles based on the datasets described in Tables 5.4 through 5.6. Tables 5.7 and 5.8 are the calculated Φs for the UF, Tran et al., and Fixed J_c method for driven concrete piles with EDC that correspond to a $\beta = 2.33$, for these data sets. Note, the UF and Tran et al. methods are presented separately from the Fixed J_c method because the summary statistics of the

Fixed J_c data set were not calculated to account for the quality of the data (only 15 and 11 values of bias). Furthermore, the efficiency factor is not calculated for the Fixed J_c method since is not being compared to others (i.e., only nominal resistance).

Table 5.7 FORM and FOSM resistance factors ($\beta = 2.33$) and Efficiency Factors for the UF and Tran et al. Methods for Dataset Excluding Voided Section Estimates

Prediction Method	Φ_{FORM}	Φ/λ (%)	Φ_{FOSM}	Φ/λ (%)
UF $\lambda = 0.918$ $\sigma_\lambda = 0.172$ $CV_\lambda = 0.188$ n = 34	0.73	79	0.62	67
Tran et al. $\lambda = 0.979$ $\sigma_\lambda = 0.182$ $CV_\lambda = 0.186$ n = 33	0.78	80	0.66	67

Table 5.8 FORM and FOSM resistance factors ($\beta = 2.33$) for the Fixed J_c Method for Dataset Excluding Voided Section Estimates

Prediction Method	Φ_{FORM}	Φ_{FOSM}
Fixed J_c $\lambda = 1.01$ $\sigma = 0.256$ CV = 0.253 n = 11	0.69	0.60

Note that less than half of the originally planned number of load tests were performed. The listed resistance factors should be used with caution due to the limited data set and the conditions they were obtained (e.g., limited soil types tested, time between BOR and load test, lack of fully instrumented tests piles). Until a sufficiently large database of static load tests is available, FDOT will continue to make use of the resistance factor contained in current documents.

REFERENCES

AASHTO (2014). *AASHTO LRFD Bridge Design Specifications (US Customary Units), Fourth Edition*, AASHTO, Washington, D.C.

Ang, A. and Tang, W.H. (1975). *Probability concepts in engineering, planning, and design*, Vol. I: Basic Principles, John Wiley & Sons, New York.

Hasofer, A. M. and Lind, N.C. (1974). "An exact and invariant first order reliability format", *Journal of Engineering Mechanics*, Vol. 100, No. 1, pp. 111-121.

Haque, M., Abu-Farsakh, M., Chen, Q., and Zhang, Z. (2014). "Case Study on Instrumenting and Testing Full-Scale Test Piles for Evaluating Setup Phenomenon," Journal of Transportation Research Board, No. 2462, pp. 37-47

Kwak, K., Kim, K.J., Huh, J., Lee, J.H., and Park, J.H. (2010). "Reliability-based calibration of resistance factors for static bearing capacity of driven steel pipe piles", *Canadian Geotechnical Journal*, 47, pp. 528-538.

Likens, G.E. and Hussein, M. (1988). "A summary of the pile driver analyzer capacity methods", Eleventh Pile Driving Analyzer User's Seminar, Cleveland, OH.

McVay, M., Birgisson, B., Zhang, L., Perez, A., and Puchta, S. (2000). "Load and resistance factor design (LRFD) for driven piles using dynamic methods – A Florida perspective", *Geotechnical Testing Journal*, Vol. 23, No. 1, pp. 55-66.

McVay, M.C., Bloomquist, D., and Tran, K. T. (2013). *Embedded data collector (EDC) evaluation phase II – comparison with instrumented static load tests*, Final Report, Florida Department of Transportation, Contract No. BDK75 977-24, Tallahassee, FL, pp. 176.

Middendorp, P., Bermingham, P., Kuiper, B. (1992). Statnamic Load testing of Foundation Pile, *Proceedings of the 4th International Conference on Application of Stress-Wave Theory to Piles*, Hague, Netherlands, pp. 581-588.

Navidi, W. C. (2006). *Statistics for Engineers and Scientists*, McGraw-Hill, 1st Edition, New York.

Paikowsky, S. G., (2004). Load and resistance factor design (LRFD) for deep foundations." *NCHRP Report 507*, Transportation Research Board, Washington D.C.

SmartPile (2013). *SmartPile Review Key Calculations: Summary Overview*, Ver. 2.0, Smart Structures Inc., pp. 1-26.

Styler, M. A. (2006). *Development and implementation of the Diggs format to perform LRFD resistance factor calibration of driven concrete piles in Florida*, Master Thesis, Department of Civil and Coastal Engineering, University of Florida.

Tran, K.T, McVay, M., Herrera, R., and Lai, P. (2012A). "Estimating static tip resistance of driven piles with bottom pile instrumentation", *Canadian Journal of Geotechnical Engineering*, Vol. 49, pp. 381-393.

Tran, K.T, McVay, M., Herrera, R., and Lai, P. (2012B). "Estimation of nonlinear static skin friction of multiple pile segments using the measured hammer impact response at the top and bottom of the pile", *Computers and Geotechnics*, 41, pp. 79-89.

Yu, Y. (2006). "Bayesian updating for improving the accuracy and precision of pile capacity predictions", *IAEG2006*, Geotechnical Society of London.

Zhang, L. and Tang, W.H. (2002). "Use of load tests for reducing pile length", *An International Perspective on Theory, Design, Construction, and Performance, Geotechnical Special Publication*, 116, pp. 993-1005.

APPENDIX
CAPWAP RESULTS FOR TEST PILES

	Measured			Predicted		
Site & Pile	Davisson Capacity (Kip)	Tip Capacity (Kip)	Skin Capacity (Kip)	CAPWAP Davisson (Kip)	CAPWAP Tip Capacity (Kip)	CAPWAP Skin Capacity (Kip)
Dixie Highway End Bent 1	430	296	134	420	315	105
Dixie Highway Pier 8	380	200	180	430	144	286
Caminada Bay Bent 1 LADOT	540	144.8	395.2	600	194	406
Caminada Bay Bent 7 LADOT	625	80	545	540	143	397
Bayou Lacassine Bent 1 Pile 1 LADOT	452	71	381	427	79	348
Bayou Lacassine Bent 1 Pile 3LADOT	850	153	697	650	162	488
I-95 Jax	380	200	180	356	137	219
Dixie Highway Pier 4			212			290
5th St Bascule Pier 2 Pile 37			185			198
5th St Bascule Pier 2 Pile 53			180			235
5th St Bascule Pier 3 Pile 9			68			135
5th St Bascule Pier 3 Pile 42			153			270
US 331 Choctawhatchee Bay Pier 25	1500	*280*	*1220*	967	317	650
US 331 Choctawhatchee Bay Pier 33	*1500*			1345	749	596
US 331 Choctawhatchee Bay Pier 59	1080	*180*	*900*	1238	349	890
US 331 Choctawhatchee Bay Pier 84	*1500*			1091	1029	62